ACTA PHYSIOLOGICA SCANDINAVICA
VOL. 26. SUPPLEMENTUM 93.

On the Theory of Counting Individual Microscopic Cells by Photoelectric Scanning An Improved Counting Apparatus

By

CARL LAGERCRANTZ

UPPSALA 1952

Digitized by the Internet Archive
in 2026

https://archive.org/details/IA41548912_0043

ON THE THEORY OF COUNTING INDIVIDUAL MICROSCOPIC CELLS BY PHOTOELECTRIC SCANNING

AN IMPROVED COUNTING APPARATUS

BY

CARL LAGERCRANTZ

AKADEMISK AVHANDLING

SOM MED TILLSTÅND AV MEDICINSKA FAKULTETEN VID UPPSALA UNIVERSITET FÖR ERNÅENDE AV MEDICINE DOKTORSGRAD OFFENTLIGEN FÖRSVARAS Å MEDICINSK-KEMISKA INSTITUTIONENS HÖRSAL LÖRDAGEN DEN 19 APRIL 1952 KL. 10 F. M.

AV

CARL LAGERCRANTZ
MED. LIC., SMÅL.

UPPSALA 1952
APPELBERGS BOKTRYCKERI AB

R. UNIV.
BIBLIOTHEEK
LEIDEN

ACTA PHYSIOLOGICA SCANDINAVICA
VOL. 26. SUPPLEMENTUM 93.

From the Central Laboratory of the University Hospital, Uppsala, and the Institute of Medical Chemistry, University of Uppsala

On the Theory of Counting Individual Microscopic Cells by Photoelectric Scanning An Improved Counting Apparatus

By

CARL LAGERCRANTZ

UPPSALA 1952

R. UNIV.
BIBLIOTHEEK
LEIDEN

UPPSALA 1952
APPELBERGS BOKTRYCKERI AB

Contents

Notation 7

Introduction 9

I. EARLIER WORKS DEALING WITH PHOTOELECTRIC COUNTING OF INDIVIDUAL MICROSCOPIC CELLS AND PARTICLES 11

1. The capillary tube method 11
2. The scanning method 12
3. Limitations of the original method 12
4. Proposed improvements 13
5. Other works concerning photoelectric counting of individual cells 14
6. Individual counting of other microscopic objects than animal and plant cells 15
7. Light-scattering 16
8. The aim of the present work 16

II. A CONTRIBUTION TO THE THEORY OF COUNTING BY SCANNING 17

9. Outlines of the method 17
10. General considerations 17
11. Impulses from individual elements 19
12. The area scanned by the aperture 20
13. Evaluation of the number of elements per unit area (no elements missed). 21
14. Counting to a predetermined number of elements (no elements missed) 23
15. The sensitivity of the scanning apparatus 23
16. Factors which may produce variations in the sensitivity of the apparatus 24
17. Corrections for missed elements. General considerations 26
18. Element centres distributed along a straight line 27
19. Elements missed 27
20. The probability of encountering intervals of length $> l$ 28

21. The mean and standard deviation of the recorded intervals in the linear case 29
22. Analogy with the counting of nuclear particles 30
23. Element centres distributed over an area. General considerations 32
24. The critical minimum distance 33
25. The mean and standard deviation of recorded intervals when the elements are situated on a plane area 36
26. Diminishing the number of missed elements 38
27. The effect of class A_2 elements 38
28. Evaluation of the number of elements per unit area 40
29. Evaluation of the effective aperture area 41
30. Successive approximations 44
31. Confidence limits of the number of elements per unit area 46

III. THE SCANNING MOVEMENT 51

32. General considerations 51
33. The area with the elements is moved while the aperture phototube system remains stationary 51
34. The aperture-phototube system is moved in the plane of the image. The object remains stationary 52
35. The scanning procedure is performed by moving the image by a prism system 53
36. Combination of the methods described in §§ 33 and 34 with that in § 35 53
37. Moving a spot of light in the object plane 53

IV. DESCRIPTION OF THE APPARATUS. THE MICROSCOPE 55

38. General considerations 55
39. Outlines of the microscope 55
40. The counting chamber and the dimensions of the scanning helix 57
41. The moving stage 57
42. Details of the moving stage 59
43. The phototube holder, the aperture holder and the scanning aperture 63
44. Determination of the apparatus constants 67
45. Element distribution not deranged by the scanning movement 68

V. THE SHAPE, DURATION AND RISE TIME OF THE IMPULSE 69

46. Shape and duration 69
47. Rise time 73
48. Dynamic range 75

VI. DESCRIPTION OF THE APPARATUS. THE ELECTRONIC SYSTEM 76

49. General considerations 76
50. The amplifier 76
51. Other electronic components 80
52. The microscope lamp 81

VII. IMPULSE SHAPE EXPERIMENTS 82

53. Experimental arrangement 82
54. Shape of impulses produced by human erythrocytes; dark field illumination 86
55. Single impulses. Effect of different aperture dimensions 87
56. Shape of impulses obtained from two erythrocytes situated close to each other. Effect of aperture dimensions 89
57. Effect of different time constants in the amplifier on the impulse shape and resolving power 91
58. Shape of a threshold impulse 95
59. Discussion 96

VIII. COUNTING EXPERIMENTS 99

60. General considerations 99
61. Experimental arrangement for testing the reproducibility of the apparatus 100
62. Tabulated values 101
63. The diagrams 102
64. The mean diameter of the elements 102
65. The counting procedure 103
66. Experiments 1—5: table I; diagrams given in Figs. 43—47 105
67. Experiments 6—9: table II; diagrams given in Figs. 48—51 108
68. Experiments 10—13: table III; diagrams given in Figs. 52—55 111
69. Statistical comparison between results obtained by the scanning method and by visual count 114

70. Conclusion 115
71. Missed elements 115
72. The apparatus error 116

IX. IMPROVEMENTS 117

73. General considerations 117
74. Standard deviation 118
75. Systematic error 118
76. The moving stage 119
77. The two-channel system 119
78. The four-apertures system 119
79. Intermittent scanning 121

X. ON THE COUNTING OF CELL NUCLEI IN HISTOLOGICAL TISSUE SECTIONS 126

80. General considerations 126
81. Impulse shape experiments 126

SUMMARY 129

ACKNOWLEDGEMENTS 134

REFERENCES 135

Notation.

a = aperture width perpendicular to the scanning direction.
A an area.
A = an element class defined in § 23.
b = a circle chord.
B = an element class defined in § 23.
c = aperture length in the scanning direction.
C = capacitance.
d maximum element length that passes inside the aperture in the scanning direction.
e = basis of the natural logarithm system.
f = number of periods per second.
F = 1. a distribution function
2. magnification factor between object plane and aperture plane.
g = see § 53.
i = an arbitrary number.
l = critical minimum interval between two consecutive element centres; defined in § 24.
L = length of the scanning track.
m = substitution for $u \cdot A$ (§ 79).
$m(i)$ = mean value of i.
n = an arbitrary number.
N = 1. number of intervals between consecutive element centres or number of elements on the scanning track.
2. number of periods the electronic system has functioned (§ 79).
N' = number of recorded intervals or number of recorded elements on the scanning track.
p = distance between the centre of a circular element and the aperture border.
P = a probability function.
Q = element group defined in § 25.
r = radius of a circular element.
R = 1. resistance
2. radius of a circular scanning aperture.
s = a substitution for $e^{-u\,l}$ (§ 21).
t = an independent variable.
T = impulse duration.
u = number of elements per unit area.
V = scanning velocity.
w = scanning width.
x = a coordinate parallel to the scanning direction.
x_i = a random variable.

z = 1. sensitivity of the recording system; defined in § 12.
2. a coordinate perpendicular to the scanning direction.
α = an arbitrary number.
ε = standard error.
λ = average number of elements on a scanning track.
μ = an arbitrary number.
ν = an arbitrary number
σ = standard deviation.
τ = recovery time of an electronic system or a period during which an electronic system functions.
ω = see § 53.
μF = microfarad (10^{-6} farads).
$\mu\mu$F = micromicrofarad (10^{-12} farads).
kc = kilocycles per second.
RC = time constant (resistance x capacitance).
N. A. = numerical aperture of a microscope objective.
Δ_i = an interval between two consecutive element centres.

Introduction.

In many fields of biology and medicine, determination of the number of individual microscopic cells in a certain specimen is an important and frequently performed procedure. Ordinarily, this process has been carried out by visual counting. On account of the tedious and time-consuming work involved, especially when a fairly large number of cells are to be counted, there appears to be good reason for replacing the visual method by some kind of automatic counting system. This problem has frequently been considered by laboratory workers who have been subjected to long periods of counting with a microscope; but no practical results have appeared until quite recently. It is apparent that the cells should be individually identified by a photo-sensitive element which is connected to some type of electronic system and a mechanical tabulator. Thus, the photo-sensitive element may be fitted to the eyepiece of a microscope on the stage of which the cells to be counted are situated. In order to be counted, the cells must pass in succession through the field of vision of the photo-sensitive element. For individual counting of microscopic cells in fluid suspensions, it would of course be very convenient if the cells could be arranged so that only one single cell could be seen at a time in the field of vision of the photo-sensitive element. Such an arrangement might conceivably be effected by forcing the fluid under pressure through a very fine capillary tube, so that the cells arrange themselves in a single line.

In 1946 the writer attempted to count erythrocytes in fluid suspension by the capillary tube method. Because this trial failed, a scanning method was evolved, where the cells were counted when lying in an area (LAGERCRANTZ, 1947, 1948). The present paper describes the history of the problem, a theory of the scanning method, an apparatus, and the results of a number of experiments performed with it.

CHAPTER I.

Earlier works dealing with photoelectric counting of individual microscopic cells and particles.

1. **The capillary tube method.** When the writer became interested in the present problem at the beginning of 1946, no reports were available indicating any successful experiments in this field. MOLDAVAN (1934) had described attempts to count erythrocytes and stained yeast cells by the capillary tube method. However, he did not obtain any signals from the cells large enough to operate a recording system, and it is not evident from his paper whether he really succeeded in passing the cells through a capillary space so small that it would pass one cell but not two abreast. He mentions some of the difficulties encountered, *i. e.* clumping of the cells, difficulties with proper focussing of the capillary tube, and lack of sufficient sensitivity of the phototube system, but fails to give any practical directions for overcoming these difficulties.

Attempting to carry through the capillary tube method, the writer made some experiments with a view to counting erythrocytes in fluid suspensions. By use of a multiplier phototube and dark field illumination, whereby the erythrocytes are seen luminous against a dark background, it was found that distinct signals from individual erythrocytes could be obtained when the cells were situated on a slide or in a counting chamber. At first, the writer attempted to arrange the erythrocytes in a suitable manner for individual counting by use of the capillary method suggested above. However, these trials were a total failure, for the following reasons. When dark field illumination was used, the curved inside borders of the capillary lumen reflected and spread light into the capillary lumen itself. Consequently, the contrast between a luminous erythrocyte and its dark background was lost; and it was no longer possible to get a sufficiently large signal-to-noise ratio to identify individual cells. Furthermore, it was found to be impossible to force any erythrocyte through a

capillary tube with inside diameter the same order of magnitude as that of an erythrocyte. When a lumen of larger diameter was used, the erythrocytes moved rapidly in the central part of the lumen; but in the peripheral parts, they moved very slowly and even stuck to the walls. Different erythrocytes passed through the capillary tube at different depths, *i. e.* at different distances from the microscope objective; and consequently the images of many erythrocytes were badly focussed and the counting procedure was disturbed. Thus, the cells could not be at all suitably arranged by this means. It was evident that counting of individual cells must be accomplished by some other method.

2. **The scanning method.** In order to count microscopic cells when distributed at random over an area, a scanning method was evolved. The essential features of this method may be summarized as follows. A diluted suspension of the cells under study is placed in an ordinary counting chamber, and the cells are allowed to settle to the bottom of the chamber. By using a special dark field system which has a field of vision not larger than a cell, the effect is achieved that only a single cell, or part of a cell, is luminous at a given time. Scanning is performed by moving the counting chamber. Cells or parts thereof become luminous in succession and produce light impulses which are recorded by a phototube electronic system. In order to calculate the number of cells per unit volume in the chamber, it is necessary to know the actual volume in which the cells have been counted. The depth of the counting chamber is known, and the length of the scanned track is easily measured. The width of the scanning track is calculated. It can be shown to be equal to the sum of the width of the field of vision and the median value of the cell diameter (cf. LAGERCRANTZ, 1947).

3. **Limitations of the original scanning method.** The width of the field of vision is not a well-defined constant quantity. In fact, the electronic system fails to record a count when a cell touches only the periphery of the field of vision, and a certain minimum part of a cell has to be inside the field of

vision in order for a threshold light impulse to be produced. Thus, the effective width of the field of vision does not coincide with its real size but is always smaller. Moreover, the effective width depends upon the intensity of light from the cells actually being scanned, upon the sensitivity and stability of the recording system as well as upon the constancy of the light source. One must also determine the median diameter of the different cell specimens.

The scanning method and an experimental apparatus for its implementation have been described in earlier communications together with certain counting experiments performed on human erythrocytes and on yeast cells (LAGERCRANTZ 1947, 1948).

4. **Proposed improvements.** In 1948, the writer proposed to elaborate a more extensive theoretical basis for the scanning method and to construct an improved apparatus. It was evident from the outset that the scanning procedure had to be carried out so that the number of cells per unit area could be calculated independently of the effective width of the field of vision mentioned above and also independently of the size of the cells to be counted. As the area scanned varies in direct proportion to the real width of the field of vision, it is obvious that the number of cells on a scanning track of fixed length is a linear function of this width, provided that the cells are uniformly distributed. With this statement as a starting point, it will be shown in the sequel that the number of cells per unit area can be evaluated without any information about the effective width of the field of vision and the size of the cells: if we perform at least two scanning runs with different real widths and if no cells belonging to the scanned area are missed.

However, it is evident that a certain number of cells must be missed, as it must sometimes happen that more than one cell is inside the field of vision when the cells have settled at random from a fluid suspension. In order get a usable result, it must be possible to estimate the number of missed cells.

Improvement of the apparatus was indicated in the two following respects. First, the scanning movement must be performed wholly automatically, second, the electronic system

must be designed more in conformity with modern impulse technique used in the counting of nuclear particles. In the original apparatus, the scanning movement was performed by hand, and the electronic system had been designed with insufficient regard to the band-width of the impulses to be recorded. The construction of the new apparatus proceeded slowly, partly on account of lack of adequate workshop facilities during the first years. The apparatus began to function satisfactorily in the latter part of 1950.

5. Other works concerning photoelectric counting of individual cells. With the writer's original scanning method as a starting point, WOLFF (1950) described in a preliminary paper some improvements on the method. He suggested that the scanning procedure be performed with two values of the width of the scanned area, so that the result could be evaluated without information about the size of the cells. Neither a detailed theoretical treatment, nor complete experimental data were given.

MELLORS and SILVER (1951) described in a preliminary report a method and an apparatus for differential detection of cancer cells in preparations of exfoliated cells obtained from secretions and spread on microscope slides. The method was based on selective staining of cell nuclei with a fluorescent dyestuff. Cancer cell nuclei combine with more of this dyestuff than normal cell nuclei and consequently emit more fluorescent light than normal cell nuclei. MELLORS and SILVER made use of a rotating disk equipped with a number of apertures arranged in a spiral and also employed a moving stage. The preparation was scanned with this device in a manner like that used in early television transmitters. Those nuclei emitting more than a certain amount of light were counted by a multiplier phototube-electronic system.

In order to obtain an objective measure of the motility of spermatozoa, BOSSELAAR and SPRONK (1952) suggested an apparatus which counted sperm cells moving in and out of a limited field of vision. We note no theoretic analysis or quantitative experimental data given in either of the two last-mentioned papers.

YOUNG and ROBERTS (1951) have suggested a new principle for visualizing microscopic objects. They propose the use of the television technique of flying spot scanning by two cathode ray tube rasters locked together. A cathode ray tube providing a televizing raster of high brilliance and very short time constant is placed in front of the eyepiece of an ordinary microscope. The microscope objective produces a minute spot of light that scans the preparation to be examined. The light passing through the preparation (the amount of which is determined by the density of the specimen) is picked up by a multiplier phototube. The output of the phototube is used for intensity modulation of the second cathode ray tube, on the screen of which an image of the specimen is seen. The authors have pointed out that their method could be used also for counting purposes. It is evident that the smaller the diameter of the flying spot, the better the resolving power is. However, it seems difficult to get a sufficiently small light spot when a large area is to be scanned.

6. Individual counting of other microscopic objects than animal and plant cells. Photoelectric methods of counting individual particles of aerosols have been described by GUCKER *et al.* (1949). These methods seem to have been developed mainly for testing respirator filters of gas masks but have also been applied, for instance, to counting bacterial spores. The aerosol flows through a narrow space under intense dark field illumination, and the light impulses from the particles are recorded by a phototube-electronic system. Spherical particles down to about 0.5 microns diameter can be counted.

The counting of stellar images on a photographic plate offers problems similar to those encountered in the counting of other individual microscopic objects. MCCUSKEY and SCOTT (1941) described a device which segregated the star images according to size into four classes, by the aid of a photoelectric photometer and a recording system. However, each star image had to be manually shifted into the optical focus of the device by aid of a microscope. Although experiments had been performed to make the counting process entirely automatic, with a mechanical scanner, that problem had not

been solved up to the date when McCUSKEY and SCOTT published their paper.

In order to analyse events in nuclear emulsions, BLAU *et al.* (1950) constructed a device that recorded range, grain density, and geometrical orientation of tracks produced by particles crossing the emulsion. It was also possible to count the number of grains along a certain track. The basic element of the apparatus was a microscope and a motor-driven stage. However, the apparatus was only semi-automatic and the operator had to control the direction, speed of motion and focussing movements by visual means.

7. **Light-scattering.** Methods involving measurement of the amount of light scattered from a cell suspension have been applied to the enumeration of the number of cells per unit volume. However, the measured light intensity is dependent not only on the number of cells but also on their size. Consequently, the results must be corrected for the cell size. This difficulty seems to have been overcome recently by LOESCHCKE and WEVER (1951) who have constructed a light-scattering apparatus for estimation of the number of erythrocytes and leucocytes in blood specimens. This apparatus is manufactured by the firm of Hellige under the name 'Elektro-Haemoskop'. The theoretical basis of the method has not yet been published, but it is claimed that the determination of the number of cells is totally independent of the size of the cells.[1] Naturally, such light-scattering methods are entirely different from those based on the counting of individual cells.

8. **The aim of the present work.** Our aim is to examine the theory and practice of counting individual microscopic cells and particles by the method of scanning. The shortcomings of the original method and the improvements mentioned in § 3 and § 4 have been taken into consideration. An improved experimental apparatus will be described. The method is applied to human erythrocytes sedimented at random on an area. Various impulse shape experiments and counting experiments will be described.

[1] A comparison between results obtained by the 'Elektro-Haemoskop' and by visual counting in estimating numbers of erythrocytes has been published by MATTHES and SCHARPF (1951).

CHAPTER II.

A contribution to the theory of counting by scanning.

9. Outlines of the method. Suppose that the cell elements to be counted are distributed in a monolayer over a certain plane area. Place the area containing the cells on the stage of a microscope. The counting procedure is now effected by passing the area with the elements relative to an optical *aperture of rectangular shape* which is oriented so that one pair of its sides is parallel to (the other therefore at right angles to) the direction of movement, *i. e.*, the scanning direction. The aperture may be situated, for example, in the image plane of the microscope objective. Its relative size is to be of the same order of magnitude as the elements to be counted. Behind the aperture, a phototube is placed and connected to an electronic recording system. Assume that the elements to be counted produce a certain light intensity change in relation to their background. Now imagine that a single element or part thereof passes through the aperture area. A transient light intensity change or signal impulse is produced which is recorded if the impulse amplitude is larger than a certain threshold value. Now consider the whole sequence of elements scanned or swept by the aperture. Elements or parts thereof pass through the aperture area in succession and give rise to impulses which are recorded. The number or elements per unit area is evaluated from the number of records and the length and width of the scanned area.

10. General considerations. Before entering upon a detailed discussion, it is convenient to give a short survey of the problems to be treated.

(1) Each individual element which is situated on the track scanned by the aperture, must be able to produce a light intensity change sufficiently large to trigger the recording system.

(2) The area scanned by the aperture must be relatively free from contamination with foreign particles, because a scanning and counting apparatus makes records of a sequence of light impulses and has no ability to distinguish between different kinds of elements which produce these light impulses.

(3) In order to evaluate the number of impulse producing elements per unit area, the area in which the recorded elements are situated must be known. The length of our track is known; to find the effective width demands some consideration.

(4) Naturally, it is desirable that the apparatus should resolve and record separately all elements in the area scanned. In counting certain kinds of element distributions, such a state of affairs seems to be attainable. On the other hand, there exist element distributions in which a certain number of elements must always escape uncounted. When the impulse producing elements are distributed at random, it can be shown (as we shall in the sequel) that the fraction of missed elements can be estimated by the theory of probability and the result corrected for missed elements. In the operations leading to this correction, it will be noted that the scanning counter does not record individual elements but rather a sequence of intervals between individual elements. When the interval between two consecutive elements is smaller than a certain minimum value, the two elements are not resolved. In order to obtain the correction for missed elements, the value of this minimum interval must be computed. If the elements were distributed at random along a straight line, this problem would be rather simple. However, the elements are distributed in an area, and the minimum interval is different for different pairs of elements. We meet here partly a geometrical problem.

(5) We now sketch the statistical considerations arising in the method of counting by scanning. When the impulse producing elements are distributed at random, Poisson's law may be assumed to be approximately valid. We must therefore consider the standard deviation of a Poisson distribution; this is of course not peculiar to the scanning method. We shall further find that for every fixed number of intervals the number of

recorded intervals is a random variable whose standard deviation must be considered. Finally, the standard error due to imperfections of the apparatus, *i. e.* the apparatus error, must be taken into account.

We shall now treat the above matters in more detail.

11. Impulses from individual elements. When the element distribution consists of the cells of a diluted fluid suspension which have settled to the bottom of a counting chamber, dark field illumination appears to be highly convenient. Provided that the elements and the surrounding medium have different refractive indices and that this medium be optically homogeneous, the elements are seen as luminous objects against a dark background. Under such conditions, when one uses multiplier phototubes and suitable amplifiers, there seems to be no difficulty in getting impulses from individual microscopic objects like human erythrocytes, yeast cells or even bacteria (LAGERCRANTZ 1947).

On the other hand, it is evident that dark field illumination cannot be used when the cell nuclei of histological tissue sections, for instance the nuclei of a liver section, are to be counted by the scanning method. Under such conditions, the whole tissue area is luminous and it is very difficult to obtain separate signals from the nuclei. However, it appears possible to obtain separate and distinct light intensity changes which identify the cell nuclei of a histological tissue section by use of ordinary microscope illumination after the nuclei have been differentially stained or identified by some other method (*e. g.* ultraviolet light absorption, or fluorescent staining of the nuclei; cf. § 5).

Besides the multiplier phototube and an amplifier, the recording system should include a scaler for reducing the impulse frequency before the signal impulses are fed to the tabulator driving circuit and the mechanical tabulator. The scaler should be driven by standard impulses delivered by an amplitude discriminator which is triggered by the signal impulses from the phototube-amplifier. Thus, the electronic recording system of the scanning counter should be rather like a counter of nuclear particles (a scintillation counter in particular).

12. **The area scanned by the aperture.** Assume that the elements to be counted are all separated from each other at least by a certain minimum distance. Under such circumstances, the dimensions of the scanning aperture can be made so that no impulse producing elements are missed. We have such a distribution when the elements to be counted consist of differentially stained cell nuclei surrounded by an unstained, or faintly stained, cytoplasma layer. Let us further assume that the impulse producing elements are of a circular or elliptical shape.

The length, L, of the scanning track is easily measured mechanically. The width, w, of the scanning track is calculated as follows.

(1) Consider an individual element belonging to the sequence to be counted. In order to record the element, it is necessary that a certain minimum part of it come within the area of the aperture.

(2) If the element is able to produce a fairly large change of light intensity, or if the amplification is high, only a minor part of the impulse producing element needs to pass through the aperture area. On the other hand, if the change is small or the amplification rather low, a major part of the impulse producing element must pass through the aperture area.

(3) We may now define the quantity z as the distance between the aperture boundary and the centre of the impulse producing element when the part of this element passing through the aperture area is just large enough to give rise to a threshold signal. From the above discussion, it will be seen that z is a function of the light intensity of the microscope lamp, of the amplifier gain, and of the bias setting of the amplitude discriminator. Further, it is evident that z is also a function of the change in light intensity produced by the unit area of the impulse producing element. Finally, z depends upon the geometric shape of the element, *i. e.*, the diameter when the element is of a circular shape. If $\bar{z}$ is defined as the average value of the z values for the element distribution in question, we may consider those elements as counted whose centres are

situated inside the width $a+2\,\bar{z}$, where a is the width of the aperture at right angles to the scanning direction. The scanning width w is thus defined as $a+2\,\bar{z}$. Consequently, the area scanned by the aperture, *i. e.*, the area of the scanning track, is equal to $(a+2\,\bar{z})\,L$.

13. Evaluation of the number of elements per unit area (no elements missed). We now set down the following equation:

$$N = u\,(a+2\,\bar{z})\,L\,, \tag{1}$$

where u means the number of elements per unit area, N the number of elements on the scanning track of length L and width $a+2\,\bar{z}$. When the same distribution of elements is scanned with different aperture widths a, it is seen from equation (1) that N is a linear function of a, if $\bar{z}$ remains unchanged during the different scanning runs (L is constant). Under such conditions, the slope of the straight line (1) is directly proportional to u, the number of impulse producing elements per unit area. Equation (1) contains two unknown quantities, u and $\bar{z}$. Consequently, two equations are necessary to evaluate u, *i. e.*, the scanning procedure must be performed at least twice, once with aperture width a_1, and once with aperture width a_2 $(a_1 \neq a_2)$. The following equations are obtained:

$$N_1 = u\,(a_1+2\,\bar{z})\,L\,, \tag{2}$$

$$N_2 = u\,(a_2+2\,\bar{z})\,L\,, \tag{3}$$

and

$$u = \frac{N_1 - N_2}{a_1 - a_2} \cdot \frac{1}{L}\,. \tag{4}$$

The quantity $\bar{z}$ has thus been eliminated. Moreover, u can be estimated without knowing the size of the impulse producing elements and without standardizing the light intensity of the microscope lamp or the phototube and amplifier gain, provided that these remain unchanged during the two scanning runs corresponding to the apertures a_1 and a_2. Naturally, all other

factors which might possibly influence $\bar{z}$ must also be held constant. In this connection, it may be pointed out that when discussing a constant value for $\bar{z}$, we do not consider random variations of $\bar{z}$ unless specially mentioned. (See further §§ 15 and 16).

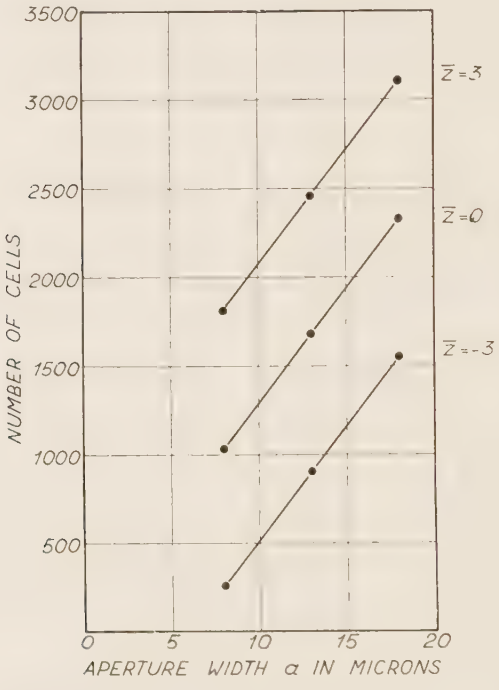

Fig. 1. Theoretical diagram where the number of recorded elements N, when no elements are missed, is plotted as a function of the aperture width at right angles to the scanning direction a, according to equation (1). The functions for three different $\bar{z}$ values are given. In order to faciliate a comparison with experimental diagrams given below, the parameters of the hypothetical functions given in the figure, are taken nearly equal to those of the experiments. Thus the scanning length L, is set to 647 mm. and the number of elements per square mm. is 200. $\bar{z}$ values are given in microns.

From equation (1), it is evident that a number of mutually parallel lines, *i. e.*, lines with the same u value, can be obtained by performing the scanning procedure with different light intensities, amplifications, or other factors which influence $\bar{z}$. A number of these relations are shown in Fig. 1.

14. Counting to a predetermined number of elements (no elements missed). Another way to perform the scanning procedure is to stop the scanning movement after a predetermined number of elements have been recorded. We then read the scanning length, L. In analogy with equation (1) of § 13, we have:

$$u\,(a+2\,\bar{z}) = \frac{N}{L}\,. \tag{5}$$

If the length L_1 is scanned with an aperture of width a_1 and the length L_2 with a_2 in order to record N elements, we find:

$$u\,(a_1 - a_2) = \frac{N}{L_1} - \frac{N}{L_2}, \tag{6}$$

$$u = \left\{\frac{1}{L_1} - \frac{1}{L_2}\right\} \cdot \frac{N}{a_1 - a_2}\,. \tag{7}$$

15. The sensitivity of the scanning apparatus. $\bar{z}$ was defined in § 12, where a number of variables which influence the magnitude of $\bar{z}$ were also mentioned. From this discussion, it is apparent that when we deal with a fixed distribution of elements, $\bar{z}$ becomes a measure of the sensitivity of the apparatus. Let us now consider other details concerning z and $\bar{z}$. When the impulse producing element has a circular shape and when its radius is r, z can assume any value between $+r$ and $-r$.

(1) $z = +r$ means that the impulse producing element needs only to touch the border of the aperture in order to produce a threshold signal. Such a state of affairs is not attainable in practice.

(2) $0 < z < r$ means that a certain part (less than half) of the impulse producing element must pass through the aperture area.

(3) $z = 0$ means that half of the impulse producing element must be inside the aperture area.

(4) $-r < z < 0$ means that more than half of the impulse producing element must be inside the aperture area.

(5) Finally, $z = -r$ means that the whole impulse producing element must be inside the aperture area in order to produce a signal which is recorded. The relations just discussed are schematically shown in Fig. 2.

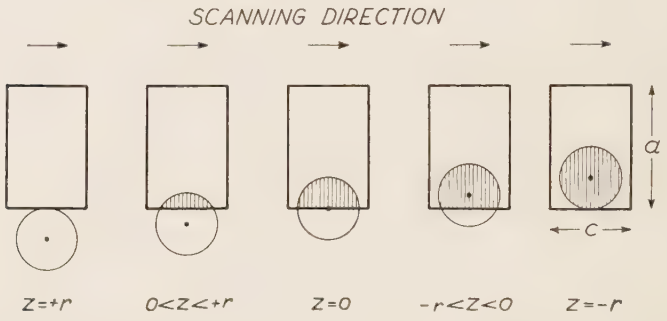

Fig. 2. z is defined as the distance between the centre of an impulse producing element and the aperture border when the element area passing inside the aperture area is just large enough to trigger the recording system. The spatial relations between a rectangular scanning aperture and a circular element are shown for several different z values, *i. e.*, different sensitivity levels of the recording system. Element area inside the aperture are shown hatched in the figure.

It is evident that the amplitude of the average threshold signal decreases as $\bar{z}$ increases and vice versa. This means that the dynamic range, *i. e.*, the ratio between the largest and smallest signals which are recorded, is a function of $\bar{z}$. Consequently, a low value of $\bar{z}$ corresponds to a relatively low dynamic range and vice versa. When $\bar{z} \to +\bar{r}$ (the mean radius of the elements), the dynamic range $\to \infty$; when $\bar{z} \to -\bar{r}$, the dynamic range $\to 1$.

16. Factors which may produce variations in the sensitivity of the apparatus. (1) In order to hold $\bar{z}$ constant during the two scanning runs, it is obviously necessary that the light intensity of the microscope lamp and the electronic recording system be reasonably stable.

(2) It is necessary that the scanning movement be performed so that the image sharpness remains unchanged during the scanning procedures. (See further § 33.)

(3) Background light: dark field illumination. The presence of diffuse background light introduces noise impulses due to the shot effect, *i. e.*, random fluctuation of the phototube current about a mean value. The shot noise is uniformly distributed over the whole transmitted frequency band. These noise impulses are always present and are superimposed upon the signal impulses. Naturally, the amount of noise is dependent on the area of the aperture. When the two scanning runs are performed with apertures of different areas, *i. e.*, $a_1 \cdot c$ and $a_2 \cdot c$, $(a_1 \neq a_2)$, c is the length of the aperture in the scanning direction, and when there is a certain amount of background light, it is evident that $\bar{z}$ cannot have the same value for the two apertures, because more noise is superimposed upon the signal impulses produced with the larger aperture than on those produced by the smaller one. Consequently, the recording system is triggered by relatively smaller element areas when the larger of the two apertures is used, and the $\bar{z}$ value is larger here than the $\bar{z}$ value corresponding to the smaller aperture. Accordingly, we find that either the background light should be kept as low as possible, or apertures of constant area should be used: *i. e.*, $a_1 \cdot c_1 = a_2 \cdot c_2$.

(4) Background light: ordinary transmitted illumination. When ordinary transmitted illumination is used, signal impulses are produced when light absorbing elements diminish the light intensity transmitted through the aperture. It is obvious that the amplitude of the signal impulses is wholly dependent upon the difference between the area of the aperture and the area of the element inside the aperture. Consequently, it is necessary to use apertures of constant area in order to obtain a constant $\bar{z}$ value for the two scanning runs.

(5) Effect of too small an aperture. Suppose the two scanning runs are performed with apertures of the dimensions $a_1 \cdot c_1$ and $a_2 \cdot c_2$. Let us further assume that the $\bar{z}$ values corresponding to the scanning runs are $\bar{z}_1$ and $\bar{z}_2$. It is evident that $\bar{z}_1 - \bar{z}_2 = 0$,

if the apparatus functions according to the specification just discussed. However, this statement is only valid when the smaller of the two apertures is not too small. Assume, for example, that $c_1 > 2\,\bar{r} > c_2$ and $\bar{z}_1 \approx 0$. In order to produce the same threshold signal, it is now evident that the centre of a certain element must be situated closer to the middle of the aperture when scanned by the aperture $a_2 \cdot c_2$ than when scanned with aperture $a_1 \cdot c_1$, and consequently $\bar{z}_1 - \bar{z}_2 \neq 0$. A similar relation is also found when $a_1 > \bar{r} - \bar{z}_1 > a_2$.

17. **Correction for missed elements. General considerations.** In order to resolve and record *all* elements lying on the scanning track, each element must be isolated enough, so that the moving aperture assumes positions both in front of and behind each individual element where the signal amplitude is smaller than the threshold level of the amplitude discriminator. Furthermore, it is necessary that the signal amplitude between two consecutive elements remain below the threshold level, at least during the time necessary for the electronic system to recover. Consequently, when the interval between two consecutive elements is equal to or less than a certain minimum value, denoted by the symbol l, the elements are not resolved. Therefore, a certain number of elements are unavoidably missed. It may be pointed out here that the recovery time of the recording system, τ, is very much smaller than the time needed for the aperture to travel the distance l relative to the elements, under the scanning velocities used in this work. Therefore τ has been neglected in the following discussion. If τ could not be neglected, it is obvious that the values of l should be increased by the distance which the object moves relative to the aperture during the time τ, *i. e.*, $\tau \cdot V$, where V is the scanning velocity.

It was pointed out in § 10 that the number of missed impulse producing elements can be derived theoretically when the element distribution has arisen from random settling of elements suspended in a sufficiently diluted fluid suspension, and that the result, *i. e.*, the number of elements per unit area, can be corrected in this case. We mention in passing that the element concentration in the counting experiments to be descri-

bed below was chosen so sparse that in average only one element was present on the scanning track for every twenty or more aperture lengths in the scanning direction. However, there exist distributions of microscopic cells and other particles such that the individual impulse producing elements are closely packed or clustered together in the whole distribution, or perhaps only in certain parts of the distribution. The elements of such a distribution are obviously impossible to count by the scanning method. In fact, such element distributions are sometimes extremely difficult to count visually. Whether or not a certain kind of elements can be satisfactorily counted by the scanning method can only be determined after careful consideration of the particular case at hand.

18. **Element centres distributed along a straight line.** Let us first assume that the centres of all elements to be counted are situated at random along a narrow strip of length L. Let us further idealize this case and assume that the centres of these elements are situated on a straight line of length L. (We use the symbol L to denote the line itself as well as its length). Assume that the rectangular aperture moves along the line and is symmetrically oriented with respect to it.

19. **Elements missed.** When the interval in the scanning direction between two consecutive elements is less than or equal to the constant critical minimum value l necessary for fulfilling the conditions mentioned in § 17, only one count is recorded and one element is therefore missed. Generally, it may be stated that n—1 out of n elements are missed if these n elements all have mutual distances in the scanning direction less than or equal to the critical value l. It is thus evident that an apparatus with the properties under consideration does not record individual elements, but rather intervals between elements, and then only the intervals larger than the critical distance l. Let us assume that the whole cell area (and not merely a part of it) is the impulse producing element. Under such conditions, there is always a certain probability that the interval between two consecutive element centres is equal to or less than the critical minimum distance l necessary for

resolving the elements, since the aperture length in the scanning direction cannot be made smaller than a certain positive number. Consequently, a certain number of elements are bound to be missed, and equations (1)—(8) are not valid unless the number of recorded elements is first corrected for missed elements.

20. The probability of encountering intervals of length $> l$. It is evident that the probability of encountering intervals of length $> l$ can be obtained from Poisson's formula; but for the sake of completeness, this probability will be computed here.

Assume that no elements are situated on L. Now place an element centre at random on L. The probability P (0, 1) that this element centre is not situated on a given segment of length l arbitrarily situated on L, is

$$P(0,1) = 1 - \frac{l}{L}. \tag{8}$$

More element centres in succession are placed at random on L, so that the total number of element centres is $N+1$ (N intervals). The probability, P(0, $N+1$) that no element centres are situated on l is

$$P(0, N+1) = \left(1 - \frac{l}{L}\right)^{N+1}. \tag{9}$$

Let the average number of element centres per unit length be equal to $u = \frac{N+1}{L}$. Equation (9) can then be written as

$$P(0, N+1) = \left(1 - \frac{u \cdot l}{N+1}\right)^{N+1}. \tag{10}$$

When l is very much smaller than L, equation (10) can be replaced by the following good approximation:

$$P(0, N+1) = e^{-u\,l}. \tag{11}$$

$u \cdot l$ is the number of elements on a segment of length l. Thus the probability that the distance between the centres of two

consecutive elements is $> l$ is equal to $e^{-u\,l}$, and the probability that this distance is $\leq l$ is equal to $1-e^{-u\,l}$.

21. **The mean and standard deviation of the recorded intervals in the linear case.** Consider a sequence of N consecutive intervals. Only those intervals of length $> l$ are recorded. Let the number of recorded intervals be equal to N'. It is evident that N' is a random variable.[1] Let us now calculate the mean value and standard deviation of N'. In order to make this calculation easier, a random variable x_i is assigned to each one of the N intervals Δ_i, i $1, 2, 3, \ldots, N$. This variable is defined as follows: $x_i = 1$ if $\Delta_i > l$; $x_i = 0$ if $\Delta_i \leq l$. Obviously,

$$N' = \sum_{1}^{N} x_i \tag{12}$$

Equation (12) means that N' is the sum of N independent random variables. All of the x_i have the same distribution function $F(t)$:

$$F(t) = P(x_i \leq t). \tag{13}$$

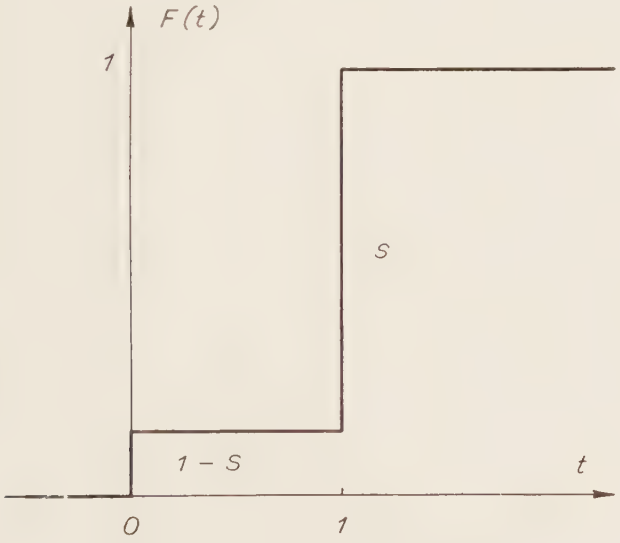

Fig. 3. The distribution function.

[1] For the following discussion of the mean and standard deviation of N', see for instance CRAMÉR, *Sannolikhetskalkylen*, 1949 and ARLEY and BUCH, *Sandsynlighetsregning*, 1943.

We write $e^{-u\,l}$ as s. The probability of intervals $\leq l$ is thus $1-s$. The distribution function is sketched in Fig. 3.

The mean value of x_i, $m(x_i)$, is

$$m(x_i) = \int_{-\infty}^{+\infty} t\, d\, F(t) = 0 \cdot (1-s) + 1 \cdot s = s, \tag{14}$$

and the square of the standard deviation is

$$\sigma^2(x_i) = \int_{-\infty}^{+\infty} (t-s)^2\, d\, F(t) = (0-s)^2 \cdot (1-s) + (1-s)^2 \cdot s = \tag{15}$$

$$= s^2(1-s) + (1-s)^2\, s = s(1-s).$$

According to rules valid for independent random variables, we obtain at once the mean value and standard deviation of N':

$$m(N') = m\left(\sum_1^N x_i\right) = \sum_1^N m(x_i) = N \cdot s = N \cdot e^{-u\,l}, \tag{16}$$

and thus

$$m(N') = N e^{-u\,l} \approx N(1-u\,l)^1, \tag{17}$$

$$\sigma^2(N') = \sigma^2\left(\sum_1^N x_i\right) = \sum_1^N \sigma^2(x_i) = N \cdot s(1-s) = \tag{18}$$

$$= N e^{-u\,l}(1-e^{-u\,l}) \approx N\,u\,l,$$

and $\sigma(N') = \sqrt{N} \cdot \sqrt{u\,l}$.

22. **Analogy with the counting of nuclear particles.** Equation (11) is analogous to the 'Interval Law' derived by MARSDEN and BARRAT (1911) for evaluating the true number of particles when ß-rays are counted. The probability that the time interval

[1] As is well known, the error (or more exactly: the correction) is approximately $\frac{\alpha^2}{2}$, when we set $e^{-\alpha} \approx 1-\alpha$ and α is a relatively small number. Thus, when $\alpha = \frac{1}{10}$, the error is 0.5 per cent. For the sake of simplicity, we often use this approximation in the sequel.

between the appearance of two successive ß-rays is longer than τ is:

(19) $$P(\tau, \infty) = e^{-N\tau},$$

where N is the average number of ß-rays expected to occur per unit time. Similarly, equation (17) is analogous to the expression

(20) $$n = N \cdot e^{-N\tau}$$

where n is the observed number of ß-rays. Furthermore, it is evident that the scanning counter is analogous to a ß-ray

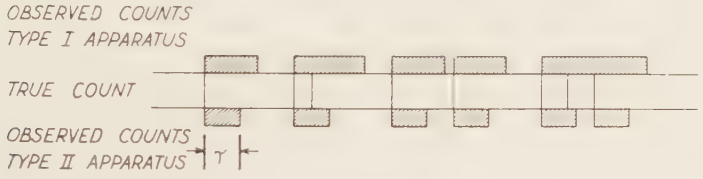

Fig. 4. Schematic illustration of the behaviour of nuclear radiation counting systems, having a resolving time τ. Time axis is from left to right. True counts occur at the times shown by vertical lines along the centre section. The responses of two different types of apparatus are shown. The number of observed counts and the time during which the apparatuses are insensitive are shown by shaded blocks. An apparatus of Type I responds only to intervals longer than τ. An apparatus of Type II is insensitive for a time τ after one impulse, but then can respond again even if the intervals between consecutive true counts is less than τ, as illustrated by the triplet on the right. In the hypothetical example shown there are 8 counts, of which 6 are recorded by a Type II apparatus, and only 5 are recorded by a Type I apparatus. The scanning counter is analogous to that used in the Type I apparatus. (From EVANS, in *Advances in Biological and Medical Physics*, ed. by LAWRENCE and HAMILTON).

counter where, for example, a quenching circuit of relaxation time τ is connected to a self quenching counter whose dead time is greater than τ. Then any β-rays occurring during the recovery time of the counter will cause new discharges and will prevent the quenching circuit from recovering, *i. e.*, n—1 particles are missed when the time between successive particles is smaller than the recovery time of the selfquenching counter (see LAWRENCE and HAMILTON, *Advances in Biological and Medical Physics*, Vol. I). See also Fig. 4.

23. **Element centres distributed over an area. General considerations.** Let us now leave the one-dimensional case and consider the situation that we actually face, *i. e.*, the case in which elements are distributed at random over a two-dimensional plane region. Suppose that such an element distribution is scanned by an aperture of width a. The elements of the distribution are divided into two classes, A and B. Class A consists of those elements which lie wholly or partly within the strip of length L and width a; class B consists of those

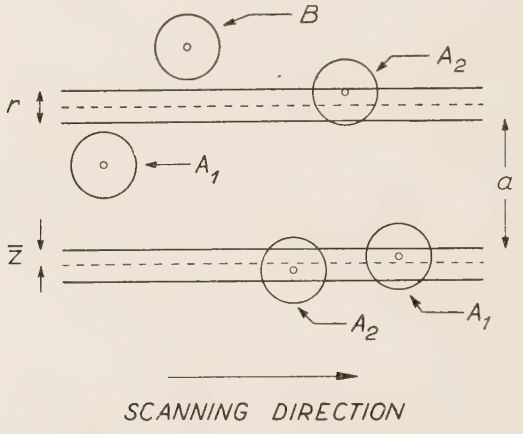

Fig. 5. Schematic diagram which shows the division into class A_1, A_2 and B elements. The centre of each element is marked by a point.

elements which lie wholly outside this strip. It is obvious that elements of class B can have no influence on the recording procedure.[1] Now divide the elements of class A into two subclasses, A_1 and A_2. These subclasses are defined as follows. An element belongs to class A_1 if its area inside $a \cdot L$ is alone large enough to trigger the recording system. Class A_2 contains the remaining elements of class A, *i. e.*, those elements which have a part of their area inside the track scanned by the aperture but which are not able individually to trigger the recording system. (See Fig. 5.)

[1] When using dark field illumination, it is sometimes possible that class B elements close to the strip $a \cdot L$ may spread diffuse light inside this area.

24. **The critical minimum distance.** Imagine that there are only two impulse producing elements on the scanning track and that these belong to class A_1. Let the aperture sweep over these elements. Let us assume that we record continuously the signal amplitude. Suppose first that the interval in the scanning direction between the element centres is relatively large. The signal then consists of two symmetrical impulses with a rising limb, a 'top' or maximum, and a descending limb (see further chapter V and Figs. 22—27). The impulses are separated by an interval in which the signal amplitude is zero. Two separate impulses are recorded by the apparatus. Now assume that the interval between the element centres is decreased by moving one of the elements in the scanning direction and that the aperture repeatedly sweeps over the elements. It is evident that the space between the impulses decreases; and when the element centres are still closer, the two impulses are no longer wholly separated from each other. The signal amplitude between the two 'tops' or maxima still has a discernible minimum value. (See Fig. 27.) The critical minimum interval, l, will now be defined as the interval between the two element centres when the signal-amplitude minimum between the two impulse maxima is equal to the triggering level of the recording system. It is evident that l is a function, among other things, of the length c of the aperture in the scanning direction and of the sensitivity of the recording system, *i. e.*, of $\bar{z}$.

We next assume that the change of light intensity produced by the unit area of the impulse producing element has a constant value for the whole impulse producing element. Under these conditions, the sum of the two element areas inside the aperture and the signal amplitude have their minimum values at the same time. The minimum occurs at the position where the aperture borders perpendicular to the scanning direction intercept the element areas so that the chords are of equal length, b. This fact is clearly seen when we move the aperture a very small distance Δx in the scanning direction, at first in one, then in the opposite direction. The net gain in area inside the aperture is $b_1 \cdot \Delta x - b_2 \cdot \Delta x$, which is 0 only when $b_1 = b_2$. Of course, the minimum sum of the element areas inside the aperture is equal to the area inside the aperture

of one element the centre of which is situated at a distance z from the aperture border, according to the definition of z (cf. § 12). See Fig. 6.

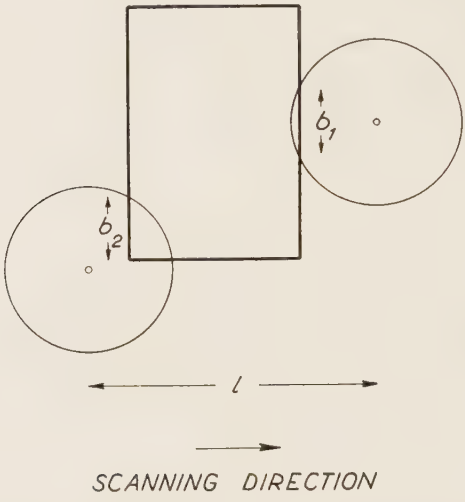

Fig. 6. For given values of the critical minimum distance l, the sum of the element areas inside the aperture has its minimum value when the chords b_1 and b_2 are equal.

Now consider a pair of circular elements whose centres are situated on the same straight line in the scanning direction. The centres of this element pair are assumed to be situated at the critical minimum distance l. Suppose first that the element pair passes wholly inside the aperture; l has now a certain value l_1. Then let the element pair pass to the side of the aperture so that only a part of the areas of the elements move through the aperture; l has now a certain value l_2. It is evident that the elements can be situated closer to each other in the latter case without the minimum of the sum of the element areas inside the aperture exceeding the trigger level of the recording system. This means that $l_2 < l_1$. For elements whose centres are situated on the same line in the scanning direction, l has a constant maximum value when the elements pass wholly inside the aperture, but smaller values when the elements pass through the aperture to the side so that only a

certain part of the element area passes through the aperture. See Fig. 7.

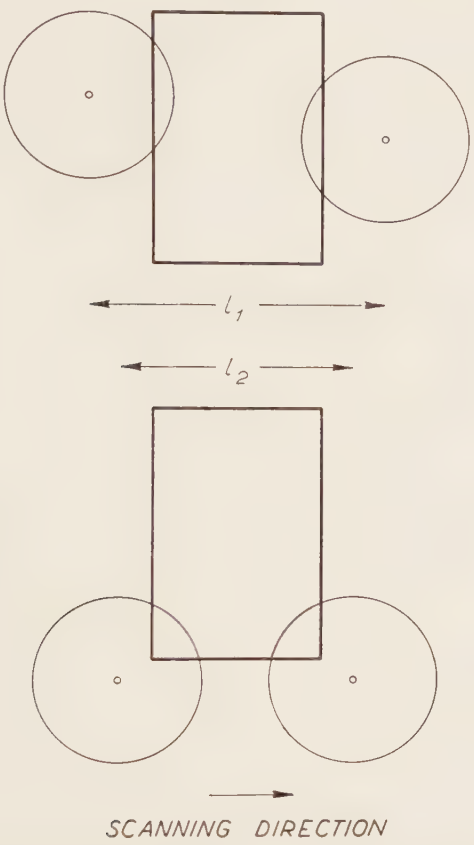

Fig. 7. When the interval between two consecutive element centres is larger than the critical minimum interval l, this interval is recorded. l depends among other things on the minimum value of the sum of the element areas which passes inside the aperture. Fig. 7. illustrates that for a given recording sensitivity of the apparatus, l is smaller when only a certain part of the elements passes inside the aperture, *i. e.*, the element centres can be situated closer together without the minimum sum being reached.

For the elements whose centres are not situated on the same line, parallel to L, it is still true that l has its maximum value when the elements are situated in the central part of the track. The number l becomes smaller when one or both elements of the pair are lying partly outside the track.

25. **The mean and standard deviation of recorded intervals when the elements are situated in a plane area.** Suppose first that we have only elements of class A_1. (The disturbing effect of class A_2 elements will be estimated below, in § 27.) Suppose that there are $N+1$ consecutive elements of class A_1 on the scanning track. Consider the N intervals Δ_i, $i = 1, 2, 3, \ldots, N$ between the element centres, measured in the scanning direction. Suppose also that the elements A_1 are divided into n groups, $Q_1, Q_2, \ldots, Q_n$, by equidistant lines parallel to the scanning direction, the position of the centre of an element

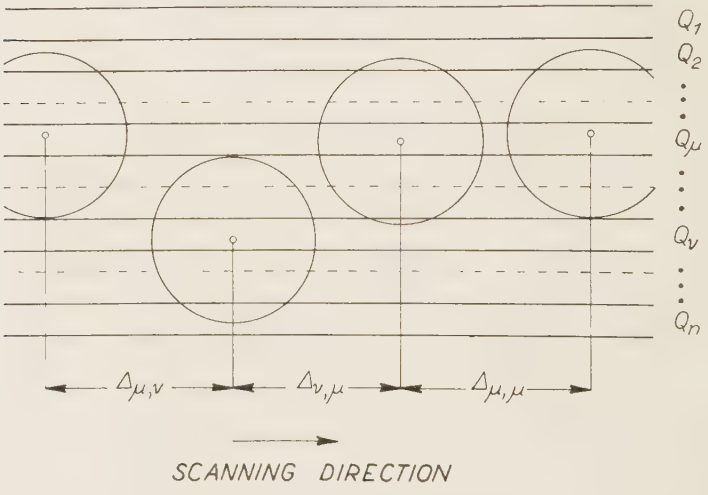

Fig. 8. A scanning track of width $a + 2\bar{z}$ is divided in n parts by equidistant lines parallel to the scanning direction. By this means, the elements on the scanning track are divided into n groups. Intervals of different types can now be combined from consecutive elements.

determining its group. By combination of elements from the n different groups into sets of two, it is evident that we can obtain $\frac{n(n+1)}{2}$ different sets. An element of class Q_μ can be combined with elements of n—1 classes $Q_\mu \neq Q_\nu$. Thus, there are $n \cdot (n-1)$ combinations between elements belonging to different classes Q_μ. We say an interval Δ_i between two elements Q_μ and Q_ν is of the type $\Delta_{\mu,\nu}$, see Fig. 8. An interval $\Delta_{\mu,\nu}$ is equivalent to an interval $\Delta_{\nu,\mu}$, because it is immaterial if the scanning movement is performed from the left to the right or vice

versa. Consequently, we have $\frac{n(n-1)}{2}$ interval groups $\Delta_{\mu,\nu}$ with $\mu \neq \nu$. Finally, there are n interval groups produced by combination of elements belonging to the same group Q_μ, *i.e.* intervals of type $\Delta_{\mu,\mu}$. In all, there are $\frac{n(n-1)}{2} + n = \frac{n(n+1)}{2}$ interval groups, and consequently also the same number of critical minimum distances, not all mutually equal. This is valid when all elements are of circular shape and have the same diameter.

When the elements are of different size and form, elliptical, for instance, it is possible to introduce an additional classification in order to describe the different critical minimum distances which may exist.

All intervals of the $\frac{n(n+1)}{2}$ groups are distributed so that the probability of obtaining an arbitrary interval with length $> l$ is equal to $e^{-u_1 l}$ where u_1 denotes the average number of elements per unit length of the track. In particular, the probability of obtaining an interval of type $l_{\mu,\nu}$ with length $> l_{\mu,\nu}$ is $e^{-u_1 l_{\mu,\nu}}$.

Consider again N consecutive intervals and introduce N random variables x_i, as in the treatment of the linear case (§ 21). If x_i refers to an interval of type $\Delta_{\mu,\nu}$, we define $x_i = 1$ when $\Delta_{\mu,\nu} > l_{\mu,\nu}$ and $x_i = 0$ when $\Delta_{\mu,\nu} \leq l_{\mu,\nu}$. The recorded number N' is equal to $\sum_1^N x_i$. Since we may assume that there are, on the average, an equal number of intervals belonging to each of the $\frac{n(n+1)}{2}$ interval groups, we find that the mean value of N', *i. e.*, of the recorded number of intervals is

$$(22) \quad m(N') = \sum_{i=1}^{N} m(x_i) = \sum_{i=1}^{N} e^{-u_1 l_{\mu,\nu}} \approx \sum_{i=1}^{N} (1 - u_1 l_{\mu,\nu}) = N(1 - u_1 \bar{l}_{\mu,\nu}).$$

This implies that $m(N') \approx N e^{-u_1 \bar{l}_{\mu,\nu}}$, where $\bar{l}_{\mu,\nu}$ denotes the arithmetic mean of all $l_{\mu,\nu}$ intervals which actually occur.

The square of the standard deviation is obtained exactly as the linear case:

$$(23)\qquad \sigma^2(N') = \sum_{i=1}^{N} \sigma^2(x_i) = \sum_{i=1}^{N} e^{-u_1 l_{\mu,\nu}}(1 - e^{-u_1 l_{\mu,\nu}}) \approx$$

$$\approx \sum_{i=1}^{N} (1 - e^{-u_1 l_{\mu,\nu}}) \approx \sum_{i=1}^{N} u_1 l_{\mu,\nu} = N u_1 \bar{l}_{\mu,\nu}.$$

After we have made one determination of N', this value is the best estimate of $m(N')$ that we can obtain. Consequently, when performing numerical evaluation we find that equation (22) assumes the following form:

$$(22')\qquad N' \approx N e^{-u_1 \bar{l}_{\mu,\nu}}.$$

In the same manner, equation (23) becomes

$$(23')\qquad \sigma(N') \approx \sqrt{N} \cdot \sqrt{u_1 \bar{l}_{\mu,\nu}}.$$

26. Diminishing the number of missed elements. From equation (22′), it follows that the percentage of missed elements in a certain scanning run is equal to

$$(24)\qquad \frac{N - N'}{N} \cdot 100 \approx u_1 \bar{l}_{\mu,\nu} \cdot 100.$$

Thus, in order to diminish the number of missed elements, the expression $u_1 l_{\mu,\nu}$ has to be made small. When we are able to vary the concentration of the elements in the fluid suspension from which they have settled, it is possible to make u_1 relatively small. Furthermore, $u_1 \bar{l}_{\mu,\nu}$ is decreased by the use of a small aperture and relatively low sensitivity of the apparatus, *i. e.*, a small $\bar{z}$ value. Sometimes it may be possible to diminish the number of missed elements to such an extent that the correction can be entirely neglected.

27. The effect of class A_2 elements. According to the definition in § 23, an element is said to be of class A_2 if it has a certain part of its area inside the region $a \cdot L$ but is unable individually to trigger the recording system. The ratio of the number of class A_2 elements, denoted by $N(A_2)$, to the total

number of class A elements, denoted by $N(A_1 + A_2)$, can be written:

$$\frac{N(A_2)}{N(A_1 + A_2)} = \frac{2(\bar{r} - \bar{z})}{a + 2\bar{r}}. \tag{25}$$

Consequently, it is evident that class A_2 elements increase in number when the sensitivity of the apparatus is made relatively low.
Elements of class A_2 can disturb the recording procedure in the following ways.

(1) By giving rise to spurious signals. A group of two or more class A_2 elements situated sufficiently close to each other may be able to trigger the recording system. It is evident that the probability $P(A_2, A_2)$ that two class A_2 elements should be situated at a distance equal to or less than the aperture length is

$$P(A_2, A_2) = 1 - e^{-2u(\bar{r} - \bar{z})c} \approx 2u\{\bar{r} - \bar{z}\}c, \tag{26}$$

where u is the average number of elements per unit area. We describe a numerical example. Let u be = 200 elements per square mm., $\bar{r} = 0.004$ mm., $\bar{z} = 0$ and $c = 0.010$ mm. Under these conditions, equation (25) gives about 44 per cent class A_2 elements and $P(A_2, A_2)$ is about 1.6 per cent (equation (26)), *i. e.*, 1.6 per cent of all intervals between consecutive elements belonging to class A_2 are equal to or less than c.

However, the number of elements per unit area is evaluated by subtraction (equation (4)) so that the effect of these signals is approximately eliminated. More accurately, the difference is a random variable with mean value = 0 and with a relatively small standard deviation. From equation (26) it is obvious that the probability is equal for two apertures only if they are of equal length c. Thus, if we use apertures of constant area with $c_1 \neq c_2$, cf. § 16, an estimation must be done.

(2) By quenching records. When the distance between the element centres of two consecutive class A_1 elements is approximately equal to or somewhat larger than the critical minimum interval, the presence of a class A_2 element may prevent the

resolution of class A_1 elements. However, this requires that at least three consecutive elements on the track be mutually situated in a distance $\leq l$, and in addition, the three elements must be very specially arranged. The probability of such an event is found to be relatively small and can be neglected when we use the method for counting relatively sparse distributions.

28. **Evaluation of the number of elements per unit area.** As stated in § 13, we perform at least two scanning runs with different aperture widths a on the same material. In order to avoid unnecessary random variation, it is found convenient to perform the scanning procedure so that track no. 2 is situated inside track no. 1. (See further §31.)

Let u denote the average number of elements per unit area. Accordingly,

$$u_1 = u\,\{a + 2\,\bar{z}\} \tag{27}$$

and equation (22′) can be written

$$N \approx N'\,\{1 + u_1\,\overline{l}_{\mu,\nu}\} = N'\,\{1 + u\,(a + 2\,\bar{z})\,\overline{l}_{\mu,\nu}\}\,. \tag{28}$$

Now let us evaluate the expression $(a + 2\,\bar{z})\,\overline{l}_{\mu,\nu}$. Under the conditions given, this is largely a geometrical problem; by taking some trouble, it is possible to obtain an arbitrarily good approximation. In order to faciliate the numerical treatment we consider the element distribution to consist of circles of the same (mean) size. Further we set

$$l_{\mu,\nu} \approx \frac{l_\mu + l_\nu}{2}\,, \tag{29}$$

where $l_\mu = l_{\mu,\mu}$ and $l_\nu = l_{\nu,\nu}$. This estimate is exact or good, except when one of the elements is situated close to the boundary of the track. Under the last-mentioned condition, equation (29) gives a value somewhat too large. The effect of this error is diminished by the subtraction which is carried out later in the calculations (see equation (38)).

The expression $(a + 2\,\bar{z})\,\overline{l}_{\mu,\nu}$ can now be written $(a + 2\,\bar{z})\,l_\mu$. It is the area of the region covered by the effective aperture area, two sides of which are straight lines parallel to each

other and to the scanning direction. The two remaining sides consist of the curves $f(z) = \pm \frac{l_\mu}{2}$. Here z is a coordinate perpendicular to the scanning direction. See Fig. 9.

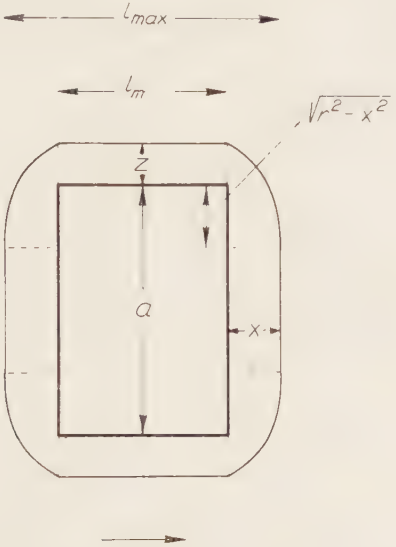

Fig 9. The effective aperture area.

29. Evaluation of the effective aperture area. The expression for the effective aperture area can be written as

$$(a + 2\bar{z})\,\overline{l}_\mu = \int l(z)\,dz. \tag{30}$$

The integral is extended over the interval of length $a + 2\bar{z}$ on which the l-function is defined. In order to evaluate this integral, Simpson's one-third rule for approximate integration (see MARGENAU and MURPHY, *The Mathematics of Physics and Chemistry*) seems to be convenient. For this operation, at least three functional values are needed; and in the actual case, these would be the maximum of l_μ, *i. e.*, l_{max}, and the two equal values $l_1 = l_n$ at the sides of the effective aperture area, *i. e.*, l_{min}. Now let us find l_{max} and l_{min}.

(1) The maximum value of l_μ. We can write

$$l_{\max} = c + 2\bar{x}. \tag{31}$$

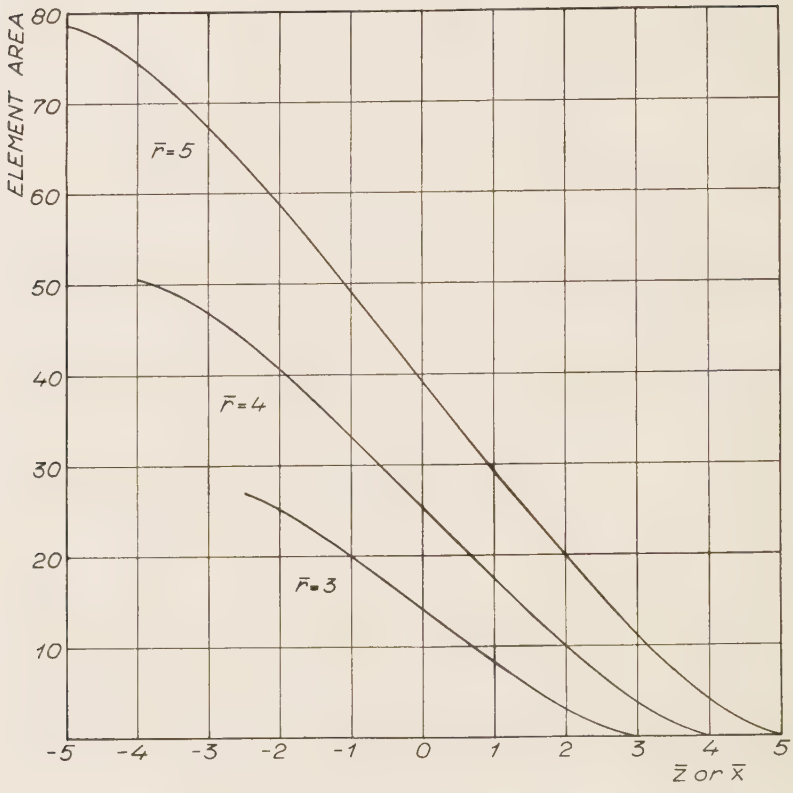

Fig. 10. The area of an impulse producing element of circular shape which passes inside the area of the scanning aperture is plotted as a function of the distance, z or x, between the element centre and the aperture border. The area inside the aperture is evaluated by use of the following formula: Area of a circle segment $= r^2 \cdot \arccos\frac{x}{r} - x\sqrt{r^2 - x^2}$. Area is given in square microns and for three different radii of the element i. e., 5, 4 and 3 microns.

The value of $\bar{x}$ can be determined graphically, as follows. In Fig. 10, the area inside the aperture is plotted as a function of $\bar{z}$ or $\bar{x}$ when the elements have a circular form. To determine $\bar{x}$, find the area inside the aperture which corresponds to the actual $\bar{z}$ value. Then find the abscissa corresponding to half of this area. This abscissa is $\bar{x}$.

(2) l_{min} is found as follows. Consider two consecutive elements both situated so that the area of each element passing inside the aperture is individually just able to trigger the recording system; *i. e.*, the centres of both elements are at the distance z from the aperture boundary. Assume that the interval between the element centres is equal to the critical minimum value. Under these conditions, it will be found

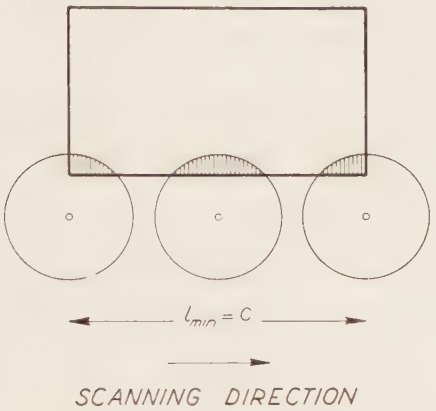

Fig. 11. The minimum value of the critical minimum interval l is equal to c the aperture length in the scanning direction. The sum of the areas inside the aperture of the two outer elements is equal to the area inside the aperture of the middle element, whose centre is situated at the distance z from the aperture broder.

that this interval is equal to c, *i. e.*, to the length of the aperture in the scanning direction, because the sum of the areas of both elements inside the aperture is a minimum at this position and is equal to the largest area of one of the two elements which can come within the aperture area at the actual z value. See also Fig. 11.

According to Simpson's rule, the effective aperture area is given by the expression

$$\int l(z)\,dz \approx l_{max} \cdot (a - 2\sqrt{\bar{r}^2 - \bar{x}^2}) + \tag{32}$$

$$+ \frac{\bar{z} + \sqrt{\bar{r}^2 - \bar{x}^2}}{3} \cdot (2c + 4\,l_{max}),$$

if $a > 2\bar{r}$. The first term in equation (32) refers to the part of the effective aperture area where l is constant and equal to l_{max}. (Cf. Fig. 9).

When $a \leq 2r$, we have:

$$\int_{\cdot}^{\cdot} l(z)\, dz \approx \frac{\bar{z} + \frac{a}{2}}{3} (2c + 4 l_{max}). \tag{33}$$

30. Successive approximations. In order to evaluate from equation (28) the number N of elements, corrected for missed elements, it is necessary to know the values of u and $\bar{z}$[1]. However, u is the quantity we want to estimate ultimately; and $\bar{z}$ can be evaluated exactly only when N_1 and N_2 are known (we make two scanning runs with aperture widths a_1 and a_2). Consequently, we have to substitute approximate values for u and $\bar{z}$ in order to perform the correction for missed elements.

We perform two scanning runs, and after introducing the expression $\int_{\cdot}^{\cdot} l(z)\, dz$ for the effective aperture area (equation (30) in equation (22′), we have

$$N_1' = N_1\, e^{-u \int l_1(z)\, dz} \approx N_1 (1 - u \int_{\cdot}^{\cdot} l_1(z)\, dz) \tag{34}$$

and

$$N_2' = N_2\, e^{-u \int l_2(z)\, dz} \approx N_2 (1 - u \int_{\cdot}^{\cdot} l_2(z)\, dz). \tag{35}$$

Our problem is to evaluate N_1, N_2, and then u from these equations.

By use of equations (2) and (3), approximate values of u and $\bar{z}$ are easily obtained from the number of recorded elements N_1' obtained with aperture width a_1, and N_2' obtained with aperture width a_2. It would perhaps be possible to use these approximate values; let us denote them u_0 and $\bar{z}_0$, directly for evaluating the effective aperture area and then N_1 and N_2.

[1] It is also necessary to know $\bar{r}$, the mean radius of the elements (see further § 64).

Nevertheless, in order to get a more accurate result, successive approximations may be performed as follows:

1. u_0 is obtained from equation (4):

$$u_0 = \frac{N'_1 - N'_2}{(a_1 - a_2) L}. \tag{36}$$

2. $\bar{z}_0$ is then obtained from equation (2):

$$N'_1 = u_0 (a_1 + 2\bar{z}_0) L. \tag{37}$$

3. Approximate value l_0 of $l_{\max}$. Using $\bar{z}_0$ and $\bar{r}$, the mean value of the element radii, we obtain an approximate value of $\bar{x} = \bar{x}_0$ according to § 29, and l_0 is calculated from equation (31).

4. A better value of $\bar{z}$ is evaluated from u_0 and l_0. Dividing equation (34) by equation (35) (equations in the exponential form), we obtain:

$$\frac{N'_1}{N'_2} = \frac{a_1 + 2\bar{z}}{a_2 + 2\bar{z}} \left\{ 1 - u_0 \left(\int l_1(z)\, dz - \int l_2(z)\, dz \right) \right\} \tag{38}$$

since $N = u (a + 2\bar{z}) L$ and $u \approx u_0$.
This yields the equality

$$\frac{N'_1}{N'_2} = \frac{a_1 + 2\bar{z}}{a_2 + 2\bar{z}} \{ 1 - u_0 (a_1 - a_2) l_0 \}, \tag{39}$$

from this, we immediately obtain $\bar{z}$.

5. A better value of $l_{\max}$ from $\bar{z}$. Now we obtain $l_{\max}$ in the same manner as in 3.

6. The effective aperture areas corresponding to the two scanning procedures are evaluated by use of $\bar{z}$ and $l_{\max}$ from equations (32) or (33).

7. A better value u_1 of u is obtained by using $\bar{z}$ and equation (4):

(40) $$u_1 = \frac{N'_1}{(a_1 + 2\,\bar{z})\,L}\,.$$

8. N_1 and N_2. Equations (34) and (35) can be rewritten in the form

(41) $$N_1 \approx N'_1 \left\{1 + u \int l_1(z)\,dz\right\},$$

(42) $$N_2 \approx N'_2 \left\{1 + u \int l_2(z)\,dz\right\},$$

In these equations, we put $u = u_1$ and insert the values for the two integrals calculated under 6.

9. The number of elements per unit area, u. After N_1 and N_2 have been obtained from equation (41) and (42); the final approximate value u^* of u is evaluated by use of equation (4). This gives us

(44) $$u^* = \frac{N_1 - N_2}{(a_1 - a_2)\,L}\,.$$

Finally, it may be remarked that all of these tedious calculations can be performed once for all and tabulated so that the corrections for missed elements can be found directly for the experimentally obtained values of u_0 and $\bar{z}_0$, when constant aperture dimensions are used and $\bar{r}$ is known (regarding $\bar{r}$, cf. § 64). Fig. 12 shows the relation between N' and N for some different $\bar{z}$ values.

31. **Confidence limits of the number of elements per unit area.** Consider a random distribution of elements like that discussed above. The number of elements, N, in regions of fixed area, A, is then a binomially distributed random variable. In analogy with the special case considered in § 20, it can be shown, that N can be considered as a variable with a Poisson distribution to a good approximation. This means that the probability of finding exactly N elements in a region of area A is $\frac{\lambda^N}{N!} \cdot e^{-\lambda}$, where λ means the average number of ele-

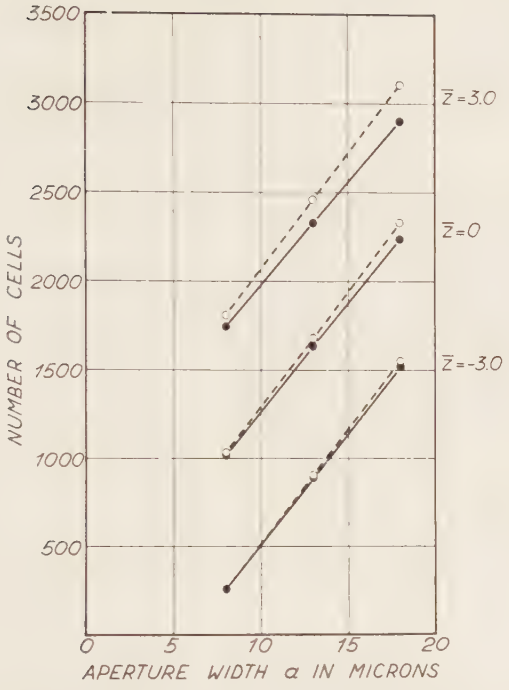

Fig. 12. Theoretical diagram which shows the number of elements recorded without correction for missed elements, N', —●—●—●— and after correction for missed elements, N, - - - ○ - - - ○ - - - ○ - - - as a function of the aperture width a. The relations are shown for three different $\bar{z}$ values. The number of elements per square mm. is taken as 200. The aperture length c is equal to 8 microns, the mean radius of the elements to 4 microns, and L to 647 mm. The curves have been constructed in the following manner. First the number of elements, N, which would have been recorded if no elements were missed, is evaluated according to equation (1). Then the number of elements, N', is evaluated from equation (34 or (35).

ments in an area A, *i. e.*, $\lambda = m\ (N)$. As is also well known, the standard deviation of a Poisson distribution is $\sigma(N) = \sqrt{\lambda}$; this is somewhat larger than the true one.[1]

In order to evaluate the number of elements per unit area, it was found convenient (equation (4)) to determine the number $N = N_1 — N_2$, where N_1 and N_2 are the number of elements on

[1] This statement seems to have been experimentally confirmed by ENGHOFF (1937).

the tracks $(a_1 + 2\bar{z}) \cdot L$ and $(a_2 + 2\bar{z}) \cdot L$ respectively. If these tracks are chosen independent of each other, the standard deviation of the random variable N should be

$$\sigma(N) = \sqrt{\lambda_1 + \lambda_2} \approx \sqrt{N_1 + N_2}, \quad (45)$$

[1]

where λ_1 and λ_2 are the average number of elements on the two tracks.

In order to diminish the standard deviation, it is desirable to effect the scanning procedure so that the smaller track is situated inside the larger one. Under these conditions, $N = N_1 - N_2$ is a variable with a Poisson distribution corresponding to the area $(a_1 - a_2)\, L$. The standard deviation in this case is

$$\sigma(N) = \sqrt{\lambda_1 - \lambda_2} \approx \sqrt{N_1 - N_2}, \quad (46)$$

i.e., in per cent, $\dfrac{100}{\sqrt{N_1 - N_2}}$.

Now assume that the number of elements $N = N_1 - N_2$ in a certain area $(a_1 - a_2)\, L$ has been determined. Our problem is now to make a statistical inference from this sample about the number of elements per unit area, u, or, in other words, the average $\lambda = u\,(a_1 - a_2)\, L$ in the area in question. As is well known,[2] the following is valid, with a probability of about 0.95:

$$-2\sqrt{\lambda} \leq N - \lambda \leq 2\sqrt{\lambda}. \quad (47)$$

By increasing the factor 2, we find that the probability is increased towards 1.

From this, we obtain the following confidence interval of λ corresponding to probability about 0.95:

$$N - 2\sqrt{N} \leq \lambda \leq N + 2\sqrt{N}; \quad (48)$$

---

[1] According to a well-known law, when N_1 and N_2 are mutually independent random variables, we have $\sigma^2(N_1 \pm N_2) = \sigma^2(N_1) + \sigma^2(N_2)$.

[2] When λ is not too small the Poisson distribution is approximately normal.

for u this becomes

$$(49) \qquad u^* - 2\frac{\sqrt{N_1 - N_2}}{(a_1 - a_2)L} \leq u \leq u^* + 2\frac{\sqrt{N_1 - N_2}}{(a_1 - a_2)L},$$

where

$$u^* = \frac{N_1 - N_2}{(a_1 - a_2)L} \quad \text{(Cf. equation (4)).}$$

The inequalities (49) can also be written as

$$(50) \qquad 1 - \frac{2}{\sqrt{N_1 - N_2}} \leq \frac{u}{u^*} \leq 1 + \frac{2}{\sqrt{N_1 - N_2}}.$$

Because the scanning apparatus is not able to perform an exact determination of N_1 and N_2, (cf. § 25) a certain degree of uncertainty is inherent in the values of N_1 and N_2 when obtained from equation (22′) and used for evaluating u^*. Consequently, the confidence interval given above must be enlarged in order to correspond to the probability in question, *e. g.*, in the example above, 0.95. In order to estimate the necessary change, let us consider possible causes of uncertainty of the evaluated N_1 and N_2 (equation (22′)).

(1) For given N_1 and N_2, the recorded number N_1' and N_2' are random variables. However, their standard deviations are relatively small for the sparse distributions we consider in this work (cf. § 17 and equation (23′)). In reverse, this means that N_1 and N_2 are obtained with good precision; the uncertainty is evident from equation (23′) where $u_1 \bar{l}_{\mu,\nu}$ is a small number. Therefore, equations (48) — (50) still hold true with a probability *about* 0.95.

(2) Random variation in the recording function of the apparatus. The standard error due to these fluctuations is measured by repeatedly performing scanning runs along the same track. The confidence interval in equation (49), for example, must be appropriately enlarged.

We now consider the total effect produced by the pure Poisson deviation and the random variations discussed under

(1) and (2). These variations may be considered as mutually independent variables; thus the resulting deviation is obtained by adding the squares of the three deviations in question and taking the square root of the sum. In the counting experiments to be described in chapter VIII, the Poisson deviation dominates the two others when the sensitivity of the recording system is not too large in proportion to the amount of diffuse background light.

We also recall, that there may be imperfections in the numerical evaluation of N_1 and N_2 from N'_1 and N'_2. We consider this uncertainty to be much smaller than the three random variations mentioned above, because the accuracy of the evaluation can always be chosen according to the actual conditions.

Finally, it should be remembered that it is a necessary condition for the scanning method that $\bar{z}_1 = \bar{z}_2$ (see § 16 and § 27). Otherwise a systematic error is introduced into the result.

CHAPTER III.

The scanning movement.

32. General considerations. There are several ways in which the scanning movement may be performed. In general, it should be carried out so that the greatest possible number of elements are recorded, in order to cut down the counting errors. Accordingly, the scanning track must be made as long as possible, of course without recording any element more than once. When counting elements settled at random and the scanning is produced by moving the area with the elements, it is necessary that the scanning movement is performed so that the movement itself does not displace the elements and derange the random distribution.

33. The area with the elements is moved while the aperture-phototube system remains stationary. Moving the object, or the stage with the object, is the usual method in microscope work where different parts of the object are to be examined. For the present work, this device offers the advantage of using only a small cross section of central rays. In order to produce an image of constant sharpness and intensity during the scanning movement, it is necessary that the plane of the object be even and that the distance between the object plane and the microscope objective, *i. e.*, the working distance, always remains constant during the scanning. Ordinary microscope stages are seldom built to comply with the last demand, since the sharpness of the image may be adjusted by visual inspection for every new position of the object. Naturally, such adjustments are not possible once the automatic scanning and counting procedure has started. The geometrical depth of focus is inversely proportional to the numerical aperture of the microscope objective and to the magnification between object and image planes (see MICHEL, *Die Grundlagen der Theorie des Mikroskops,* 1950). This means that a certain change in

the working distance resulting from imperfections of the moving stage produces more disturbances of the image sharpness when working with a small geometrical depth of focus than with a larger one. Consequently, we shall use as low a numerical aperture and magnification as possible, evidently without obtaining an image of too bad a quality and without using scanning apertures of too small physical dimensions.

In order to get a uniform response of the electronic system, the scanning velocity must be made fairly uniform in all parts of the scanning track, since the rise time and duration of the impulses are proportional to the scanning velocity. The movement of the stage may be performed either so that the scanning aperture crosses back and forth over the object field with a side displacement between every stroke, *i. e.* a linear motion, or so that the aperture moves in a spiral track relative to the object. In the linear method, the counting process may be disturbed each time the direction is reversed, but if the reverses occur outside the object field, the effect of the interruption can be nullified. The velocity of the scanning movement can be made constant during each stroke, so that uniform rise time and duration of the impulses are obtained. The effective length of each stroke must be held nearly constant in order to get a reproducible scanning length, L. The spiral track method gives an even and uninterrupted movement, but the velocity decreases continuously as the radius of the helix diminishes. This may be compensated for by a synchronized increase in the speed of revolution, but this modification would complicate the apparatus. However, the difference between the maximum and minimum scanning velocity of a helical track can be made relatively small and of minor importance if the central part of the helix is not used. The proportion between the area available for the scanning process and the total area of elements is thus decreased.

34. **The aperture-phototube system is moved in the plane of the image. The object remains stationary.** By this means, the high precision moving microscope stage is eliminated. The

movement of the aperture-phototube system does not demand such a high degree of precision as the movement of a stage, because the errors due to mechanical imperfections are reduced in proportion to the magnification factor between object and image plane. The relatively large image which must be produced by the microscope objective must be free from image curvature. If not, the scanning aperture-phototube system has to follow the curvature of the image. Furthermore, the light intensity must be uniform over the whole image. In order to produce a nearly plane image, it is necessary to use plane-achromatic objectives, special objectives for photo-micrography, or objectives for profile projectors.

35. **The scanning procedure is performed by moving the image by a prism system.** In this case both the object and the aperture-phototube system remain stationary. A helical scanning track can be produced by rotating the image with the use of a Dove or Wollaston prism. Radial displacements are made by tilting the axis of the rotating prism or by using another prism incorporated in the optical system. The system for producing the prism movements can be made quite small. Mechanical imperfections of the prism movements do not influence the image sharpness and brightness, provided the optical distance between the objective and the scanning aperture plane is not changed. The requirement for image quality of the microscope objective are the same as in § 34.

36. **Combinations of the methods described in §§ 33 and 34 with that in § 35.** One component of the scanning movement is performed by one method and the perpendicular component of the movement by another method.

37. **Moving a spot of light in the object plane.** The spot should be of the same order of magnitude as the elements which are counted and should be of rectangular shape. By reversing a microscope objective, a diminished image of a small aperture is projected on the object plane. The scanning motion is then performed by moving the projecting system

or by another of the methods described above. It would perhaps also be possible to use the television technique of flying spot scanning by a cathode ray tube, cf. § 5. Irrespective of the method for producing and moving it, the spot must be moved with a high degree of precision and in such a way that no changes in the dimension and brightness of the projected spot are produced.

CHAPTER IV.

Description of the apparatus. The microscope.

38. General considerations. It was decided to apply the scanning method to the counting of human erythrocytes sedimented to the bottom of a counting chamber from a diluted fluid suspension. A scanning counting apparatus which we shall now describe, was constructed for the purpose. It was decided to scan by the method described in § 33, where the microscope stage is moved in a helix. At the time the present work was planned (1948), no microscope objectives fulfilling the demands given in the discussion in § 34 were available to the author, so that the scanning procedure had to be performed by moving the microscope stage. Moving a spot of light, according to § 37, seemed to be inconvenient on account of the difficulty to obtain a constant size of the projected spot. Thus, the choice lay between the linear or the helical motion of the microscope stage. Without any doubt, a larger area might be scanned by linear motion of the stage than by the helical track method, but, when the apparatus was planned, the smooth and even motion of the helical track method was considered to be of major importance.

39. Outlines of the microscope. A schematic diagram of the scanning counter constructed is shown in Fig. 13. The microscope 'Ortholux', manufactured by Leitz, was found to have a relatively stable and firm stand and to be generally suitable as the basic component of the scanning counter. A microscope of this type was rebuilt and equipped with a framework for the aperture-phototube system, and with a specially constructed microscope stage for the helical scanning motion. A photograph of the scanning counting microscope is given in Fig. 60. Dark field illumination, which gives a relatively high contrast light intensity between the cells to be counted and the background, was used as in the first appa-

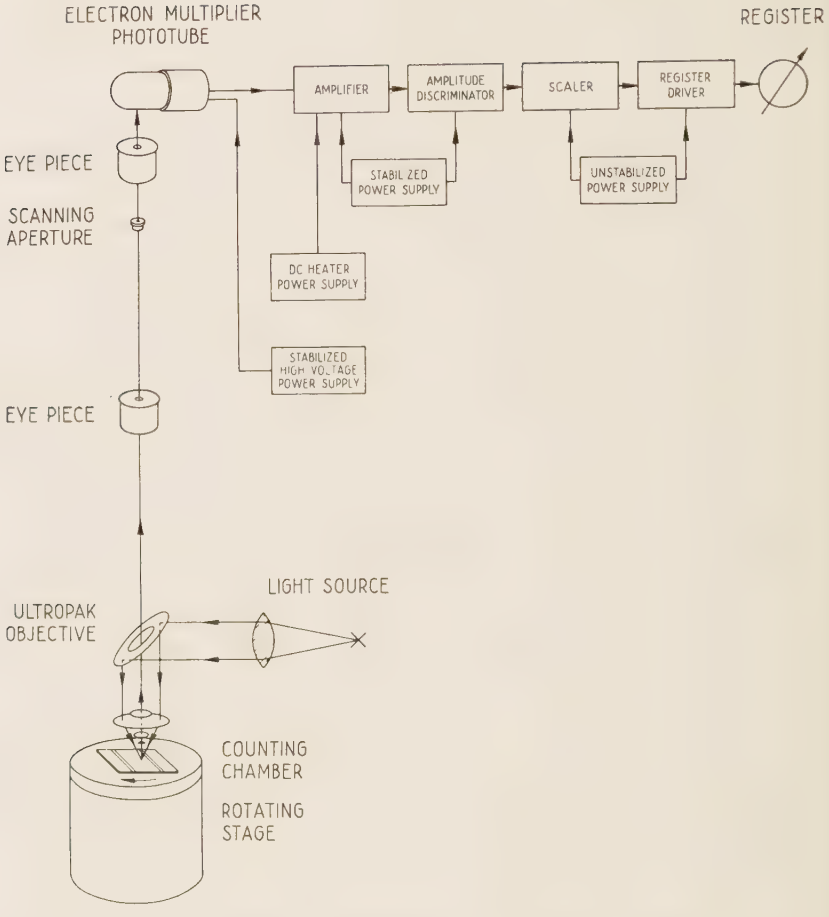

Fig. 13. Schematic diagram of the scanning counter.

ratus (LAGERCRANTZ 1947, 1948); but this requirement was now effected by use of the optical system 'Ultropak', manufactured by Leitz. In this device dark field illumination is combined with illumination from above. Thus the need was eliminated for any optical devices under the plane of the stage for transmitting light from below; this fact simplified the construction of the moving stage. In order to increase the contrast and light intensity from the cells, it was found desirable to place a mirror just below the counting chamber. This arrangement functioned very well when human eryth-

rocytes were counted, using the 'Ultropak' objective 11 x, N. A. – 0.25, and a counting chamber about 3.8 mm. in thickness. The mirror was fixed on the rotating stage and is shown in Fig. 17 (38).

40. **The counting chamber and the dimensions of the scanning helix.** A counting chamber of the one-field ruling type was filled with a diluted suspension of the cell to be counted.[1] The maximum dimensions available for the scanning procedure, outside the ruled field of the counting chamber area, were about 6 × 25 mm. The ruled area could not be used for the scanning counting because the rulings gave rise to an inhomogeneous background. Accordingly, the maximum usable diameter of the scanning helix was about 5 mm., as the helix had to be well inside the usable area in order to avoid disturbing reflections from the borders of the counting chamber field. In the discussion of the helical scanning movement (§ 33), it was stated that the minimum diameter of the helix should not be made too small. Rather arbitrarily, the minimum diameter of the helix was set at about 3 mm. In order to avoid the recording a single cell more than once, the distance between two adjacent revolutions on the helix had to be made equal to or larger than the scanning width w, *i. e.*, $a+2\bar{z}$. The minimum distance between two adjacent revolutions was set at 0.02 mm. This corresponds to 50 revolutions when the maximum and minimum diameter of the helix are 5 and 3 mm. $\left(\frac{5-3}{2} \cdot \frac{1}{0.02} \cdot 50\right)$. The diameter of the medium revolution is 4 mm.; and from this value and the number of revolutions, the total length of the scanning track is found to be equal to $\pi \cdot 4.0 \cdot 50 = 628$ mm.

41. **The moving stage.** The helical scanning track is produced in the manner described below, and is shown schematically in Figs. 14 and 15. The counting chamber is placed on a horizontal table rotating about its centre. At a certain distance from the centre of rotation, a small field of the counting

[1] The counting chamber used was manufactured by W. Schreck, Jena.

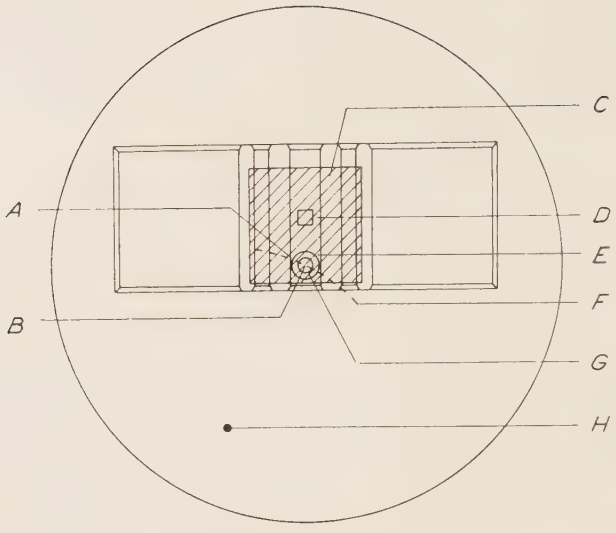

Fig. 14. Schematic diagram of the rotating table with the counting chamber, seen from above, and the geometrical arrangement, used to produce the helical scanning track. A. The aperture field when situated on the outer border of the helix. B. Centre of rotation of the table. C. Cover glass (shaded). D. Ruled field. E. Outer border of the helix. F. Periphery of side displacement. G. Inner border of helix. H. Centre of side displacement.

chamber is viewed through the scanning aperture, which is placed in the image plane of the eyepiece of the microscope. The scanning aperture and the microscope are stationary. When the table with the counting chamber is rotated, an annular area in the counting chamber passes the aperture. During the rotation, however, the centre of rotation of the table moves continuously towards one side, so that the distance between the centre of rotation of the table and the stationary aperture is continuously changed. The field of the counting chamber which passes the aperture has the form of a helix. The positions of the rectangular scanning aperture and the rotating stage must be adjusted in relation to each other so that the aperture borders corresponding to the aperture width a are perpendicular to the scanning direction. In order to effect this, the aperture must actually be situated on the periphery of the side displacement movement (see Figs. 14 and 15). Otherwise, the aperture might be correctly

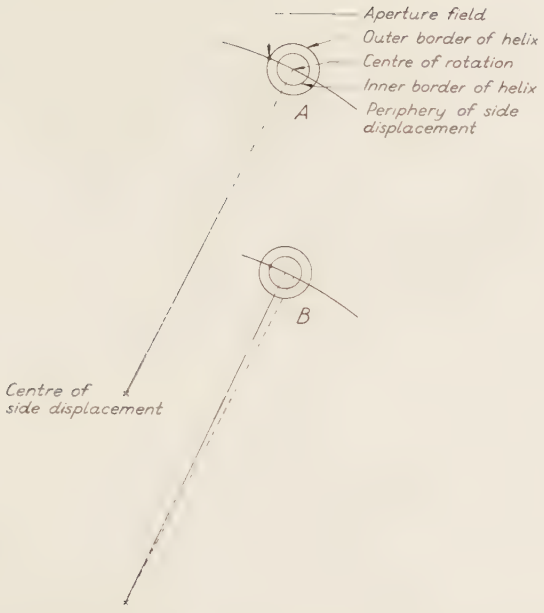

Fig. 15. Geometrical relations in the helical scanning track.
A. The aperture area (in fig. denoted aperture field) is situated on the periphery which gives maximum radius of the helix.
B. The aperture area is situated on the periphery which gives minimum radius of the helix.

oriented, in the outer part of the helix, for example, but obliquely in the inner part. Such an oblique position of the aperture in relation to the scanning direction changes the aperture width a, and an error is introduced into the final result.

42. Details of the moving stage. A drawing of the moving stage is given in Figs. 16 and 17. The counting chamber (not shown in these figures) is placed on the horizontal circular table (1), which is in turn fixed on the vertical spindle (2). This spindle is mounted in the frame (3) by use of the two precision-type radial ball bearings (4) and (5) (SKF 6304/C02 and ELY/C02), which permit a minimum of backlash. The larger bearing (4) is placed close to the table, the smaller one (5) on the opposite end of the spindle. The frame (3) with the counting chamber table (1) and the spindle (2) is supported by the two bearings (6) and (7), and is able to make the

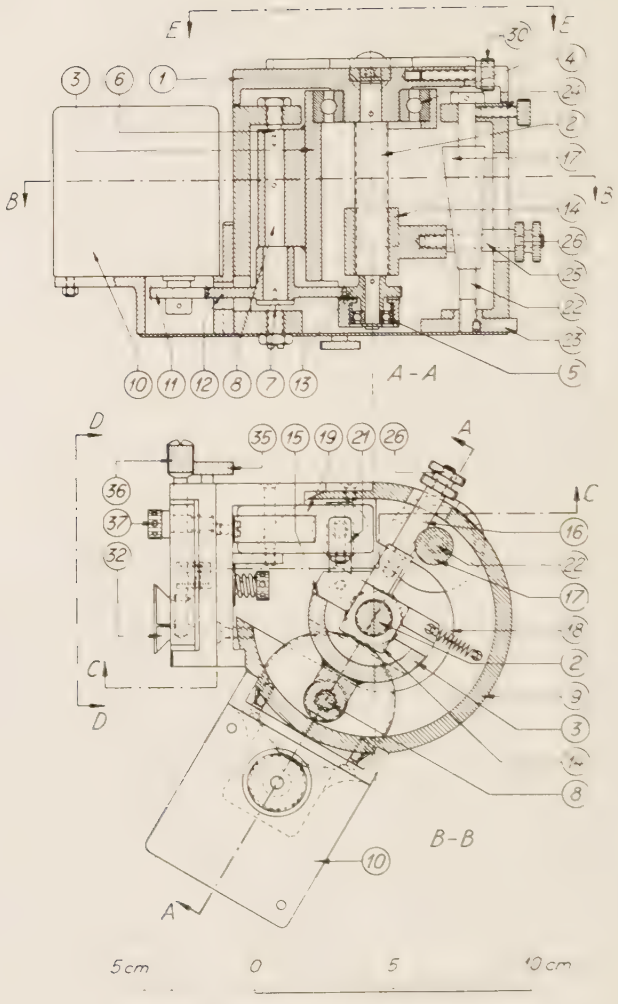

Fig. 16. The moving stage.

above-mentioned side displacement by a rotation of a few degrees round the vertical spindle (8), the ends of which are parts of the bearings. The cylindrical housing (9) which surrounds the internal parts of the stage also serves as a framework and supports the bearings (6) and (7). The driving motor (10) (Bodine synchronous motor KYC-22, 60 r m) is placed on a shelf fixed to the side of the cylindrical housing (9). Power is fed from the motor to the table spindle (2) by

use of the three helical gears (11), (12) and (13). Gear (11) is placed on the motor shaft and gear (13) on the table spindle (2). In order to transfer power to the table and at the same time allow the side displacement to take place, gear (12) is mounted so that it is free running on the spindle (8). The spindle (2) is threaded and is equipped with a nut (14), fitted without any backlash to the slide way (15), which is part of the frame (3). The nut (14) is mounted with the lever (16), which is pressed against the tapered shaft (17) by means of the spring (18). When the spindle (2) is rotated, the nut (14) with the lever is moved up or down (depending on the direction of rotation); and the frame (3) supporting the counting chamber table is displaced to one side or the other as the lever is forced to follow the profile of the tapered shaft (17). When the nut (14) has reached its top or bottom position, the motor is automatically stopped by one of the two microswitches (19) or (20) (Burgess Micro Switch Ref. CR) which are activated by the spring lever (21) also mounted on the nut (14). In order to adjust the dimensions of the scanning helix, the tapered shaft (17) is mounted eccentrically on its spindle (22). By turning the dial (23) attached to the lower end of the spindle (22), which is locked by the screw (24), profiles of different slopes are made available for the side displacement. The distance between the scanning aperture and the centre of rotation of the table can be adjusted by rotating sleeve (25), which has an oval cross section and which slides on lever (16). The sleeve can be fixed in any position by means of clamping nuts (26). The exact number of revolutions, usually 50, which the counting chamber table makes, is controlled by adjusting the level of the lower micro switch (20) using the screw (27). The counting chamber is held in its proper position on the table by heavy clips (28) and (29), and by stopper (30). The position of the chamber is radially adjustable by the vernier screw (31). The moving stage is attached to the 'Ortholux' microscope by the dovetail slide (32) and locked by screw (36) in the place otherwise occupied by the conventional stage and substage apparatus. The joint bracket between the dovetail slide (32) and the cylindrical

housing (9) is constructed so that the counting chamber table (1) can be adjusted relative to the horizontal plane by rotating the stage about two horizontal and mutually perpendicular

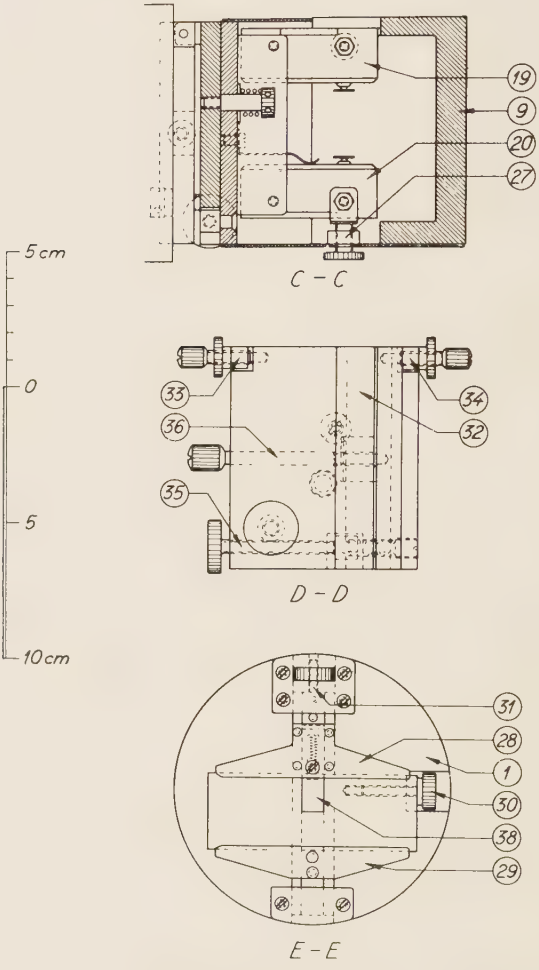

Fig. 17. The moving stage (further details).

axes with screws (35) and (37). A side displacement of the whole stage is effected by screws (33) and (34). The spindles (2), (8) and (22), the tapered shaft (17), the lever (16) with the sleeve (25), and bearings (6) and (7), are all made of steel. The remaining parts are made of brass. Extraordi-

nary precautions were taken in turning out the moving parts of the apparatus and in mounting the bearings in order to achieve the highest precision possible. The counting chamber table was ground to a nearly prefect plane configuration. Finally, the apparatus was tested when in motion by use of a dial displacement gauge, the lever of which turned against the bottom of an accurate-plane counting chamber placed in its correct position on the table. Choosing properly the force effected by spring (18), the pressure of lever (16) against the tapered shaft (17) was adjusted so that the lever glided along the profile of (17) with a smooth and even motion. Too high a pressure caused an elastic deformation of spindle (2), resulting in an unsatisfactory motion with vertical deviation of the table as indicated by the gauge. On the other hand, insufficient pressure by the lever caused an uneven and rattling motion. In order to increase the stability of the moving stage, it was found necessary to support the apparatus by five holders, shown in Fig. 61. With the force of spring (18) properly adjusted and with these five holders in their correct positions, the vertical deviations of the table were less than $\pm$ 0.0025 mm. during the entire operation. The lever of the dial displacement gauge was placed at a distance of about 2.5 mm. from the centre of rotation.

43. **The phototube holder, the aperture holder and the scanning aperture.** These parts of the scanning counter are shown in Figs. 18, 19 and 20. The two plates (41) and (42) are attached to the sides of the arm (40) of the 'Ortholux' which carries the microscope tube (68). On the horizontal square base (43), which is screwed to the ends of the side plates (41) and (42), the vertical centre plate (44) is erected and equipped with the dovetail slide (45). Bracket (46) is fitted to this slide so as to be movable in a vertical direction. It can be clamped in any position along the slide by screw (47). The horizontal shelf (48) part of bracket (46) carries the scanning aperture holder (49), which is adjustable in the horizontal plane by the three screws (50), (51) and (52). Each

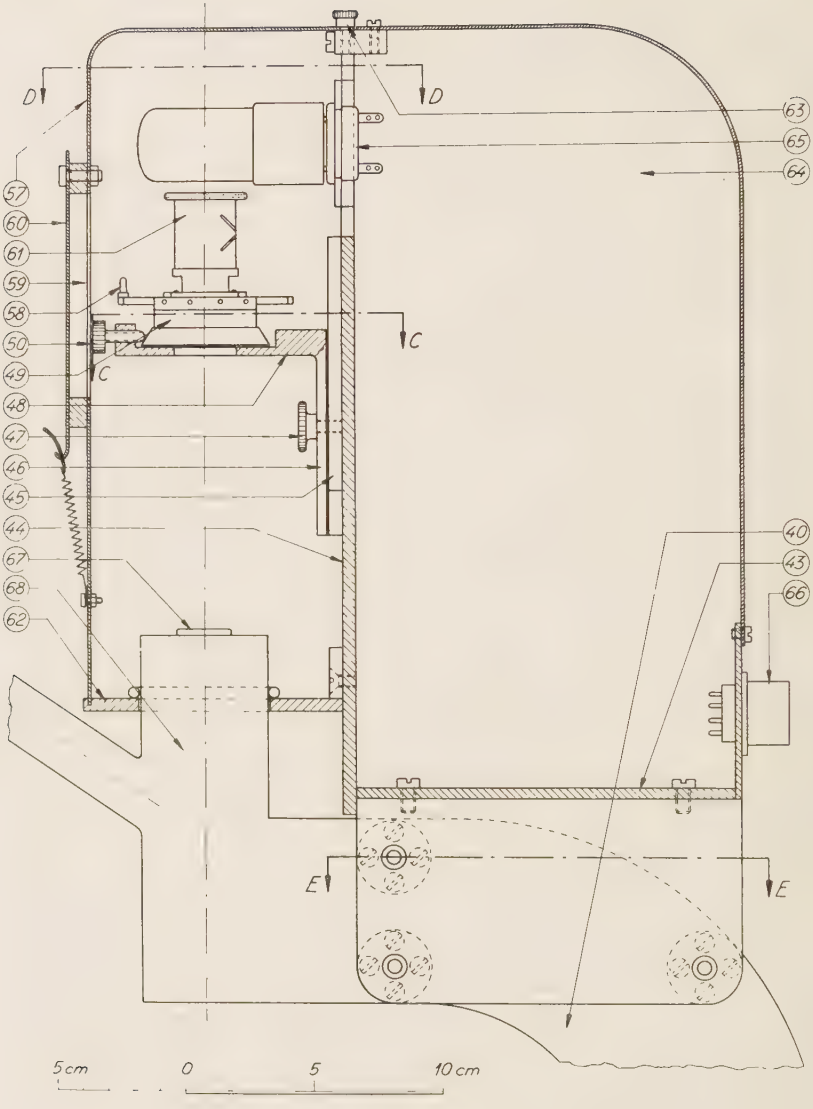

Fig. 18. Upper parts of the scanning and counting microscope.

of the screws is locked by a separate stop screw (not shown in the figure). The aperture holder (49) is made in the shape of a frustum of a cone, which forms the base (53) on which the slide (54) is fitted. The apertures are made of cylindrical

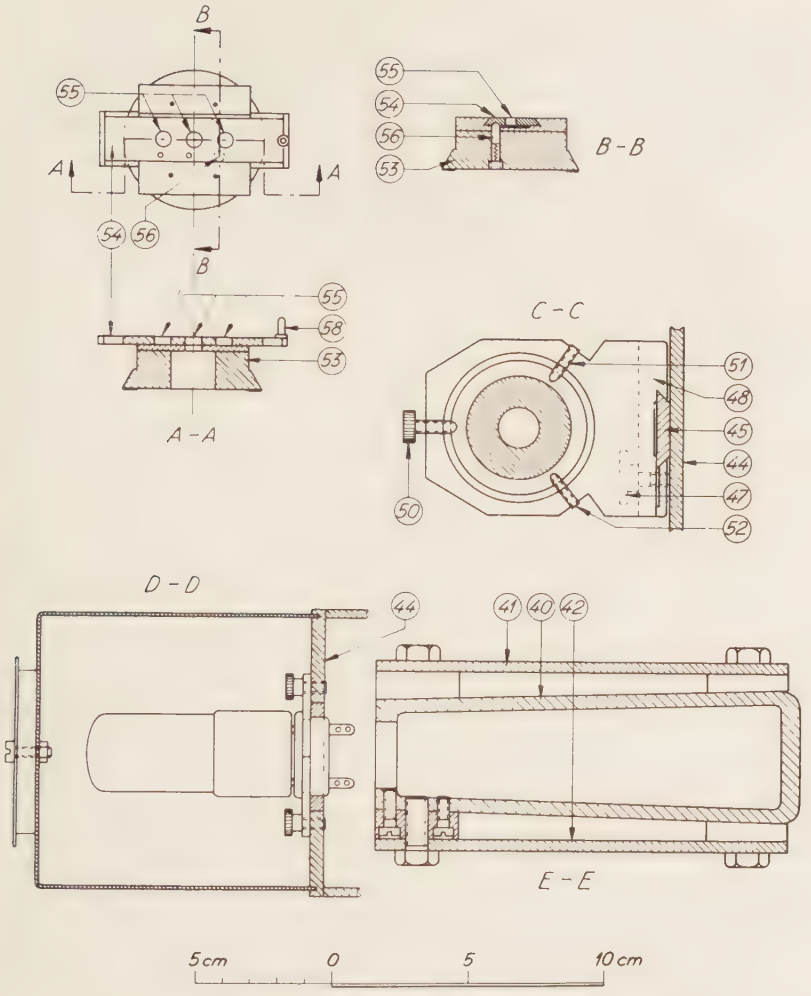

Fig. 19. The aperture holder and the phototube holder.

pieces of brass. The rectangular slit which forms the aperture is broached through the upper surface as an extension of the conic hole so that the edges are sharp and well defined. The construction of the aperture frame and the aperture is shown separately in Fig. 20. The smallest aperture used has dimensions about 0.2×0.2 mm., the largest about 0.8×0.4 mm. The aperture frames are equipped with a flange and are made to fit into any of the three holes (55) in the slide (54). By moving

the slide, we can insert any one of the three apertures into the optical system and use it as the actual scanning aperture. In order to bring the centre of the aperture always to the same

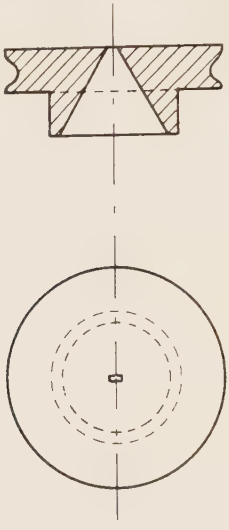

Fig. 20. The scanning aperture (not in scale with the other drawings).

position in the optical path, a spring plunger (56) fixed in the conic base (53) is slipped into one of three slots in the slide, each of which corresponds to one of the three apertures inserted in the slide. When the light shield (57) is mounted, the aperture slide (54) is moved by use of the knob (58) and a spanner through the window (59) normally covered by the shutter (60). The phototube socket (65) is placed at the upper end of the plate (44), and its position is adjustable vertically. In order to adjust the image in the aperture plane before the phototube is put into place, and in order also to bring the light to fall on the photocathode, the Ramsden eyepiece (61) is inserted between the scanning aperture and the phototube. The light shield (57), equipped with the window (59) and the shutter (60), slips into corresponding slots in the centre plate (44) and in the bottom plate (62). This shield is locked by screw (63). The space (64) situated behind the centre plate (44) is occupied by the amplifier.

44. Determination of the apparatus constants. The length of the helical scanning track is determined from the number of revolutions of the rotating table and the mean of the maximum and minimum diameter of the helix. These two diameters are measured by the following method. A sketch of

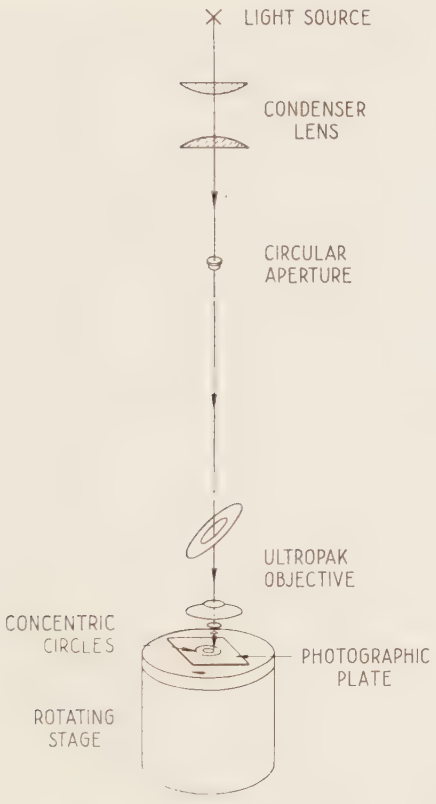

Fig. 21. Schematic diagram of the arrangement for determining maximum and minimum diameters of the helix.

the arrangement is given in Fig. 21. The condenser lens focusses an image of the lamp filament in the principal plane of the microscope objective. This is adjusted to give a diminished image of a small circular scanning aperture situated at its ordinary position in the optical system, in the object plane on the stage, where a photographic plate is fixed. The plate is exposed twice, once during one revolution which starts

from one end of the helix, and once during one revolution which starts from the other end of the helix. In this manner, two concentric circles are produced which correspond to the maximum and minimum circumferences of the helix. The two diameters are measured on the plate in a measuring microscope. Thus:

$$L = \pi \frac{\textit{maximum diameter} + \textit{minimum diameter}}{2} \cdot \textit{number of revolutions}. \tag{51}$$

The magnification factor F is determined by using an object micrometer placed on the stage and a large calibrated scanning aperture. The physical dimensions of the scanning apertures are measured in a microscope with the aid of a screw micrometer eyepiece.

The scanning length used in all experiments to be described below is 647 mm. The magnification factor, F, is equal to 44.4 in experiments 1—5, and is 50.0 in the remaining experiments.

45. Element distribution not deranged by the scanning movement. The helical scanning movement does not change the position of the erythrocytes settled to the bottom of the counting chamber (cf. § 32). This fact was shown as follows. An arbitrary area in the counting chamber corresponding to the periphery of the helix was photographed before and after the table had rotated the number of revolutions corresponding to the scanning length L. It was found that the erythrocytes occupied identical positions when the two photographic plates were compared.

CHAPTER V.

The shape, duration and rise time of the impulses.

46. Shape and duration. Assume that the light intensity change produced per unit area of the impulse producing element has a constant value for the whole impulse producing element. Under such conditions, the instantaneous impulse amplitude produced by the element is directly proportional to the area of the element actually inside the aperture area. The shape of the impulse produced by an element of circular form depends upon a number of factors, among others, upon the magnitude of the element area which passes inside the aperture and upon the aperture dimensions. In Figures 22—27, the relative impulse amplitude is plotted against the position of the element centre along the scanning track, and in relation to a rectangular aperture. The position of the element in the figures (except in Fig. 27), is given just as the element is about to pass over the aperture border. The part of the element that will pass inside the aperture area is shown hatched in the figures. The amplitudes, which are plotted in arbitrary units, are obtained from evaluation of the area of the circle intercepted by the aperture borders by use of the formula:

$$(52) \qquad 2\int_0^x \sqrt{r^2-(r-x)^2}\,dx = r^2 \cdot \arccos\frac{r-x}{r} + (x-r)\sqrt{2rx-x^2}.$$

In Fig. 22, the diameter of the element, $2 \cdot r$, is set equal to the aperture length in the scanning direction, c. The element passes wholly inside the scanning aperture. It is seen that the symmetrical impulse curve reaches its maximum when the element centre has reached the position $x = r + \frac{c}{2}$, *i. e.*, when the element is wholly inside the aperture. Further, it follows that the impulse duration, T, consists of two parts: the time

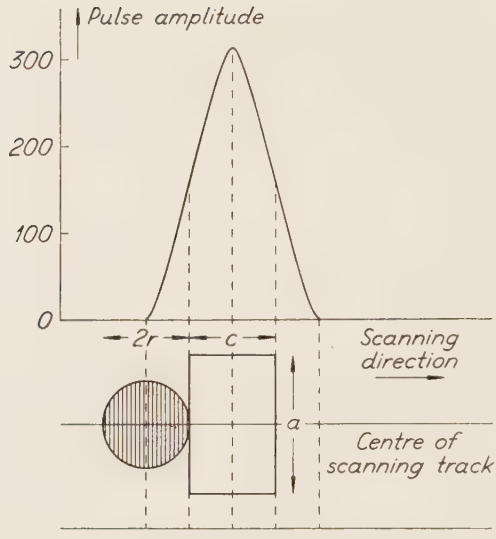

Fig. 22. Schematic diagram of the impulse shape when a circular element passes wholly through the aperture area. $2 \cdot r = c$.

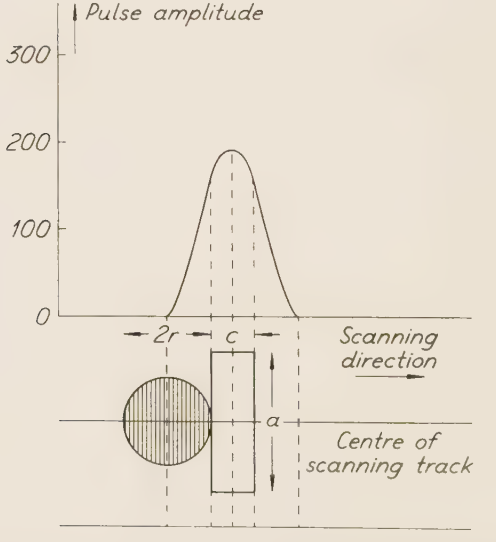

Fig. 23. Schematic diagram of the impulse shape when a circular element passes wholly through the aperture area. $2 \cdot r > c$.

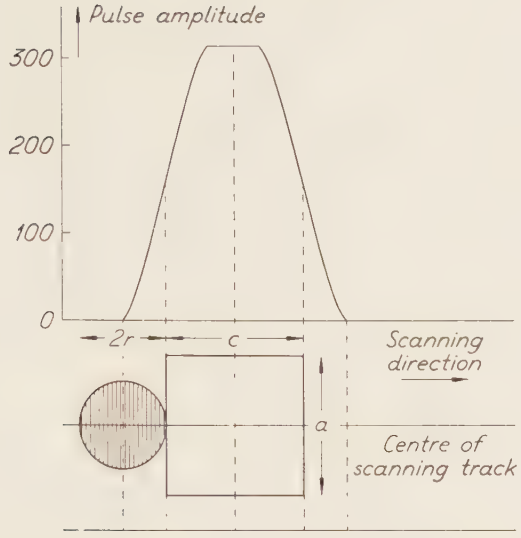

Fig. 24. Schematic diagram of the impulse shape when a circular element passes wholly through the aperture area. $2 \cdot r < c$.

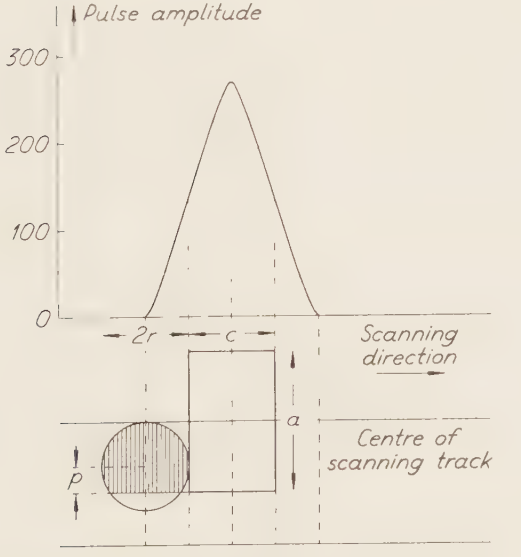

Fig. 25. Schematic diagram of the impulse shape when a circular element passes only in part through the aperture area. $2 \cdot r = c$.

for the leading edge of the element to pass the aperture length, c, and the time for the trailing edge to pass over the aperture border at right angles to the scanning direction. The first part is equal to $\frac{c}{V}$, the second $\frac{d}{V}$, where V denotes the scanning velocity and d the maximum element length that passes inside the aperture in the scanning direction. In those cases where the element centre passes inside the aperture area, d is always equal to $2 \cdot r$, *i. e.*, the element diameter. Thus:

$$T = \frac{c + d}{V} . \tag{53}$$

Fig. 23 shows what happens when the aperture length $c < 2 \cdot r$. The maximum impulse amplitude is smaller, and the impulse duration shorter, than in Fig. 22.

Fig. 24 presents the situation when the aperture length $c > 2 \cdot r$. The maximum impulse amplitude is equal to that in Fig. 22, but the impulse is longer because of the flat top of the impulse, which $= \frac{c - 2r}{V}$.

In Fig. 25, the element meets the aperture so that the major part of the element, but not the entire element, passes inside the aperture area. Here we have $c = 2 \cdot r$. The centre of the element moves at a distance, p from the aperture border in the scanning direction. The maximum impulse amplitude is smaller than that of Fig. 22 but the impulse duration is the same.

In Fig. 26, the element meets the aperture so that less than half of the element passes inside the aperture area, again we have $c = 2 \cdot r$. The centre of the element moves outside the aperture area at a distance p from the border of the scanning direction. The maximum element length that passes inside the aperture is now $2 \sqrt{r^2 - p^2}$, and the impulse duration is

$$T = \frac{c + 2\sqrt{r^2 - p^2}}{V} . \tag{54}$$

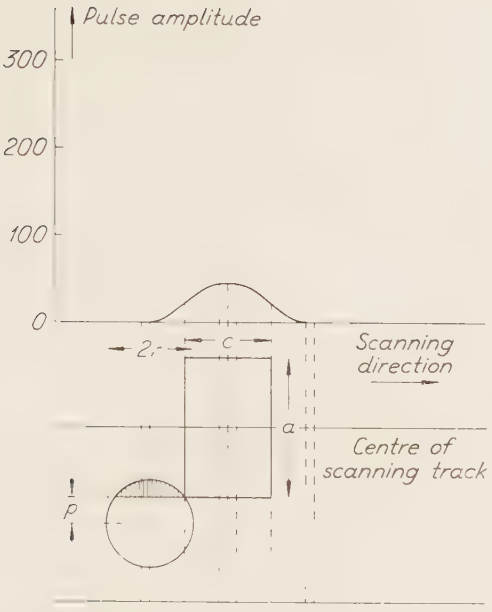

Fig. 26. Schematic diagram of the impulse shape when less than half of a circular element passes through the aperture area. $2 \cdot r = c$.

In Fig. 27, the impulses produced by two elements close together are shown. The distance in the scanning direction between the two elements is somewhat smaller than c, and this causes incomplete separation of the two impulses. In order to resolve and record both elements, it is necessary that the actual l-value be less than the distance between the element centres.

The maximum scanning velocity of the described apparatus is about 15.7 mm. per second, and the minimum velocity about 9.4 mm. per second. Assuming a mean radius of the elements about 4 microns, and an aperture length, c, equal to 8 microns the maximum impulse duration is about $1{,}700 \cdot 10^{-6}$ seconds and the minimum duration about $850 \cdot 10^{-6}$ seconds when we set $\bar{z}$ equal to 3.0 microns.

47. **Rise time.** From the above discussion, it is evident that the rise time of the impulses, *i. e.*, the time for the impulses

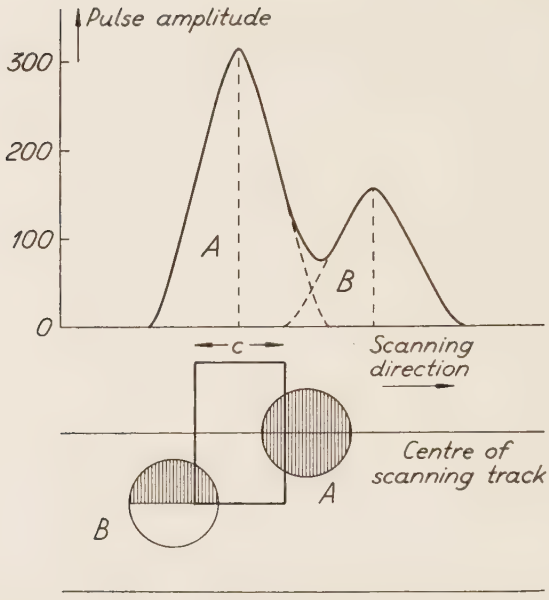

Fig. 27. Schematic diagram of the impulse shape when two consecutive circular elements pass through the aperture, the first element with the whole area, the second one with only half its area inside the aperture area.

to reach maximum amplitude, is equal to $\frac{d}{V}$ for $d \leq c$ and $\frac{d+c}{2V}$ for $d > c$. When $c > 2 \cdot r$, it follows that the minimum rise time is equal to $\frac{2 \cdot \sqrt{\bar{r}^2 - \bar{z}^2}}{V}$ and that the maximum rise time is equal to $\frac{2\,\bar{r}}{V}$. Let us assume that we do not use a $\bar{z}$ value above 75 per cent of the mean radius of the elements. In this case, the ratio of the maximum to the minimum rise time is:

$$(55) \qquad \frac{\text{max. rise tim.}}{\text{min. rise tim.}} = \frac{2 \cdot \bar{r}}{2\sqrt{\bar{r}^2 - \left(\frac{3}{4}\bar{r}\right)^2}} = \frac{4}{\sqrt{7}} \approx 1.51 : 1.$$

Assuming the values of scanning velocities, aperture length, element radius and $\bar{z}$ to be the same as in the numerical

example given above, we find a maximum rise time of about $850 \cdot 10^{-6}$ seconds, and a minimum rise time about $567 \cdot 10^{-6}$ seconds.

48. **Dynamic range.** Finally, it may be pointed out that the dynamic range (cf. § 15) is approximately equal to 13.4 : 1 when $\bar{z}$ is 75 per cent of $\bar{r}$ and $\bar{r}$ is = 4 microns. This value is obtained directly from Fig. 10, as the ratio of the area of the whole element to the area inside the aperture for the actual $\bar{z}$ value.

CHAPTER VI.

Description of the apparatus. The electronic system.

49. General considerations. In order to record the impulses of light produced by the cells when passing inside the area of the scanning aperture, the electronic system shown in Figs. 13, 28 and 29 is used. The impulses of light are detected by the highly sensitive multiplier phototube RCA 1P21. The very high gain obtained by this phototube restricted the need for more gain in a separate amplifier to a factor of about 100 when human erythrocytes were counted by means of the apparatus described. The remaining components of the electronic system, *i. e.*, amplitude discriminator, scaler, tabulator driving circuit, and stabilized power supplies are all conventional components used in counting of nuclear particles.

50. The amplifier. From the discussion in §§ 46—48 and 49, it can be seen that the demands put on the amplifier for rise time, gain, dynamic range and design of minimum overshoot circuits are not very high. When other elements than erythrocytes are counted, however, it may perhaps be necessary to introduce more amplifier gain; and the circuits must be designed more carefully. It is vital of course to make the amplifier and other electronic parts as stable as possible, in order that the sensitivity of the recording system, *i. e.*, $\bar{z}$, may remain as nearly constant as possible during the scanning runs necessary for evaluating the number of elements per unit area.

The directly coupled amplifier described by MARSHALL, COLTMAN and BENNETT (1948) for use in a scintillation counter was modified. The circuit diagram of the amplifier used is shown separately in Fig. 29. The amplifier is very simple and consists of only two stages, a relatively high-gain pentode stage and a cathode follower output stage. The output from the multiplier phototube where the signal has negative

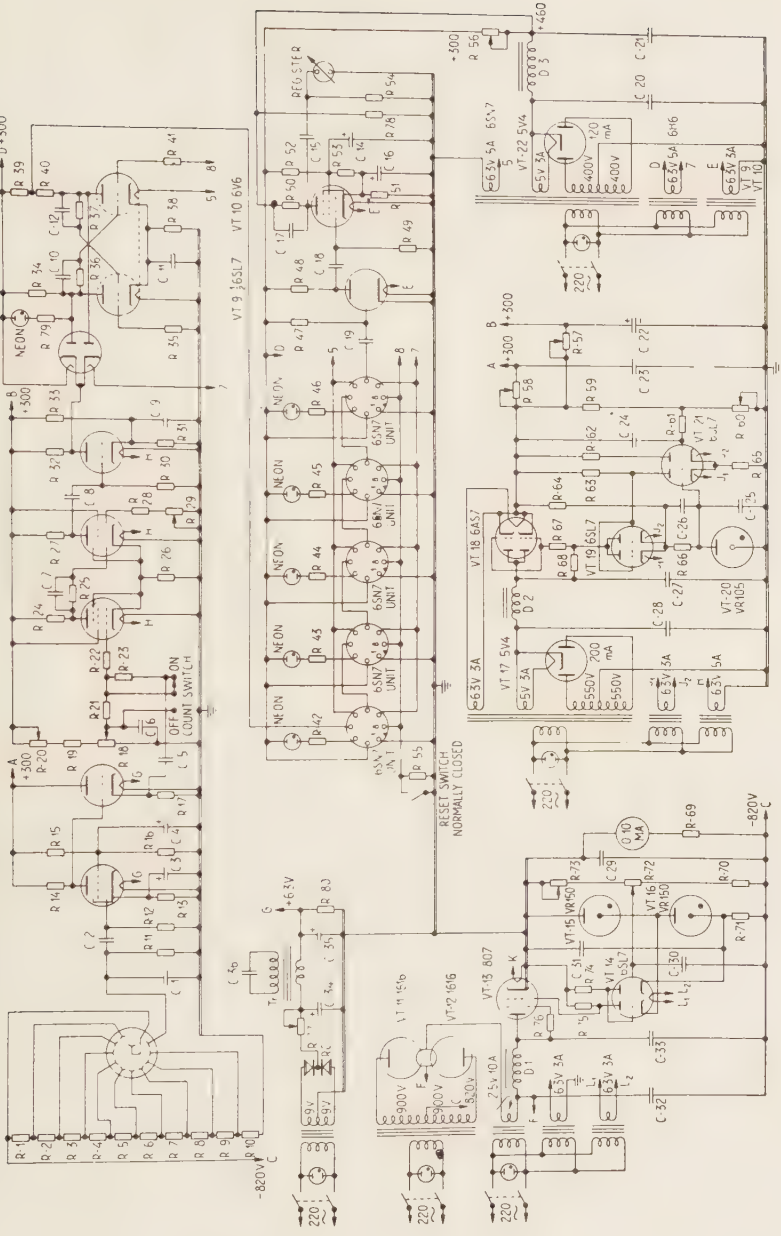

Fig. 28. The electronic system.

$R_1 - R_{10} = 100$ K — 1/2
$R_{11} = 2$ M — 1/2
$R_{12} = 2$ M — 1/2
$R_{13} = 3.3$ K — 1/2

R_{14} = 250 K — 4
R_{15} = 17 K — 4
R_{16} = 10 K — 2
R_{17} = 33 K — 2
R_{18} = 50 K pot. G.R. 314 — A
R_{19} = 75 K — 12 W.W.
R_{20} = 50 K — 12 W.W. scr. adj.
R_{21} = 1 M — 1/2
R_{22} = 1 K — 1/2
R_{23} = 2 M — 1/2
R_{24} = 3.9 K — 1
R_{25} = 100 K — 12 W.W.
R_{26} = 10 K — 2
R_{27} = 5 K — 1/2
R_{28} = 40 K — 12 W.W.
R_{29} = 20 K — 12 W.W. scr. adj.
R_{30} = 50 K — 1/2
R_{31} = 10 K - 1/2
R_{32} = 20 K — 1/2
R_{33} = 150 K — 2
R_{34} = 20 K — 2
R_{35} = 100 K — 1/2
R_{36} = 200 K — 1/2
R_{37} = 200 K — 1/2
R_{39} = 5 K — 1/2
R_{40} = 15 K — 2
R_{41} = 100 K — 1/2
R_{42} = 1 M — 1/2
R_{43} = 1 M — 1/2
R_{44} = 1 M — 1/2
R_{45} = 1 M — 1/2
R_{46} = 1 M — 1/2
R_{47} = 2 M — 1
R_{48} = 200 K — 2
R_{49} = 1 M — 1/2
R_{50} = 50 K — 2
R_{51} = 1.5 K — 1/2
R_{52} = 20 K — 12
R_{53} = 10 K — 1/2
R_{54} = 1 M — 1/2
R_{55} = 100 K — 1
R_{56} = 2—5 K — 12 scr. adj.
R_{57} = 10 K — 12 scr. adj.
R_{58} = 10 K — 12 scr. adj.
R_{59} = 225 K — 12
R_{60} = 75 K — 12 scr. adj.
R_{61} = 1 M — 1/2
R_{62} = 1 M — 1
R_{63} = 1 M — 1
R_{64} = 10 K — 12
R_{65} = 200 K — 1
R_{66} = 10 K — 12
R_{68} = 500 K — 1
R_{69} = 100 K — 12 W.W.
R_{70} = 50 K — 12
R_{71} = 50 K — 12
R_{72} = 10 K pot. G.R. 314 — A
R_{73} = 25 K — 12 scr. adj.
R_{74} = 500 K — 1
R_{75} = 500 K — 1
R_{76} = 100 ohms — 2
R_{77} = 5—10 ohms W.W. scr. adj.
R_{78} = 50 K — 12
R_{79} = 1 M — 1/2
R_{80} = 120 ohms — 2

C_1 = 47 μμF
C_2 = 0.1 μF
C_3 = 100 μF el. 12 V
C_4 = 8 μF el. 450 V
C_5 = 0.05 μF
C_6 = 0.01 μF
C_7 = 25 μμF
C_8 = 50 μμF
C_9 = 500 μμF
C_{10} = 50 μμF
C_{11} = 0.01 μF
C_{12} = 50 μμF
C_{14} = 8 μF el. 450 V
C_{15} = 4 μF paper 1500 V
C_{16} = 25 μF el. 50 V
C_{17} = 0.15 μF
C_{18} = 0.005 μF
C_{19} = 0.05 μF
C_{20} = 6 μF oil 600 V
C_{21} = 6 μF oil 600 V
C_{22} = 16 μF el. 450 V
C_{23} = 2 μF paper 1500 V
C_{24} = 0.1 μF
C_{25} = 0.1 μF
C_{26} = 0.1 μF
C_{27} = 6 μF oil 600 V

C_{28} = 6 μF oil 600 V
C_{29} = 4 μF oil 1500 V
C_{30} = 4 μF oil 1500 V
C_{31} = 0.25 μF paper 600 V
C_{32} = 4 μF oil 1500 V
C_{33} = 4 μF oil 1500 V
C_{34} = 4,000 μF el. 12 V
C_{35} = 4,000 μF el. 12 V
C_{36} = 0.6 μF

Interpolator lamps LUMA GL 4
R C selenium rectifier
ELEKTROSCANDIA type
EPF 1/1—1, max. 3 amp.
D — 1 10 H., 200 mA
D — 2 15 H , 200 mA
D — 3 15 H., 150 mA.
Tr transformer p:s = 220: 6.3.
Sec. tuned by use of C_{36} to 100 c/s.

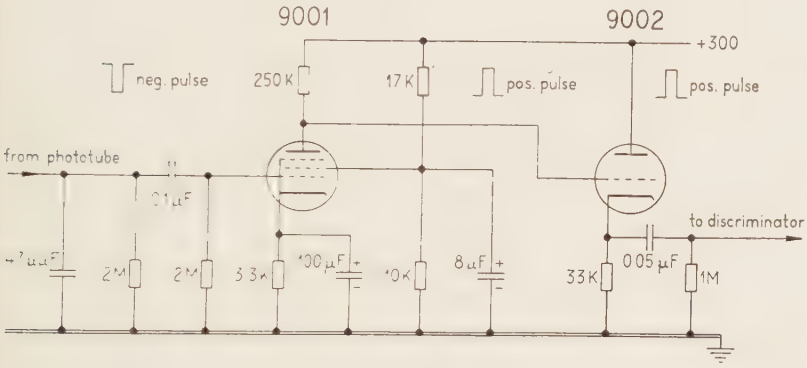

Fig. 29. The amplifier.

polarity is capacitively coupled to the pentode in order to depress slow fluctuation due to the background. In order to suppress noise which might cause change in $\bar{z}$ (cf. § 16) or even spurious impulses, it was found necessary to decrease the band width by placing a shunt capacitor (C_1 in Fig. 28) of about 50 μμF across the load resistance of the phototube. We may define the rise time of a parallel resistance-capacitance combination as the time for a rectangular current step impulse to develop a voltage of 90 per cent of its maximum value across the RC-combination. If we assume a total shunt capacitance of about 60 μμF (C_1 + output capacitance of the phototube + stray and wiring capacitances + input capacitance of the pentode), a minimum rise time of about $120 \cdot 10^{-6}$ seconds is available. (Rise time = 2.2 RC) (cf. VALLEY and WALLMAN, *Vacuum Tube Amplifiers* (1948)). Comparing this value with the minimum rise time of the actual impulses (cf. § 47), it

is obvious that we can consider the phototube-amplifier system as infinitely fast.

In order to minimize impulse distortion due to imperfect d. c. response, *i. e.*, low frequency overshoots, the time constants of coupling, decoupling and bypass circuits were made as large as possible relative to the maximum impulse duration (see § 46). The time constant of the coupling circuit between the cathode follower and the amplitude discriminator was made somewhat shorter in order to depress microphonics. The chief advantage of the cathode follower was to reduce the output impedance of the amplifier and thereby eliminate the effect of the shunt capacitance of the coaxial cable on the rise time, and to short circuit hum and extraneous voltages induced in this cable. Since the d. c. component of the impulses, *i. e.*, the flat top of the impulses, is relatively small, if the length of the aperture is not made fairly large, and since the dynamic range is very small, special low frequency compensation seems to be unnecessary.

According to a traditional view, the frequency response of an impulse amplifier should be of the same order of magnitude as the inverse value of the impulse duration. The actual circuit seems to correspond to a band width of about 2.3 kc per second. The inverse value of the minimum impulse duration is about 1.2 kc per second.

Oscillograph patterns that illustrate the effect of various time constants on the impulse shape are given in chapter VII.

51. **Other electronic components.** The regulated high voltage power supply for the multiplier phototube was of a type described by HEIGL, DUDENBOSTEL, BLACK and WILSON (1950) for use in a Raman spectrometer. The electronic impulse counter was of the type described by HIGINBOTHAM, GALLAGHER and SANDS (1947), and by ELMORE and SANDS (1949) in their monograph on electronics for nuclear investigation under the name of 'Model 200 Pulse Counter'. It consists of an amplitude discriminator based on the Schmitt trigger circuit, a scale of 128 and a register driving circuit. The input to the scales-of-two units was diode coupled. The output from the scaler could be coupled by a suitable switch (not shown in the figures) to

the register driving circuit so that the impulse rate could be reduced by a factor of 2, 4, 8, 16, 32, 64 or 128. The amplifier and discriminator were fed from the same regulated power supply, which was of the type called 'Model 100 Power Supply' by ELMORE and SANDS (loc. cit.). The amplifier and amplitude discriminator were isolated from each other by suitable resistors and decoupling capacitors. The heaters of the amplifier tubes were fed from a d. c. power supply. The amplifier was built on a metal plate that was shock mounted on the microscope and placed in the space (64) shown in Fig. 18, behind the multiplier phototube. The other electronic equipments were built into four chassis which were mounted in a 19″ standard rack. This rack was made very stable so that the microscope could be placed on a wooden plate fixed on the top of the rack. Shielded coaxial cables and cable connectors (Amphenol model AN and 83) were used for the necessary connections between the electronic parts in the microscope and in the rack. A diagram of the whole electronic system is given in Fig. 28. All electronic equipment was built and trimmed in the laboratory.

52. **The microscope lamp.** In order to get as stable a light intensity as possible, the microscope lamp (Philips Microprojection lamp, type 6019 M, 8 volts, 6 ampères) was fed from a storage battery (Tudor type OE4, capacity 64 ampères hours). The battery was charged from a selenium rectifier (Tudor type CLAS 16/7).

CHAPTER VII.

Impulse shape experiments.

53. Experimental arrangement. In order to investigate the effect of different aperture dimensions and different time constants on the impulse form and on the resolving power, the impulses were visualized on the screen of a cathode ray oscillograph during a scanning run on a distribution of human erythrocytes. However, it was found rather difficult to arrive at any conclusions from these observations, since the impulses were distributed at random. Consequently, an experimental arrangement was set up, whereby the same single cell or group of cells, now stationary, was scanned repeatedly by a moving aperture that was placed on the periphery of a rotating disc. A schematic diagram of the experimental arrangement is shown in Fig. 30. By this means, it was possible to observe the effects both of different circuit parameters and different aperture dimensions on the impulse shape and on the resolving power under identical light signals. The relation between the scanning velocity, V, the number of revolutions per unit time, ω, and the dimension of the rotating disc, *i. e.*, the distance between the scanning aperture and the centre of rotation, g, and the magnification factor, F, is

$$V = \frac{\omega \cdot 2 \cdot \pi \cdot g}{F}. \tag{56}$$

During an ordinary helical scanning run, the maximum scanning velocity is about 15.7 mm. per second, and the minimum velocity about 9.4 mm. per second. The disc was rotated by a Bodine synchronous motor, KYC—22, which made 100 revolutions per minute at 50 cycles per second. By feeding the motor from a power oscillator, the frequency of which could be varied, the number of revolutions could be decreased to 60 per minute. From these values and the magnification factor F 50.0, it was found by means of equation (56) that the

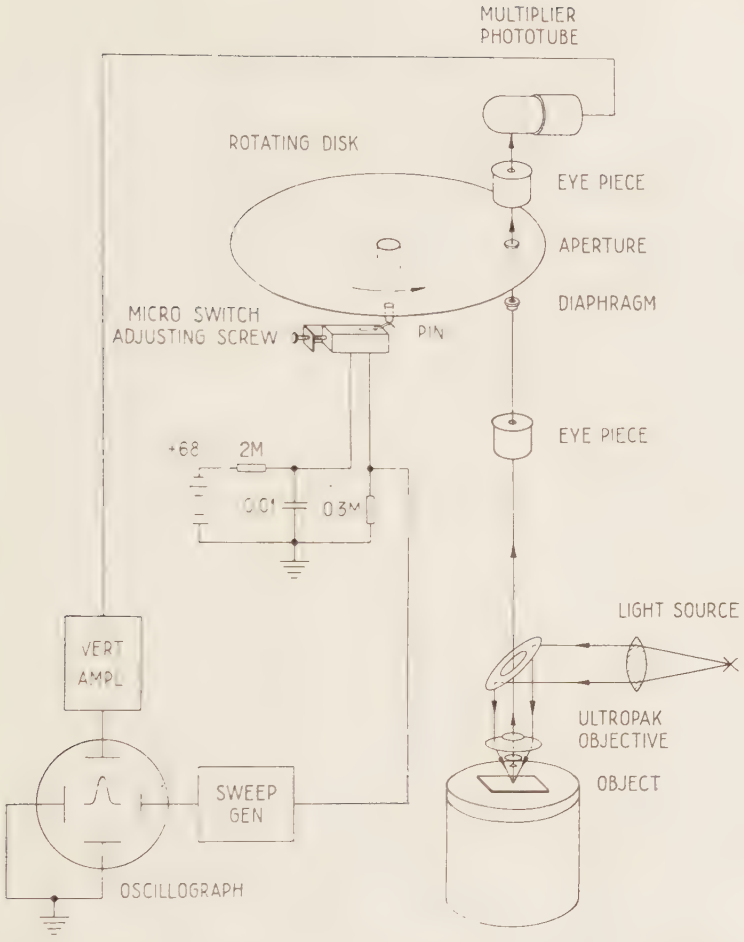

Fig. 30. Schematic diagram of the arrangement for visualizing the impulse shape of a single element or group of elements.

aperture should be placed at a distance of 75 mm. from the centre of rotation in order to obtain the above mentioned maximum and minimum scanning velocities. The disc was made of aluminum sheet, 1.5 mm. thick, had a diameter of about 100 mm., and was mounted on the motor shaft by means of a chuck. The construction of these parts is shown in Fig. 31. Four holes (65), (66), (67) and (68) were bored in the disc (69), symmetrically and equidistant from each other, at a distance of exactly 75 mm. from the

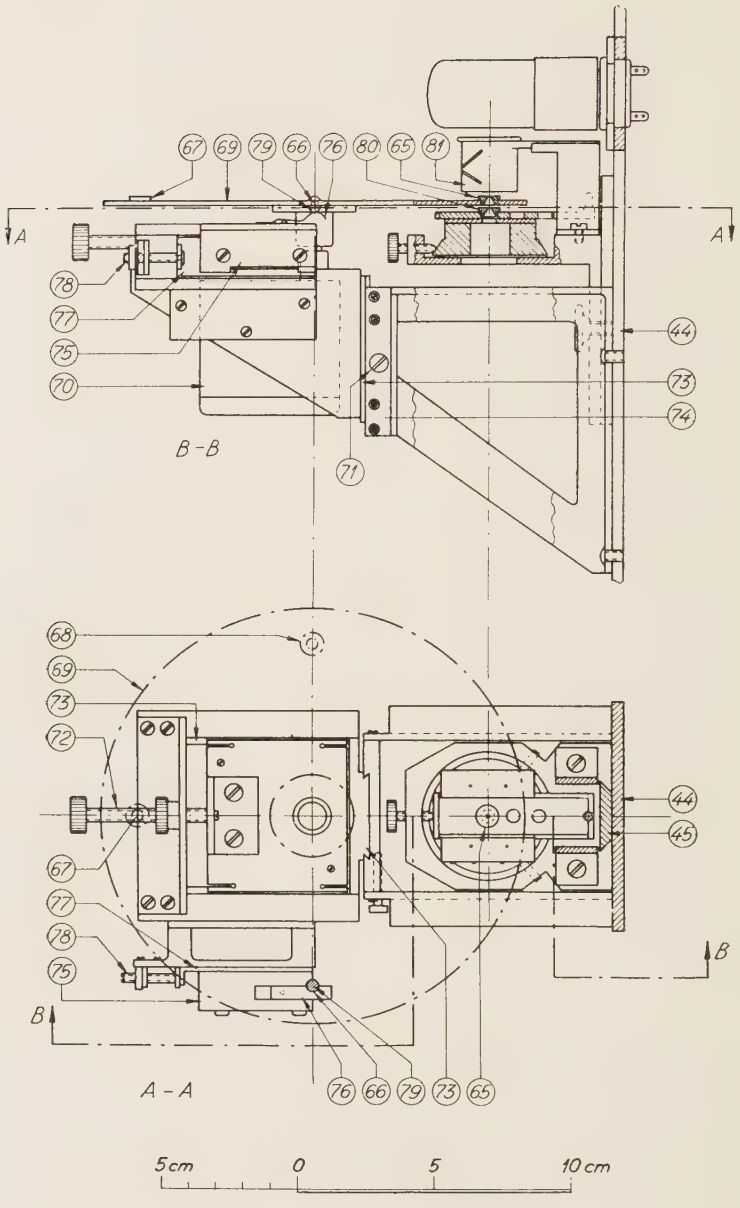

Fig. 31. The rotating disc.

centre of rotation. The diameter of the holes was so chosen that the aperture frames described in § 43 could

be inserted. The motor (70) with the disc (69) was mounted on a slide system so that its position could be adjusted vertically and locked by screw (71), and horizontally by use of the vernier screw (72). The base of the vertical slide (73) was made a part of bracket (74) which was fixed to the centre-plate (44). The vertical position of the disc was adjusted until the scanning aperture moved in exactly the same plane as that otherwise occupied by the stationary aperture when it was placed on the rotating disc. In order to start the oscillograph sweep about half an impulse length before the arrival of the impulse, so as to visualize the beginning of the impulse and the region before the impulse on the screen, the following arrangement was used. To one side of the motor holder, a Burgess micro switch, Ref. CRL (75), equipped with a leaf spring (76) was mounted on a dovetail slide (77), so that the position of the switch could be adjusted by the vernier screw (78) along a line tangential to the disc. By means of pin (79) fixed in hole (66) in the disc, the switch was actuated once for each revolution of the disc. When the switch was operated, a condenser (see Fig. 30) was discharged through a resistance, and an impulse was produced that triggered the oscillograph sweep. The aperture was inserted in hole (65) of the disc. The last two holes (67) and (68) were occupied by dummies of the same form as the aperture to balance the disc properly. By moving the stage, the cell or group of cells whose impulses were to be investigated were brought into the field of vision and isolated from other cells by means of the circular diaphragm (80) of suitable diameter placed below the plane of the scanning aperture on the slide where the scanning apertures are placed during an ordinary scanning procedure. The spatial relations of the cell or group of cells under investigation to the scanning aperture were adjusted by moving the motor with the disc by means of the vernier screw (72) under visual control through the eyepiece (81). The position of the micro switch was adjusted to trigger the sweep as mentioned above. A special light shield was used when the arrangement described was functioning. The output from the amplifier of the scanning counter was fed to both the oscillograph and to the amplitude discriminator. The directly coupled amplifier of the oscillograph

was used which had d. c. response and was infinitely fast relative to the actual impulses. The oscillograph patterns were photographed. A photograph of the microscope when mounted with the described arrangements is shown in Fig. 61.

54. Shape of impulses produced by human erythrocytes; dark field illumination. In the following diagrams, the posi-

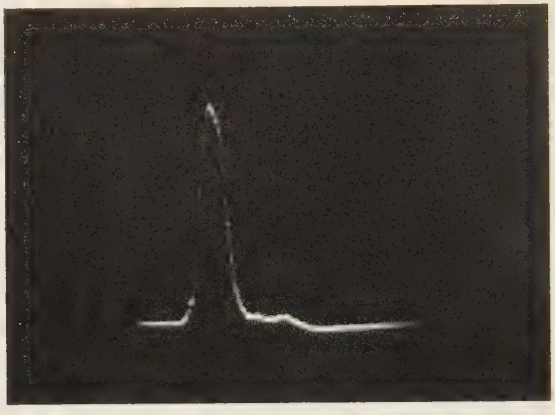

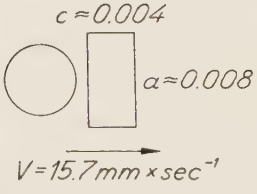

Fig. 32 A. Impulse shape of a single erythrocyte. Relatively small aperture and maximum scanning velocity.

tion of a human erythrocyte or pairs of erythrocytes is given in relation to the scanning aperture, together with the recorded impulse shape. The erythrocyte-aperture diagrams are made from visual observation through the eyepiece, and the impulse patterns are reproductions from photographs. The same sweep time and oscillograph amplifier gain were used in all records.

In all these experiments, the diameter of the erythrocytes was about 0.0075 mm. The dimensions of the scanning apertures used in the different experiments are given in the figures.

55. **Single impulses. Effect of different aperture dimensions.** In the first three diagrams, the impulse shapes are shown for several different aperture lengths in the scanning direction,

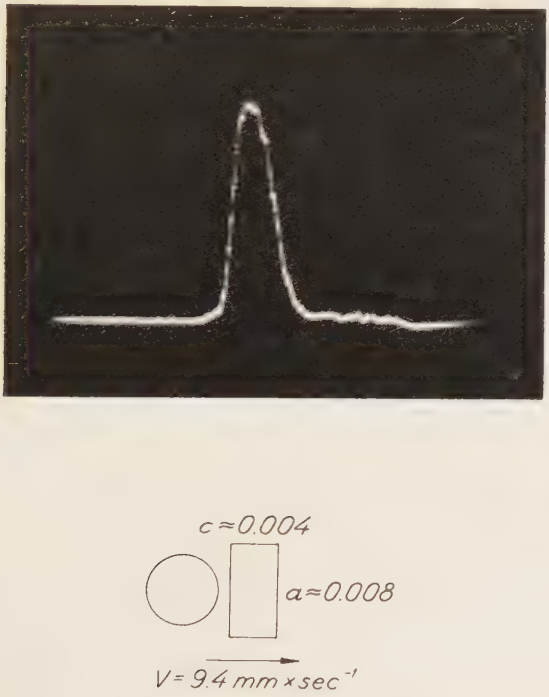

Fig. 32 B. Impulse shape of a single erythrocyte. Minimum scanning velocity.

i. e., *c*, when a single erythrocyte passes through the middle of the scanning aperture area. In this case, *d*, (the maximum length of the cell which passes inside the aperture in the scanning direction) is equal to the diameter of the cell. In Fig. 32, the aperture length *c* is relatively small in relation to the diameter of the cell (cf. the theoretically derived impulse shape in Fig. 23). Fig. 32 A gives the impulse-shape when the

scanning velocity, V, is equal to 15.7 mm. per second; Fig. 32 B gives the impulse shape when $V = 9.4$ mm. per second (*i. e.*, the maximum and minimum velocities on the helical scanning track). The amplitude of the background noise is reasonably small but is clearly seen as the upward step in the flat region behind the impulse. In Figs. 33 and 34, the aperture length, c,

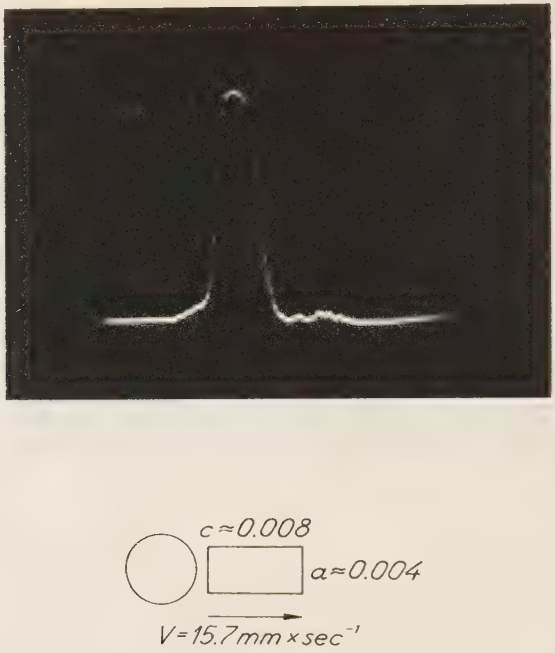

Fig. 33. Impulse shape of a single erythrocyte. The aperture has been rotated through 90° so that c is the larger aperture dimension.

has been made larger than the diameter of the cell. In Fig. 33, the aperture used in Fig. 32 was rotated through 90°. In Fig. 34 a larger aperture was used. The flat top of the impulse is seen (cf. Fig. 24), and a small sag is present. Because the area of the aperture used in Fig. 34 is larger than those in Figs. 32 and 33, the noise is also prominent here. The background noise amplitude is not so clearly seen in Fig. 34. It is made up of the curled 'foot' on either side of the impulse.

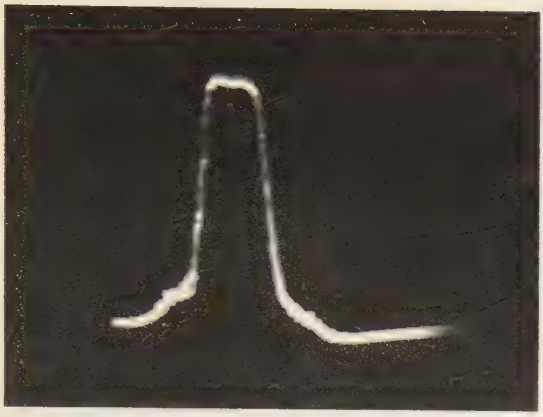

Fig. 34. Impulse shape of a single erythrocyte. Large aperture (*c*, very large).

56. Shape of impulses obtained from two erythrocytes situated close to each other. Effect of aperture dimensions. In Figs. 35—40, the impulses of two erythrocytes lying close together are given. In Figs. 36 and 37, the first erythrocyte passes through the scanning aperture to one side of the middle line, but with the major part inside the aperture area. In the remaining diagrams, the first erythrocyte passes along the middle line through the aperture area and wholly within it. Only a part of the other erythrocyte passes inside the aperture area, and the impulse produced by this cell is smaller than that produced by the first cell (cf. Fig. 27). In the impulse patterns, two horizontal lines are drawn which indicate schematically the position of two different amplitude discriminator

bias settings, *i. e.*, two different l values. In Fig. 35, the two impulses are resolved and properly recorded only if the higher value of the two discriminator bias settings is used, *i. e.*, the smaller l value. The background noise and the noise that over-

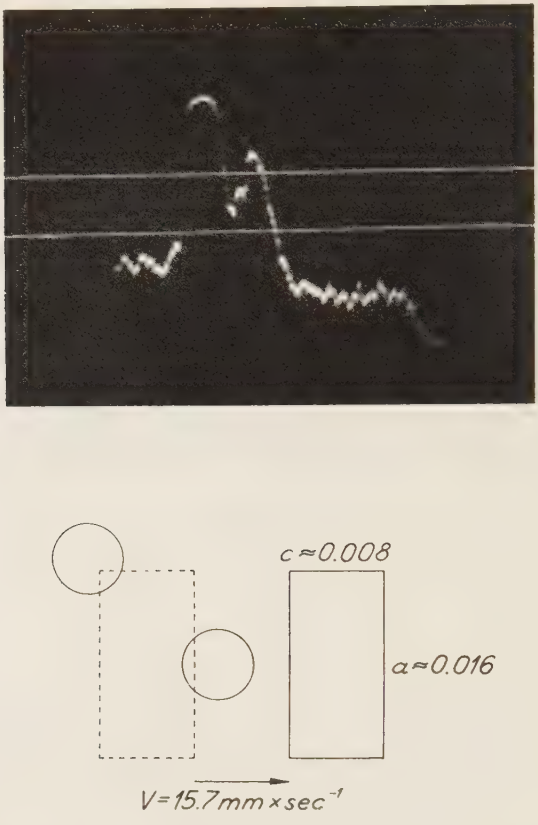

Fig. 35. Impulse shape of two consecutive erythrocytes lying close together. Two different discriminator bias levels are schematically given by the two horizontal lines.

lies the signal impulse are rather prominent, but no spurious counts are recorded with the bias setting used. In Fig. 36, the aperture has been rotated through 90° so that the aperture dimension, c, is the larger aperture dimension, and accordingly l is increased. The two impulses are not separated

and are not resolved at any discriminator bias setting. In Fig. 37, a smaller aperture is used, and the two impulses are very well separated and resolved at both discriminator bias settings.

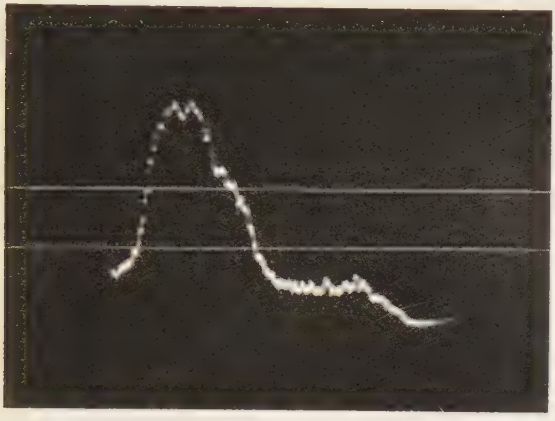

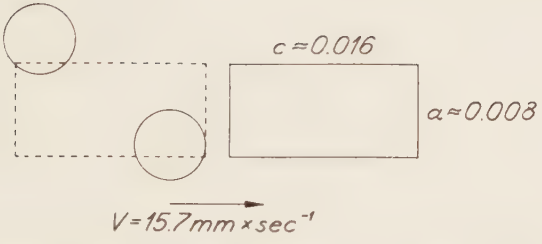

Fig. 36. Impulse shape for two consecutive erythrocytes. The aperture of Fig. 35 has been rotated through 90°. Resolution of the two impulses is impaired.

57. **Effect of different time constants in the amplifier on the impulse shape and the resolving power.** In Fig. 38, the shunt capacitance across the multiplier phototube load has been disconnected (cf. Fig. 29 and C_1 in Fig. 28). The separation of the two impulses is rather good compared with the experiments where the same aperture dimensions were used, but

where the shunt capacitance was functioning (cf. Fig. 35). The noise is very prominent, giving rise to many spurious counts at all bias settings except the very high values, where only the first impulse, *i. e.*, the largest one, was recorded. In Fig. 39,

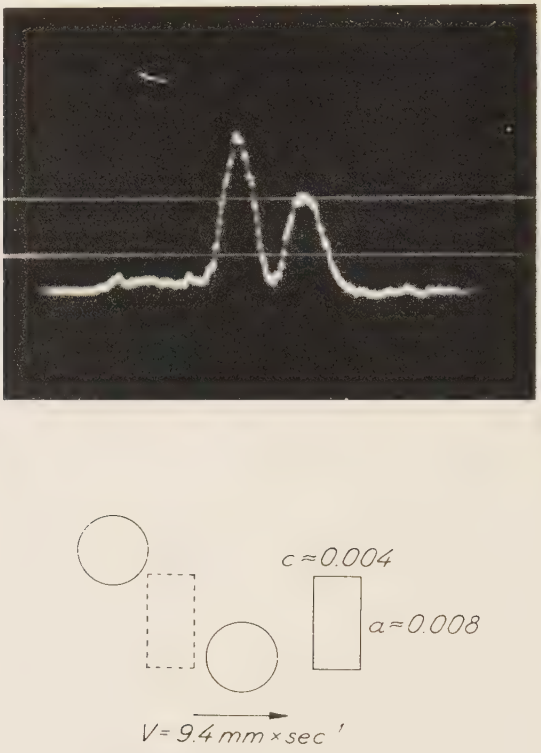

Fig. 37. Impulse shape of two consecutive erythrocytes lying close together. A relatively small aperture was used, and the resolution is complete.

the same aperture dimensions and scanning velocity were used as in Fig. 38; but a shunt capacitance of about 350 μμF was placed across the multiplier phototube load. The impulse separation is very bad. The two impulses can hardly be distinguished and the cells are consequently not resolved. The actual band width is only about 500 cycles per second and the rise time of the amplifier about $770 \cdot 10^{-6}$ seconds. The noise

is eliminated to a large extent, and the impulse curve is very smooth. The form of the impulse complex is very like that of Fig. 36. In Fig. 40, the shunt capacitance of 50 μμF is replaced across the multiplier phototube load but the time constant of the

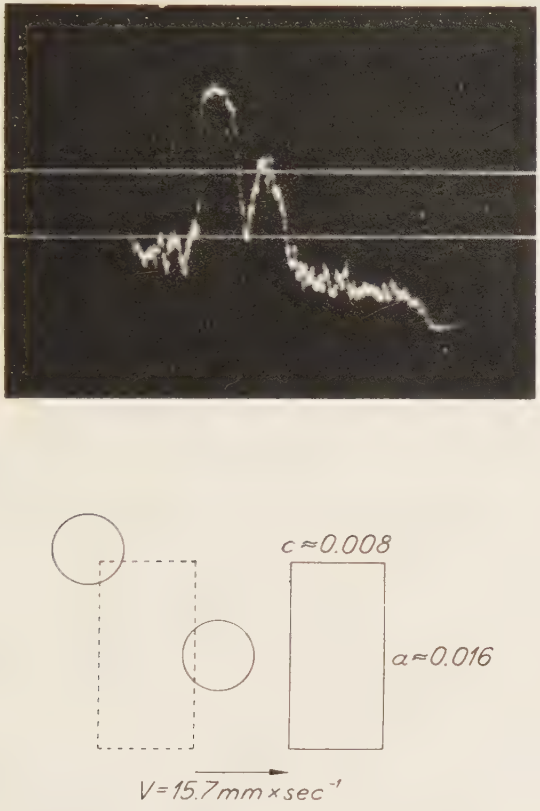

Fig. 38. Impulse shape for two consecutive erythrocytes lying close together. Shunt capacitance across the multiplier phototube has been disconnected, and noise has increased.

coupling circuit between the amplifier output and the amplitude discriminator is lowered from about $(1.0 + 0.033) \cdot 50{,}000 \cdot 10^{-6}$ seconds to about $(1.0 + 0.033) \cdot 500 \cdot 10^{-6}$ seconds which is about the length of the impulse at the actual scanning velocity (V = 15.7 mm. per second). The separation of the two impulses

is very good, but the short time constant introduces an appreciable overshoot and impulse distortion. The overshoot produced

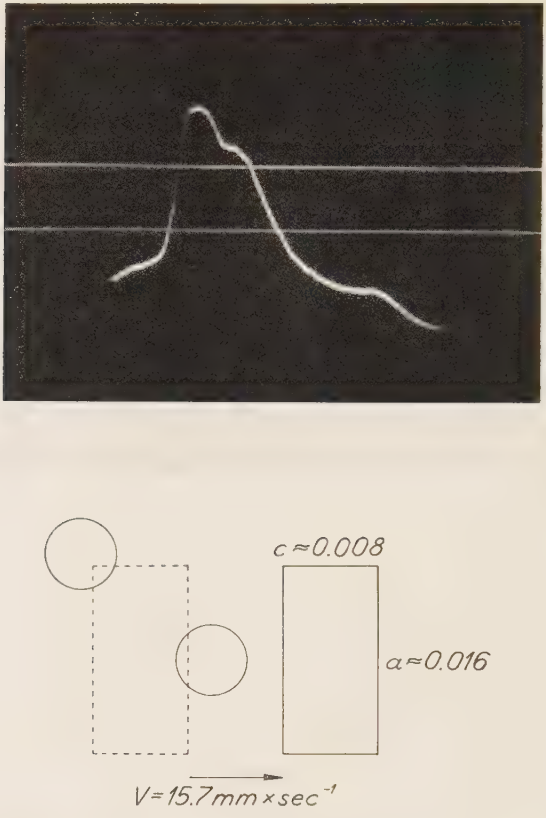

Fig. 39. Impulse shape of two consecutive erythrocytes lying close together. There is a relatively large shunt capacitance across the multiplier phototube load, and noise has decreased. Resolution of the two elements is impaired.

by the first impulse submerges the impulse of the second erythrocyte, and the real impulse amplitude is reduced; thus two impulses are recorded only at the lower one of the two discriminator bias settings shown in the figure.

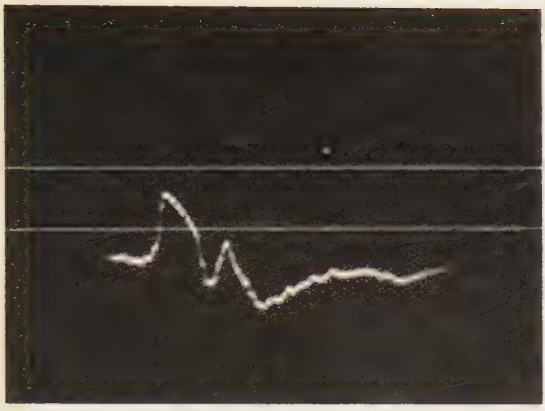

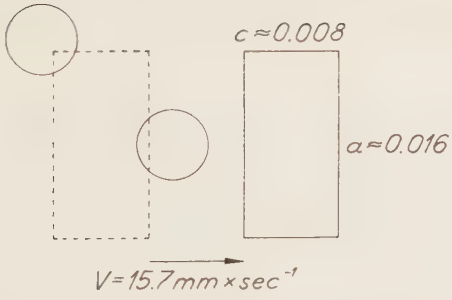

Fig. 40. Impulse shape of two consecutive erythrocytes lying close together. Overshoot was produced by improper time constant in the amplifier.

58. **Shape of a threshold impulse.** Fig. 41 shows the impulse produced by a cell when only a small part of its area passes inside the scanning aperture area, and the light impulse is just large enough to produce a threshold signal (z about 0.003 mm.). (Cf. the theoretically derived impulse shape in Fig. 26). In this case, d is smaller than the diameter of the cell: and consequently the impulse length is shorter according to equation (54). This fact is also clearly seen from the impulse pattern in Fig. 41.

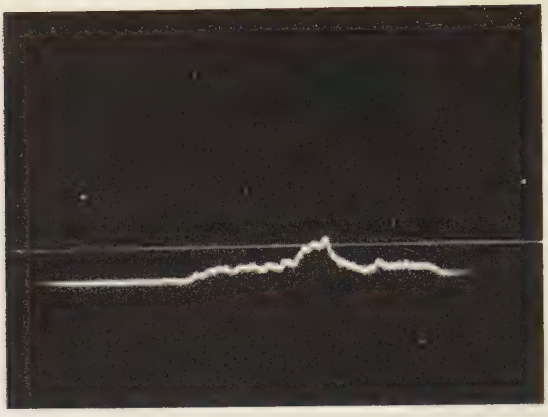

Fig. 41. Impulse shape of a single erythrocyte when only a small part of its area passes inside the aperture area, so that a threshold signal is just released.

59. Discussion. A comparison of the theory and the results of the impulse shape experiments shows satisfactory agreement. It has already been pointed out (see § 46) that the impulse shape was derived by assuming that the elements to be counted were homogeneous in the whole of their area. However, human erythrocytes are biconcave discs, the light intensity from which is somewhat stronger in the periphery. No marked differences between the theoretical and experimental impulse shapes that might be due to this fact have been found in these semi-quantitative experiments.

Experiments where both the maximum and minimum values of the scanning velocity were used indicate that the impulse shape, impulse amplitude, and resolving power corresponding

to the two velocities, are nearly equal. The slower velocity produces a somewhat larger impulse length. It is clearly shown that the resolving power is better when the aperture length in the scanning direction, c, is relatively small. The background

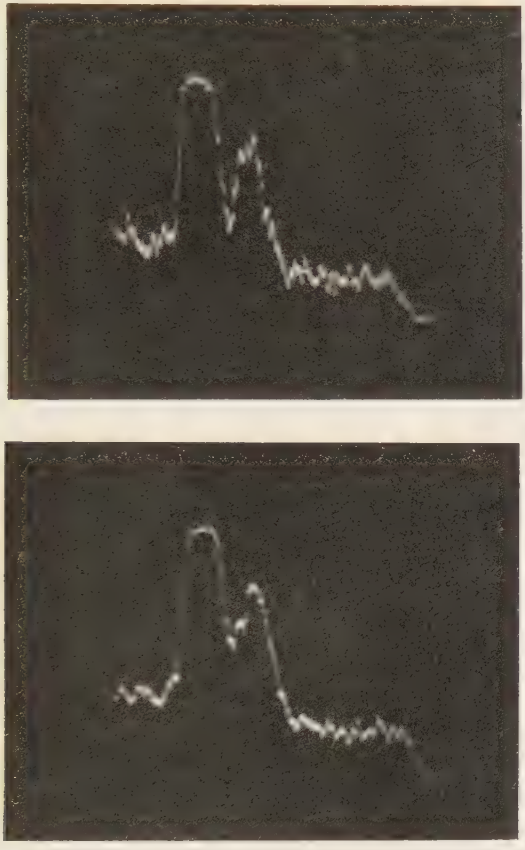

Fig. 42. Impulse shape for two consecutive erythrocytes. Shunt capacitance over the multiplier phototube is disconnected. Two different exposures are given. Randomness of the impulse outline, due to noise, is clearly seen.

noise increases as the aperture area increases, this area should therefore be kept rather small. Otherwise, the contrast in the dark field system has to be improved (cf. § 16). Moreover, it is evident that an impulse overlayed by too much noise has a non-constant amplitude because the noise impulses increase

the real signal impulse at random (cf. § 16). This phenomenon is clearly seen from the two different exposures of the same pattern (Fig. 38) which are given in Fig. 42.

The effects of the different time constants were discussed in the description of the electronic system and in the account of each impulse shape experiment.

In order to decide whether certain types of cells or other elements can be satisfactorily counted by the scanning counting method, the experimental arrangement described for investigation of the impulse shape of a single cell or group of cells is very usable.

CHAPTER VIII.

Counting experiments.

60. General considerations. The aim of the counting experiments described below is to determine whether or not the apparatus functions according to the theory presented. As experimental distributions, the author selected the element distributions which arise when human erythrocytes in a sufficiently diluted and thoroughly mixed fluid suspension have settled to the bottom of a counting chamber. The erythrocytes were considered to be situated at random. As mentioned above (cf. § 59), human erythrocytes are biconcave discs; and because of this fact, the light intensity change produced by such elements is more pronounced on the periphery of the elements than in the centre. Thus the apparatus was tested on elements of a shape somewhat different from that assumed when the theory was first proposed, *i. e.*, a constant light intensity change from all parts of the element area.

When erythrocytes which have settled randomly are counted by the apparatus, a certain number of elements should be missed, according to the theory proposed. The proportion of missed elements should decrease as the effective aperture area decreases and as the number of elements per unit area decreases. When the number of experimentally obtained elements has been corrected for missed elements, and when the corrected numbers are plotted against the aperture width a, a straight line should result provided we ignore random variations. (We assume that scanning runs have been performed with at least three different aperture widths a; cf. also Fig. 12.). The slope of the straight line should be the same as that of a line constructed from the number of elements per unit area obtained by visual count, again provided that we ignore random variations. All this is possible only if the sensitivity of the apparatus, *i. e.*, $\bar{z}$, is constant for the scanning runs corresponding to the different aperture sizes, or in other words if the difference $\bar{z}_1 - \bar{z}_2$ has the value $= 0$.

Counting experiments were performed on three different fillings (denoted I, II, and III) of the counting chamber. On each of these three element distributions four different scanning experiments were performed (in filling I five experiments were performed), each corresponding to a certain $\bar{\varepsilon}$ value. Three different aperture widths, a_1, a_2 and a_3 and the same aperture length c, were used in each experiment, *i. e.*, the aperture dimensions were $a_1 \cdot c$, $a_2 \cdot c$ and $a_3 \cdot c$.

61. Experimental arrangement for testing the reproducibility of the apparatus. In the counting experiment described below, fifteen scanning runs were performed in each experiment, five for each of the three apertures (in experiments nos. 10, 11 and 12: six). These scanning runs were performed in the same element region and in such a way that the aperture was always shifted between every two runs, *i. e.*, the sequence of apertures used was: a_1, a_2, a_3, a_1, a_2, a_3, . . . This arrangement was made in order to minimize the effect of possible systematic errors due to long-time fluctuation of the sensitivity of the recording system, *i. e.*, change in the light intensity of the lamp, fatigue of the multiplier phototube, and instability of the electronic system.

In these experiments, it is obviously important that every one of the three apertures be always brought to the same position relative to the element distribution when the apertures are shifted. Furthermore, the scanning track corresponding to aperture a_3 should be situated inside track a_2 which in turn should be situated inside track a_1 ($a_3 < a_2 < a_1$); cf. § 31. However, on account of mechanical imperfections of the stop mechanism of the aperture holders ((54) of Fig. 19), the scanning apertures did not always assume exactly the same position. The displacement of the apertures is estimated to be of the order of magnitude of about 0.05 mm. in the image plane, which corresponds to about 1 micron in the object plane (magnification 50 x). Consequently, the apparatus error, which we measure by the standard error, will be increased by a certain factor because of inexact coincidence of the five scanning tracks corresponding to each aperture: *i. e.*, the apparatus error contains a certain contribution from the random

distribution of the elements. It may be remarked that this part of the standard error would have been eliminated if all five scanning runs corresponding to each aperture had been performed without shifting the apertures. On account of mechanical imperfections in the rotating table, it is not sure, however, that the position of an aperture relative to the element distribution is perfectly reproduced in different scanning runs, even if the apertures are not shifted. Consequently, the apparatus error contains a certain contribution from the random distribution of the elements whether the apertures are shifted according to the above description or not. Further discussion of the apparatus error is given in § 72.

62. Tabulated values. The results of the counting experiments are collected in three tables, corresponding respectively to the three fillings of the counting chamber. The first column gives the sensitivity $\bar{z}$ evaluated by means of equation (39). All values for the number of recorded elements given in the tables and the diagrams represent the mean of the five (or six, see above) separate scanning runs of each aperture mentioned above, here denoted as N'. The apparatus error is given in the tables in the form of the percentage standard error of N'. The standard error is

$$\varepsilon = \sqrt{\frac{\sum_{\mu=1}^{5} (N_\mu' - N')^2}{5 \cdot 4}} . \tag{57}$$

Besides N' and the percentage standard error, the following data are given for each of the three apertures used: the dimensions of the aperture relative to the object (the ratio between the physical size and the magnification factor, F); and the number of elements recorded, corrected for missed elements according to equations (41) or (42). In the last columns at the right in the tables N_1—N_3 is given (in filling III: N_1—N_2) together with the percentage standard deviation due to the Poisson distribution. Further, the standard error, ε_D of N_1—N_3 (the apparatus error) is given in per cent. ε_D is obtained from:

$$\varepsilon_D^2 = \left[\varepsilon_1 \cdot \frac{N_1}{N_1'}\right]^2 + \left[\varepsilon_3 \cdot \frac{N_3}{N_3'}\right]^2; \tag{58}$$

where ε_1 and ε_3 denote the standard errors of N_1' and N_3' respectively. The number of cells per square mm. obtained by the scanning method and by the visual count are given. Finally, the percentage difference between the results obtained by the scanning method and by the visual count is given.

63. **The diagrams.** Each diagram corresponds to a separate experiment. The numbers of experimentally recorded cells, N', are represented by black circles connected by solid lines (—●—●—●—) and the experimentally recorded numbers, after correction for missed cells, N, are represented by open circles connected by dashes (- - ○ - - ○ - - ○ - -). After introducing the number of cells per unit area obtained by visual counting in equation (2), and by use of the value of $\bar{\varepsilon}$ corresponding to the actual experimental data obtained with the scanning method, the numbers of cells corresponding to the different aperture widths a are evaluated. By use of these values, the lines referring to the visual count are drawn in the diagrams. They are represented by partly shaded circles connected by dotted lines (· · ◑ · · · ◑ · · ◑ · ·). In the experiments described, the $\bar{\varepsilon}$ value was varied by changing the light intensity (moving a condenser lens situated close to the microscope lamp), by changing the multiplier phototube voltage, and by changing the amplitude discriminator bias setting (given in arbitrary units below each diagram).

64. **The mean diameter of the elements.** In all numerical calculations, it is assumed arbitrarily that the mean diameter of the erythrocytes is 8 microns. When the number of missed elements is of the order of magnitude met with in the experiments described here (below 10 per cent), it is clearly seen from equations (36)— (44) that a 25 per cent change in the diameter of the elements, for example, has very little influence on the result. Let us evaluate the result of experiment no. 2 (table I) assuming a mean diameter of 6 microns instead of 8 microns (we give the figures referring to a mean diameter

of 8 microns between brackets): number of recorded elements corrected for missed elements, aperture no. 1: 2992 (2997); aperture no. 3: 1730 (1731). The number u^* of elements per unit area computed from these values is equal to 216.7 (217.4). Thus the difference is about 0.3 per cent.

65. The counting procedure. When the counting experiments were performed, the following procedure was used. Capillary blood is diluted with a 0.9 per cent solution of sodium chloride. Before filling the counting chamber, we mix the cell suspension for about 10 minutes in an apparatus of the type described by Bryan and Garrey (1934). In most of the experiments, it is essential that one obtains several scanning runs with one filling of the counting chamber. In order to avoid evaporation of liquid from the cell suspension in the chamber during this time, the open entrances to the chamber space are occluded with vaseline[1]. By this means, the same filling can be used for several hours without perceptible change. After the filled counting chamber has been placed in position on the stage and the erythrocytes have settled to the bottom, the image is focussed by visual control through the side tube eyepiece of the microscope, which is adjusted so that the same image sharpness is obtained through this eyepice and the eyepice (61) placed over the scanning aperture (see Fig. 18). Then the holders described in § 42 and shown in Fig. 61 are carefully adjusted and the image sharpness is readjusted. Before a series of counting experiments is started, the electronic system and the microscope lamp are allowed to warm up for about 10 minutes. The moving stage is set in motion after the scanning aperture to be used has been pushed into place, the high voltage supply of the multiplier phototube switched on, and the scaler and mechanical tabulator reset. When the rotating stage has stopped, the tabulator and scaler are read. In order to protect the multiplier phototube from damage by excessive light, it is necessary to disconnect its high voltage supply before the light shield is removed or the shutter moved to the side to change the scanning aperture.

[1] The author is indebted to Dr. G. Wallenius for this suggestion.

Table I.

Experiment no.	z in μ	Aperture no. 1				Aperture no. 2				Aperture no. 3				Scanning method				Visual count		Difference between the methods $\frac{u_n - u_v}{u_v} \cdot 100$ in per cent
		Aperture dimensions: a and c in μ	Number of cells			Aperture dimensions: a and c in μ	Number of cells			Aperture dimensions: a and c in μ	Number of cells			$N_1 - N_3$	Standard deviation (Poisson) $\frac{100}{\sqrt{N_1 - N_3}}$ in per cent	Standard error (apparatus error) of $N_1 - N_3$ in per cent	Scanning method number of cells u_n per mm²	Visual count number of cells u_v per mm²	Standard deviation (Poisson) $\frac{100}{\sqrt{N_v}}$ in per cent	
			experimentally obtained: N_1'	after correction for missed elements: N_1	standard error, ε_1, in per cent		experimentally obtained: N_2'	after correction for missed elements: N_2	standard error, ε_2, in per cent		experimentally obtained: N_3'	after correction for missed elements: N_3	standard error, ε_3, in per cent							
1	+1.56	$a = 17.9$ $c = 9.0$	2834	2999	0.42	$a = 13.4$ $c = 9.0$	2255	2357	0.18	$a = 8.9$ $c = 9.0$	1663	1716	0.53	1283	2.79	1.21	219.8	224.2	2.23	— 1.74
2	+1.70	„	2831	2997	0.27	„	2256	2360	0.45	„	1677	1731	1.10	1266	2.81	1.60	217.4	„	„	— 3.03
3	+2.43	„	3106	3319	0.35	„	2518	2655	0.30	„	1931	2008	0.52	1311	2.76	1.18	225.1	„	„	+ 0.40
4	+2.68	„	3237	3471	0.33	„	2666	2819	0.41	„	2043	2130	0.52	1341	2.73	1.19	230.3	„	„	+ 2.72
5	+1.77	$a = 8.6$ $c = 5.0$	1830	1876	0.70	$a = 6.9$ $c = 5.0$	1578	1611	0.32	$a = 4.7$ $c = 5.0$	1253	1273	0.77	603	4.07	2.64	239.0	„	„	+ 6.60

66. Experiments 1—5: Table I: diagrams given in Figs. 43—47. Capillary blood is diluted in the ratio 1: 2.000. The total number of erythrocytes visually counted is 2018 (9 square mm.). The number of erythrocytes per unit area found by the

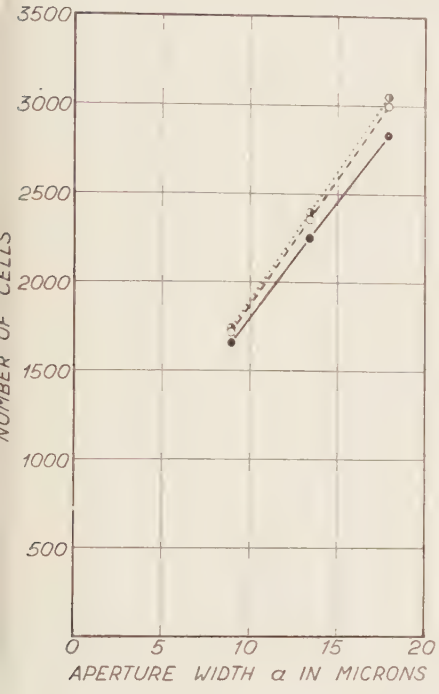

Fig. 43.

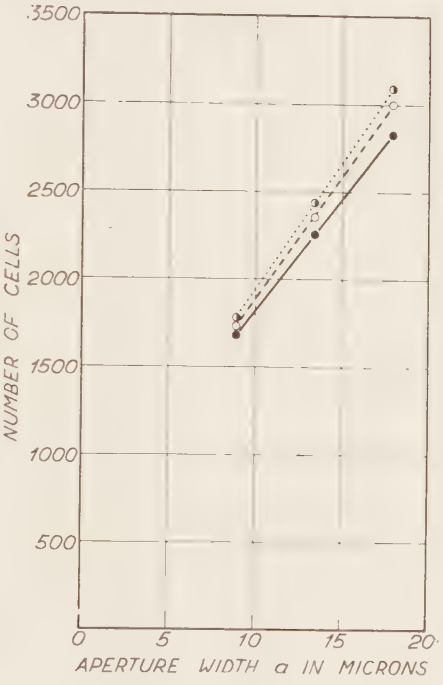

Fig. 44.

Fig. 43. Diagram referring to exp. 1. In this and the following diagrams ●—●—● denotes the number of cells experimentally obtained. ○----○----○ denotes this number after correction for missed cells. ◑····◑····◑ denotes the number of cells obtained by visual count. In exp. 1 a relatively high light intensity was used. Multiplier phototube voltage about 820. Discriminator bias = 80 (arbitrary units).

Fig. 44. Diagram referring to exp. 2. Relatively low light intensity. Multiplier phototube voltage about 820. Discriminator bias = 60.

scanning method was evaluated by use of the largest[1] and smallest of the three apertures used. Because of the relatively large effective aperture area, (large aperture size and high

[1] In experiments 1—4 aperture width a_1 is somewhat too large resulting in a small overlapping between adjacent turns of the scanning track.

value) used in experiments 1—4, the number of missed erythrocytes was quite noticeable. As is clearly seen from the diagrams of experiments 1—4 (Figs. 43—46) and from table I, the slopes of the curves referring to the scanning method without correc-

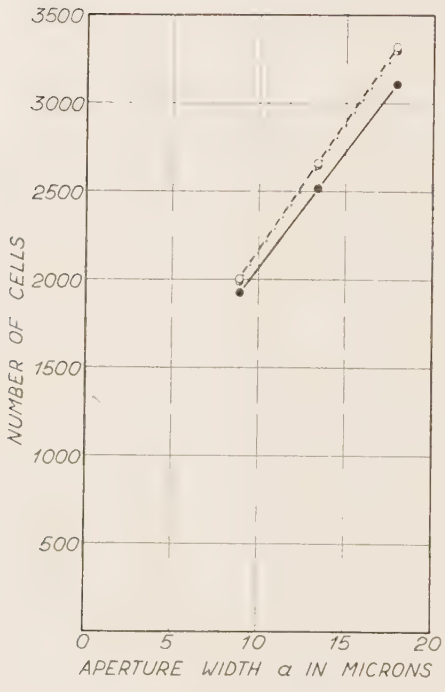

Fig. 45.

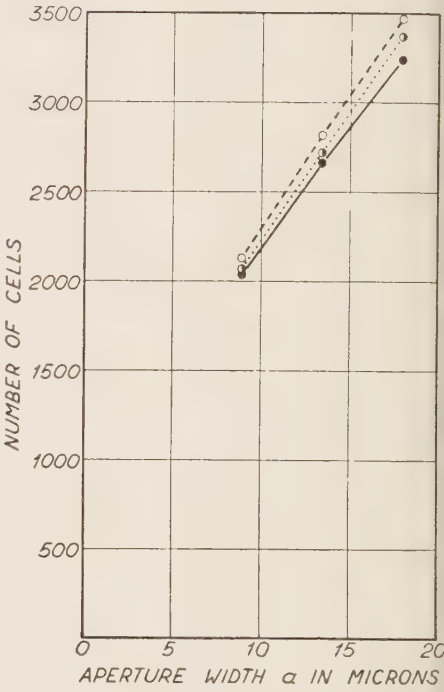

Fig. 46.

Fig. 45. Diagram referring to exp. 3. Relatively low light intensity. Multiplier phototube voltage about 880. Discriminator bias = 60.

Fig. 46. Diagram referring to exp. 4. Relatively high light intensity. Multiplier phototube voltage about 820. Discriminator bias = 60.

tion for missed elements are considerably less than those referring to the visual count. However, after correction for missed elements according to equations (41)—(42), the slopes of the curves of the scanning method agree very well with those of the visual count, in conformity with the theory. The linearity of the scanning method curves after correction for missed elements is good (visual judgment). In these experiments, it is evident that the $\bar{z}$ value is nearly constant and

equal in the records of all three aperture sizes used. Furthermore, it is seen from the diagrams that the deviation between the uncorrected and corrected curves is more pronounced the larger the effective aperture areas are, also in good conformity

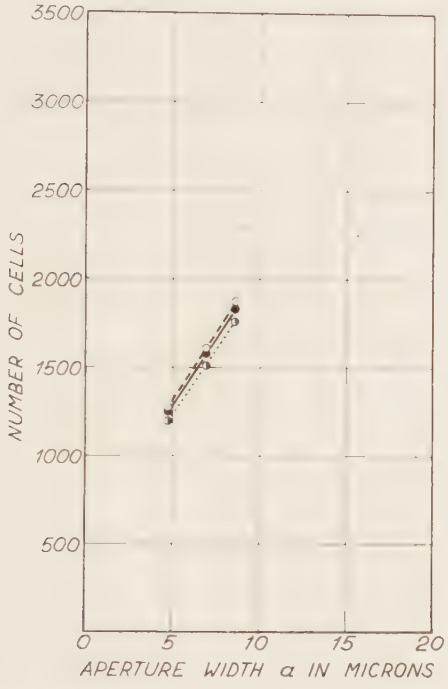

Fig. 47. Diagram referring to exp. 5. Smaller apertures than used in experiments 1—4. Relatively high light intensity. Multiplier phototube voltage about 820. Discriminator bias = 60.

with the theory (cf. Fig. 12). Uncorrected, the number of erythrocytes per unit area is 8.7 per cent in experiments nos. 1 and 2, 10.4 per cent in experiment no. 3, and 11.0 per cent in experiment no. 4, below the corrected results. The standard error ε, as a percentage of N', is rather low and is below 1 per cent in most experiments The standard error of the difference N_1—N_3 *i. e.*, the standard error of the obtained number of erythrocytes per unit area, ε_D is below 2 per cent in experiments 1—4, and is considerably lower than the Poisson deviation.

In experiment no. 5 smaller apertures were used and therefore the number of missed elements is lower. The number of erythrocytes per unit area obtained by the scanning method is somewhat higher than in experiments 1—4.

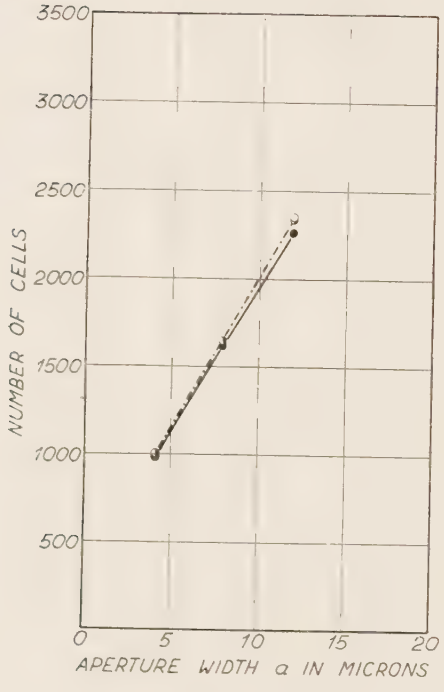

Fig. 48.

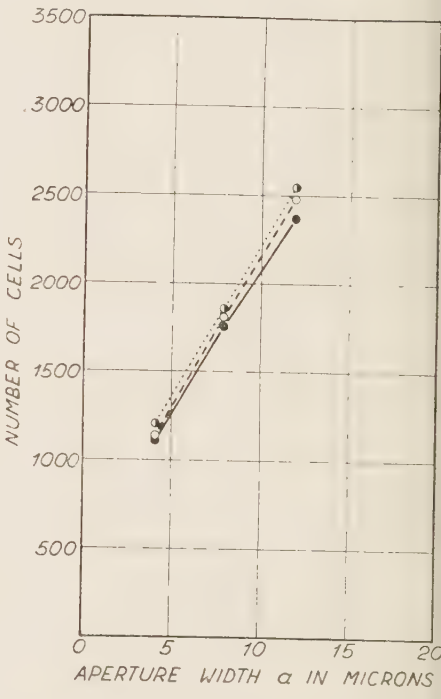

Fig. 49.

Fig. 48. Diagram referring to exp. 6. Relatively high light intensity. Multiplier phototube voltage about 820. Discriminator bias = 80.

Fig. 49. Diagram referring to exp. 7. Relatively high light intensity. Multiplier phototube voltage about 820. Discriminator bias = 60.

67. Experiments 6 – 9: Table II: diagrams given in Figs. 48 -51. Dilution 1: 1,500. The number of erythrocytes visually counted is 2915 (9 square mm.). In evaluating the number of elements per unit area, the largest and smallest of the three apertures were used. The apertures in this group of experiments were of a size between those used in experiments nos. 1—4 and those used in experiment 5 (see table II). The

Table II.

Experiment no.	$\bar{z}$ in μ	Aperture no. 1				Aperture no. 2				Aperture no. 3				Scanning method				Visual count		Difference between the methods in per cent $= \frac{u_a - u_v}{u_v} \cdot 100$
		Aperture dimensions: a and c in μ	Number of cells			Aperture dimensions: a and c in μ	Number of cells			Aperture dimensions: a and c in μ	Number of cells			$N_1 - N_3$	Standard deviation (Poisson) in per cent $= \frac{100}{\sqrt{N_1 - N_3}}$	Standard error (apparatus error) of $N_1 - N_3$ in per cent	Scanning method number of cells, u_a per mm²	Visual count number of cells u_v per mm²	Standard deviation (Poisson) in per cent $= \frac{100}{\sqrt{N_v}}$	
			experimentally obtained: N_1'	after correction for missed elements: N_1	standard error, ε_1, in per cent		experimentally obtained: N_2'	after correction for missed elements: N_2	standard error, ε_2, in per cent		experimentally obtained: N_3'	after correction for missed elements: N_3	standard error, ε_3, in per cent							
6	+0.88	$a = 11.9$ $c = 8.0$	2265	2355	0.73	$a = 7.9$ $c = 8.0$	1621	1665	0.72	$a = 4.1$ $c = 8.0$	986	1001	1.2	1354	2.72	1.56	268.3	265.0	2.05	+1.25
7	+1.48	„	2374	2478	0.61	„	1757	1811	0.53	„	1117	1138	0.38	1340	2.73	1.18	265,5	„	„	+0.19
8	+1.78	„	2321	2423	0.25	„	1740	1795	0.37	„	1086	1108	0.40	1315	2.76	0.57	260.6	„	„	−1.66
With too high a light intensity and sensitivity of the recording system; systematic error introduced (cf. § 69)																				
9	+2.11	„	2761	2909	1.1	„	2105	2187	1.6	„	1347	1382	1.2	1527	2.56	2.42	302 6	„	„	14.2

curves, corrected for missed elements, referring to experiments 6—8 show good linearity, except experiment no. 8, which shows a slight displacement of the point referring to the medium sized aperture. The slopes of the curves after correction

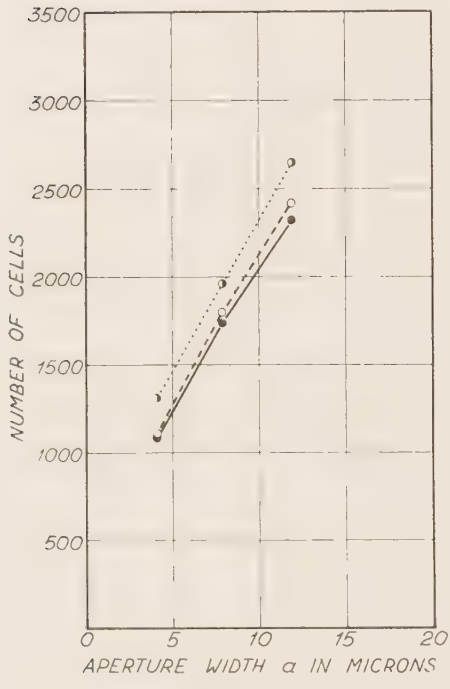

Fig. 50.

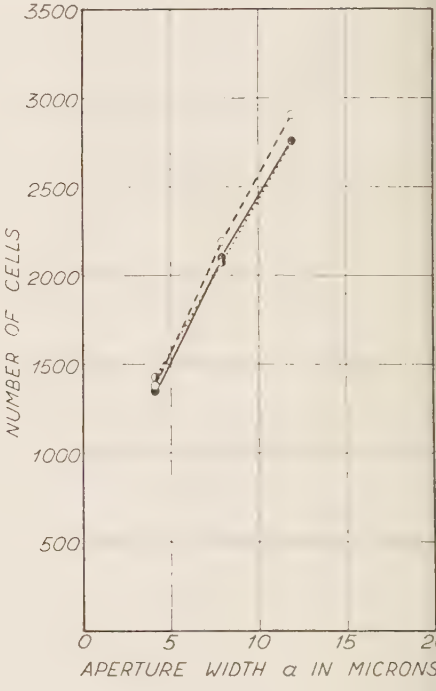

Fig. 51.

Fig. 50. Diagram referring to exp. 8. Relatively high light intensity. Multiplier phototube voltage about 900. Discriminator bias = 120.

Fig. 51. Diagram referring to exp. 9. Relatively high light intensity. Multiplier phototube voltage about 900. Discriminator bias = 60. In this experiment the conformity with the result obtained by visual count is lost (see text).

agree very well with those of the visual count. Uncorrected, the number of erythrocytes per unit area is 5.6 per cent in experiment no. 6, 6.2 per cent in experiments nos. 7 and 8, below the corrected results. The standard error of the difference $N_1 - N_3$, for the number of erythrocytes per unit area, is below 2 per cent. In experiments 6—8 the Poisson deviation dominates over the apparatus error.

In experiment no. 9, the slope of the corrected curve is considerably larger than that of the visual count: and the result is about 14 per cent too high. The linearity is also somewhat impaired, and the curve is convex upward even after correction for missed elements. The reason for these discrepancies is probably to be found in excessive light intensity and amplifier gain, which introduces a systematic error due to change in $\bar{z}$ with change in aperture size (cf. § 16) or by giving rise to spurious impulses.

68. Experiments 10—13: Table III: diagrams given in Figs. 52—55. Dilution 1: 1,100. The number of erythrocytes visually counted is 3617 (9 square mm.). The same apertures were used

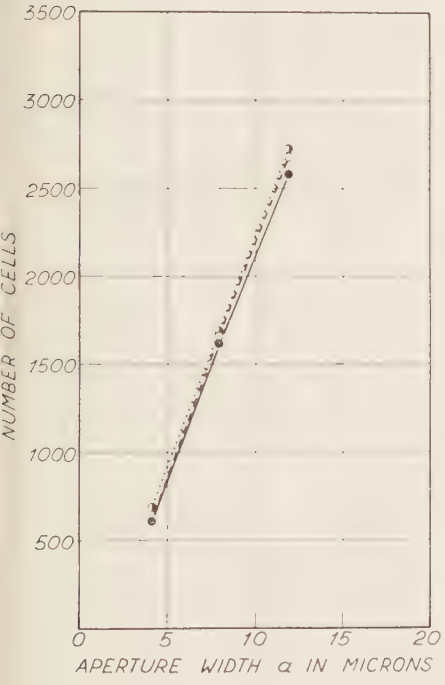

Fig. 52.

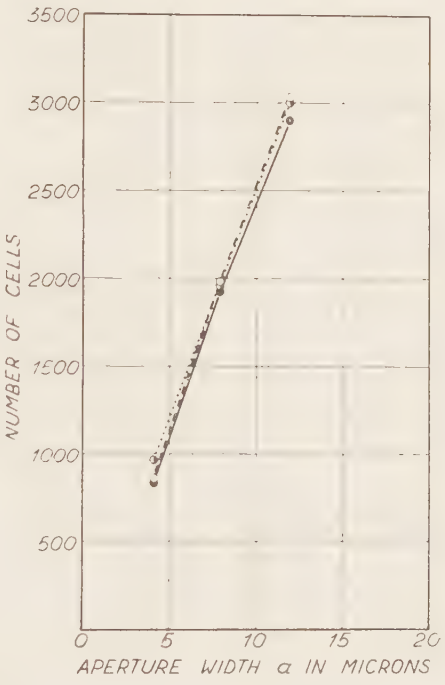

Fig. 53.

Fig. 52. Diagram referring to exp. 10. Relatively low light intensity. Multiplier phototube voltage about 820. Discriminator bias = 100.

Fig. 53. Diagram referring to exp. 11. Very low light intensity. Multiplier phototube voltage about 820. Discriminator bias = 60.

Table III.

Experiment no.	z in μ	Aperture no. 1				Aperture no. 2				Aperture no. 3				Scanning method				Visual count		Difference between the methods in per cent $= \frac{u_a - u_v}{u_v} \cdot 100$
		Number of cells			Aperture dimensions: a and c in μ	Number of cells			Aperture dimensions: a and c in μ	Number of cells			Aperture dimensions: a and c in μ	$N_1 - N_2$	Standard deviation (Poisson) in per cent $= \frac{100}{\sqrt{N_1 - N_2}}$	Standard error (apparatus error) of $N_1 - N_2$ in per cent	Scanning method number of cells, u_a per mm²	Visual count number of cells u_v per mm²	Standard deviation (Poisson) in per cent $= \frac{100}{\sqrt{N_v}}$	
		experimentally obtained: N_1'	after correction for missed elements: N_1	standard error, ε_1, in per cent		experimentally obtained: N_2'	after correction for missed elements: N_2	standard error, ε_2, in per cent		experimentally obtained: N_3'	after correction for missed elements: N_3	standard error, ε_3, in per cent								
10	−0.71	2578	2680	0.55	$a = 11.9$ $c = 8.0$	1619	1658	1.1	$a = 7.9$ $c = 8.0$	609	614	1.2	$a = 4.1$ $c = 8.0$	1022	3.13	2.50	394.9	401.9	1.66	−1.74
11	−0.19	2900	3036	0.45	„	1925	1982	0.52	„	843	854	0.85	„	1054	3.08	1.62	407.3	„	„	+1.34
12	0.26	3020	3165	0.82	„	1993	2053	1.4	„	925	937	2.0	„	1112	3.00	3.49	429.7	„	„	+6.91
With too high a light intensity and sensitivity of the recording system; systematic error introduced (cf. § 69)																				
13	±0.0	3363	3548	0.76	„	2279	2360	0.96	„	1094	1112	2.2	„	1188	2.90	2.98	459.0	„	„	+14.2

as in experiments nos. 6—9. On account of the relatively large number of erythrocytes per unit area and the more concentrated blood plasma (presence of chylomicrons) in this group of experiments, the diffuse background light was more trouble-

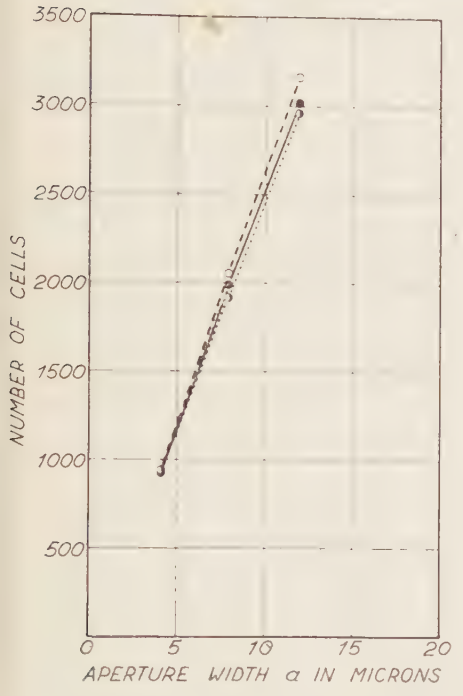

Fig. 54.

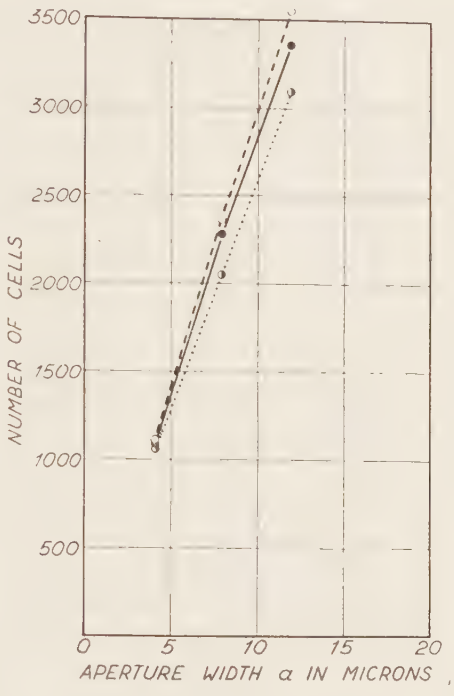

Fig. 55.

Fig. 54. Diagram referring to exp. 12. Relatively low light intensity. Multiplier phototube voltage about 820. Discriminator bias = 80.

Fig. 55. Diagram referring to exp. 13. Relatively high light intensity. Multiplier phototube voltage about 900. Discriminator bias = 120. The conformity with the result obtained by visual count is lost in this experiment. (see text.)

some than in the experiments so far described. In order to keep the $\bar{z}$ value as nearly constant as possible from one aperture to the other, relatively low light intensity and amplifier gain were used, *i. e.*, $\bar{z}$ was made rather low. Furthermore, the effect of changes in the value of $\bar{z}$ from one aperture to the other was decreased by employing the two largest apertures in

evaluating the number of elements per unit area. This was because the difference in $\bar{z}$ was less pronounced between these two apertures than between the largest and smallest apertures. As long as $\bar{z}$ is negative, conformity with the visual count and the linearity are as good as in the experiments of tables I and II. Uncorrected, the number of erythrocytes per unit area is 6.2 per cent in experiment no. 10, 7.5 per cent in experiment no. 11, and 7.7 per cent in experiment no. 12, below the corrected results. The standard error of the difference N_1—N_2 is perceptibly greater than in the experiments of tables I and II, partly because the difference N_1—N_2 is smaller, thus giving a somewhat larger percentage error (in the experiments of tables I and II, N_1—N_3 was used). In experiments nos. 12 and 13 the percentage apparatus error is equal to or somewhat larger than the Poisson deviation (spurious counts?).

Experiment no. 13 gives too great a number of erythrocytes per unit area. The interpretation of this experiment is the same as that given for experiment no. 9 (table II).

69. Statistical comparison between results obtained by the scanning method and by visual count. Let us denote the standard deviation of u_a, (the number of elements obtained by the scanning method) by σ_a, and the standard deviation of u_v (the number of elements obtained by the visual count) by σ_v. The standard deviations are reduced to unit area (square mm.). Thus, setting down only the main term in σ_a, (see end of § 31); we obtain:

$$\sigma_a \approx \frac{\sqrt{N_1 - N_3}}{(a_1 - a_3)\, L} \tag{59}$$

and

$$\sigma_v = \frac{\sqrt{N_v}}{A}. \tag{60}$$

N_v denotes the number of elements counted visually in the area A ($A = 9$ square mm. in all experiments).

Let us now consider the random variable $u_a - u_v$. Obviously, the mean value of $u_a - u_v$ should be equal to zero. We will now see whether the experiments described are in conformity with

this statement. The standard deviation of $u_a - u_v$, denoted by σ_D, is

$$\sigma_D = \sqrt{\sigma_a^2 + \sigma_v^2}, \tag{61}$$

as u_a and u_v are mutually independent random variables. As mentioned in § 31, the following is valid with a probability of about 0.95:

$$-2\,\sigma_D \leq u_a - u_v \leq 2\,\sigma_D. \tag{62}$$

Examination of our experiments shows that the difference $u_a - u_v$ is situated inside the above-mentioned interval except in experiments nos. 9 and 13, where $u_a - u_v$ is about 3 times σ_D.[1] The discrepancies found in these two experiments can be considered as due to a systematic error depending partly on the difference between $\bar{z}_1$ and $\bar{z}_3$ and partly on the recording of noise impulses (cf. § 16 and § 67).

70. **Conclusions.** The results obtained from the scanning counting experiments recounted above indicate that the apparatus functions in agreement with theory, when we count an element distribution like human erythrocytes sedimented from a diluted fluid suspension, and when dark field illumination is used. When the diffuse background light is relatively low and the sensitivity $\bar{z}$ of the apparatus is not too large, $\bar{z}$ seems to have been nearly the same for each of the three different apertures used in each experiment, and the results agree with those obtained by visual counting. On the other hand, conformity with visual count and with the experiments performed with a low background light and a relatively low sensitivity of the recording system is seriously disturbed when the diffuse background light is more prominent, as in experiments nos. 9 and 13.

71. **Missed elements.** The number of missed elements is more prominent when relatively large apertures are used, as shown in experiments 1—4. (See Figs. 43—46.) After correction for missed elements, the results of these experiments agree satisfac-

[1] When evaluating σ_D of experiments no. 9 and 13, we use the exact expression for σ_a in stead of equation (59).

torily with the visual count. On the other hand, the number of missed elements is rather low when smaller apertures and a low $\bar{z}$ value are used, as shown in experiment no. 10 (Fig. 52), also in good conformity with the theory.

72. **Apparatus error**. This error, which is given as standard error in the tables, is rather small when the intensity of the diffuse background is low. We mention some possible imperfections in the apparatus and method which may have contributed to the apparatus error. Too high a diffuse background gives rise to spurious counts (see § 68). The effect of the position of the apertures relative to the element distribution has been discussed above (§ 61). Displacements between the aperture and the element distribution may also be produced by mechanical imperfections of the rotating table or by temperature effects. Deviations of the rotating table that cause incorrect focussing are discussed in the description of the apparatus (cf. § 33 and § 42). The error introduced by variation in the scanning length, L, due to different stop positions of the rotating table is about $\pm$ 0.5 per cent of the scanning length, as the stage always stops within a quarter of a revolution (50 revolutions per scanning run). Fluctuation of the light intensity and occasional instability of the electronic system may cause change and drift in the $\bar{z}$ value, and by this means contribute to the apparatus error. It may also be pointed out that the position of the apertures discussed above (cf. § 61), which varies slightly from one scanning run to another introduces a displacement of the light pencil relative to the photocathode of the multiplier phototube. Thus, the response of the multiplier phototube may be slightly changed by displacement of the light pencil from one area to another of the photocathode. It is also possible that displacements relative to the wire of the screen in front of the photocathode or different absorption or refraction of the light pencil in the curved glass bulb of the phototube are of importance.

CHAPTER IX.

Improvements.

73. General considerations. It is possible to improve the method and the apparatus in the following ways.

(1) The percentage standard deviation due to random distribution of the elements can be decreased by counting more elements.

(2) It is desirable further to minimize the apparatus error and the tendency towards systematic error due to inequality between $\bar{z}_1$ and $\bar{z}_2$. This can be done by use of a more accurate optical system or by use of apertures of constant area (cf. § 16).

(3) The apparatus will be more flexible if the moving stage is constructed so that both transmitted and vertical illumination ('Ultropak system') can be used.

(4) Linear scanning motion (cf. § 33) seems to be more convenient and easier to adjust than helical motion.

(5) It seems possible to minimize the apparatus error due to instability of the light intensity and the recording system, or to imperfect reproducibility of the aperture position (cf. § 61), by use of a two-channel system where scanning runs corresponding to two different apertures are performed simultaneously.

(6) Scanning counting systems may be advanced which involve a less tedious numerical treatment of the results. Two such systems will be sketched below: a four-aperture system and counting by means of intermittent scanning.[1]

We shall now consider the above proposals in more detail.

---

[1] An improved apparatus is under construction. Linear scanning motion is used and the object can be illuminated both from below and from above ('Ultropak'). The apparatus will be equipped with four channels for simultaneous recording with four different apertures.

74. **Standard deviation.** The percentage standard deviation will be decreased by increasing the number $N = N_1 - N_2$ (cf. § 31). This is most simply effected by increasing the scanning length. Let us consider a numerical example. Assume that an area of 5×10 mm. of the counting chamber is available for the scanning procedure. By use of the linear scanning method (cf. § 33), one can obtain a scanning length of 200×10 mm., *i. e.*, 2 metres, with a distance of 0.025 mm. between every linear stroke. Assume that the aperture widths a_1 and a_2 are 0.018 and 0.008 mm. and that $\bar{z}$ is about 0.001 mm. (Human erythrocytes are being counted). By use of an element concentration of about 200 per square mm., N_1 is 8,000, $N_2 = 4{,}000$ and $N_1 - N_2 = 4{,}000$. Under such conditions, the standard deviation is about 2 per cent $\left(\frac{100}{\sqrt{4000}}\right)$. (Cf. description of the counting experiments.)

Further diminution in the percentage standard deviation seems to be impossible without a denser cell suspension, unless special counting chambers are available without a ruled network that disturbs the counting procedure. A cell concentration of about 400 per square mm. instead of 200 in the example above, will give a percentage standard deviation of about 1.1.

75. **Systematic error.** It is probable that dark field illumination effected by means of transmitted light ensures a better contrast between the luminous elements and the background than did the 'Ultropak' system used in the apparatus described. With a better illumination system, the tendency towards systematic error due to inequality between $\bar{z}_1$ and $\bar{z}_2$ and due to spurious impulses will be depressed even when relatively high light intensity is used.

In the theoretical part (§ 16), it was proposed that the sensitivity $\bar{z}$ of the apparatus corresponding to the various apertures used for one experiment could be made more independent of the element background if the areas of the different apertures were made equal. Experiments for checking this claim have not been performed up to now, partly because it is very

difficult to prepare the small apertures used in this work. This difficulty can be relieved by use of a higher magnification so that apertures of larger physical dimension can be used.

76. The moving stage. It is evident that the apparatus will be much more flexible if the moving stage is constructed so that both transmitted and vertical illumination can be used. With such an arrangement, illumination systems other than 'Ultropak' can be used. It is possible that microscope objectives of larger numerical apertures than that used in this work can be used if the vertical deviation of the moving stage can be further suppressed. However, such a modification would make the apparatus very expensive.

With the linear scanning method, it will be easier to adjust the position of the aperture relative to the scanning direction, and a larger part of the element distribution will be available for the counting procedure (cf. § 33).

77. The two-channel system. Fluctuations and instability of the light intensity and of the electronic system can be decreased further and the inconvenience of shifting the apertures (cf. § 61) eliminated, if in addition to the use of a more stable electronic system, an apparatus can be constructed wherein the light from the microscope objective is divided into two parts and led to two aperture-phototube-recording systems, where records corresponding to the two aperture widths a_1 and a_2 can be taken simultaneously, or where only the difference between the two channels is recorded. With the electronic elements of the two channels fed from the same power supplies, fluctuations in light intensity and power supplies cancel each other out. Once adjusted, the apertures of such an apparatus can remain fixed relative to the rest of the optical system. Furthermore, it is evident that only one scanning run is necessary for evaluating the result.

78. The four-aperture system. By the following manoeuver, the number of elements per unit area can be obtained in a simpler manner than that given in § 30 and used in evaluating the counting experiments. In addition it will be seen that even

the correction for missed elements can be performed without any information about the average size of the elements.

(1) Make two scanning runs with the aperture length in the scanning direction equal to c_1 and c_2 respectively. The aperture width a is equal to a_1 in both scanning runs. The number of recorded elements is N_1' and N_2'. According to equation (34), we have:

$$N_1' = N_{a_1} e^{-u\,(a_1+2\,\bar{z})\,\bar{l}_{\mu,\nu}}, \tag{63}$$

$$N_2' = N_{a_1} e^{-u(a_1+2\bar{z})\,(\bar{l}_{\mu,\nu}+c_2-c_1)}, \tag{64}$$

and

$$\frac{N_1'}{N_2'} = e^{-u\,(a_1+2\bar{z})\,(c_1-c_2)}. \tag{65}$$

This can be written:

$$u\,(a_1+2\,\bar{z}) \approx \frac{1}{c_1-c_2} \cdot \frac{N_2'-N_1'}{N_2'}, \tag{66}$$

multiplication by L now gives:

$$N_{a_1} = \frac{L}{c_1-c_2} \cdot \frac{N_2'-N_1'}{N_2'}. \tag{67}$$

(2) Make two scanning runs with the aperture lengths c_1 and c_2 used in (1). Let the aperture width a be equal to a_2 in both scanning runs. The number of recorded elements is now N_3' and N_4'. In analogy with equation (67), we have:

$$N_{a_2} = \frac{L}{c_1-c_2} \cdot \frac{N_1'-N_3'}{N_4'}. \tag{68}$$

(3) The number of elements per unit area, u, is now obtained from equation (4):

$$u = \frac{N_{a_1}-N_{a_2}}{(a_1-a_2)\,L}. \tag{69}$$

All the four scanning runs can be performed simultaneously by use of a four-channel scanning counter.

79. Intermittent scanning. Let us consider a different method for counting individual microscopic elements by photoelectric scanning. We perform the scanning movement as before: *i. e.*, the area with the elements moves relative to the aperture. Now suppose that the recording system or the microscope lamp functions only intermittently during the scanning procedure. Let us suppose further that the periods of function have a very short duration time, τ, and that these periods are continuously repeated with a frequency of f times per second. With a scanning velocity of, for example, 20 mm. per second and $\tau = 2 \times 10^{-6}$ seconds, the area with the elements moves relative to the aperture only 0.04 microns during a period of function, and in practice, we can consider that the element distribution remains completely stationary during this time.

Under these conditions, the aperture-recording system 'views' a sequence of f different fields of vision per second. We assume that the dimension of the scanning aperture relative to the scanning velocity is chosen so that there is no overlapping of consecutive fields of vision. The following possibilities occur when we consider one period:

(1) There is no element centre situated inside the effective aperture area, and no elements are recorded.

(2) There are one or more element centres inside the effective aperture area. One record is obtained.

Suppose that there are u elements per unit area and that the effective aperture area is equal to A. If the elements are distributed at random and if we assume Poisson's law valid, we obtain immediately the following probabilities:

(1) The probability that no element centres are situated inside the effective aperture area A is equal to e^{-m}, where m is equal to $u \cdot A$.

(2) The probability that one or more element centres are situated inside the effective aperture area is equal to $1-e^{-m}$.

Suppose we have obtained N' records when the recording system has functioned N times. We can then set down the following equation:

$$(70) \qquad N' = N(1 - e^{-m}) \approx N\left\{1 - \left(1 - m + \frac{m^2}{2!}\right)\right\} = N\left(m - \frac{m^2}{2}\right)$$

from which m is easily obtained.

Let us now assume that we perform two scanning runs and that we use apertures of circular shape with radii R_1 and R_2 respectively (see Fig. 56).

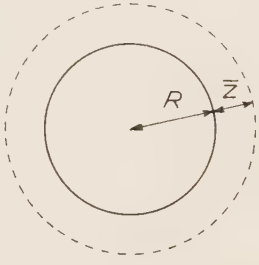

Fig. 56. Intermittent scanning. Circular aperture of radius of R. The figure illustrates the effective aperture area, which is equal to $\pi(R+\bar{z})^2$.

The following relations hold:

$$(71) \qquad N'_1 \approx N\left(m_1 - \frac{m_1^2}{2}\right)$$

$$(72) \qquad N'_2 \approx N\left(m_2 - \frac{m_2^2}{2}\right),$$

from which m_1 and m_2 are immediately obtained. We also have:

$$(73) \qquad m_1 = u\,\pi\,(R_1 + \bar{z})^2,$$

$$(74) \qquad m_2 = u\,\pi\,(R_2 + \bar{z})^2,$$

and

$$(75) \qquad \sqrt{m_1} = \sqrt{u} \cdot \sqrt{\pi} \cdot (R_1 + \bar{z})$$

(76) $$\sqrt{m_2} = \sqrt{u} \cdot \sqrt{\pi} \cdot (R_2 + \bar{z}).$$

After subtraction, we obtain:

(77) $$\sqrt{m_1} - \sqrt{m_2} = \sqrt{u} \cdot \sqrt{\pi} \cdot (R_1 - R_2),$$

and

(78) $$u = \frac{(\sqrt{m_1} - \sqrt{m_2})^2}{\pi (R_1 - R_2)^2}.$$

Let us now consider a numerical example. (Human erythrocytes are being counted.); Assume that R_1 and R_2 are 0.010 and 0.005 mm., respectively, and that $\bar{z}$ is about 0. From these figures and with a scanning velocity V of 20 mm. per second, it is evident that the repetition rate of the periods of function, f, cannot be made larger than 1,000 per second without overlapping between consecutive fields of vision, *i. e.*, the aperture must travel at least one aperture length between two consecutive periods of function $\left(f = \frac{V}{2 R_1}\right)$. If there are about 200 elements per square mm., m_1 and m_2 are 0.0628 and 0.0157 respectively. In order to record about 8,000 elements with the larger of the two apertures, the total number of periods of function N during a scanning run should be about 127,000. With $f = 1{,}000$ per second, such a scanning run would take about 2 minutes. The scanning length will be about 2.54 metres ($V = 20$ mm. per second), cf. § 44.

Very short periods of recording function with a duration of only a few microseconds can be produced in several ways. Thus, it would be possible to use as a light source an electronic stroboscope which produces intermittent light flashes with a constant repetition rate. By use of a continuous light source and a Kerr cell, it is possible to produce light flashes of extremely short duration. Another way of producing the very short periods of function is to feed the multiplier phototube by high voltage impulses. POST and SHIREN (1950) have used this technique in an attempt to develop high speed counting equipment for scintillation counters. These authors used impulses of an amplitude of about 5,000 volts and of 2.5 micro-

seconds duration. This performance gives also an improved signal-to-noise ratio, a more stable secondary emission, and a very high current gain.

The simplest way to produce repeated periods of recording function is perhaps to perform electronic switching of the impulse amplifier. It is possible to turn on an amplifier tube by use of a repeated gate impulse applied on the screen grid

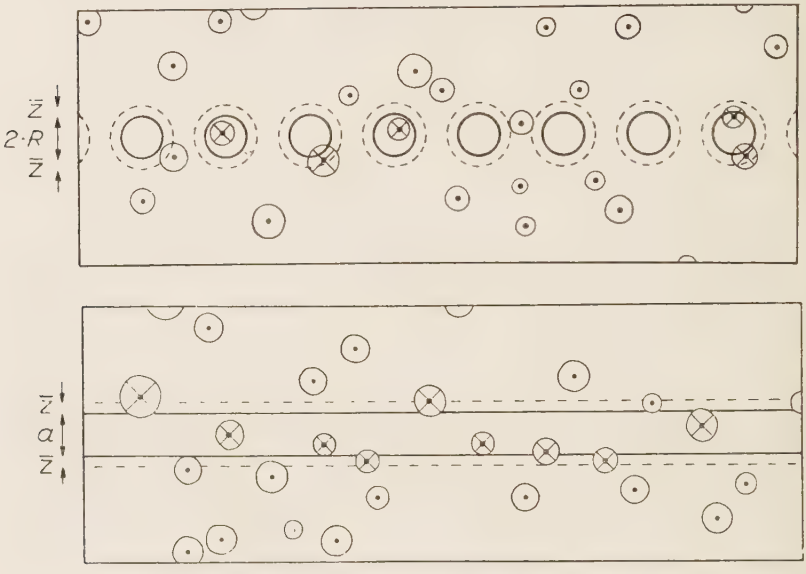

Fig. 57. Comparison between intermittent and continuous scanning.

or used for turning off an extraneously generated current through the cathode resistor of the tube which is cut off by the voltage produced by this extraneous current between the periods of recording function. In order to measure the total number N of periods of recording function, a separate counting channel may be added, from which N can be exactly determined.

The advantage of the intermittent scanning system lies in the very simple evaluation of the result and the use of circular apertures, which are much easier to manufacture than apertures of rectangular shape.

There is a complication inherent in intermittent scanning not yet mentioned. The probability of obtaining two or more class A_2 elements is larger in the larger of the two apertures (cf § 27). However, the disturbing effect of class A_2 elements will probably not be large, and if necessary, we can enter a suitable correction. In this connection, it may be pointed out that the probability of obtaining two or more class A_2 elements is not equal for the different apertures used, both in the constant area system (cf. § 16 and § 75), and in the four-aperture system (cf. § 78). Finally a comparison between continuous and intermittent scanning is sketched in Fig. 57.

CHAPTER X.

On the counting of cell nuclei in histological tissue sections.

80. General considerations. Although so far applied only to the counting of human erythrocytes and yeast cells sedimented from fluid suspensions (cf. also LAGERCRANTZ 1947), the scanning counting method may also be used in counting cells of histological tissue sections as well as other kinds of cells and particles settled from fluid suspensions. (cf. § 12). It seems likely that the method is especially suitable for counting cell nuclei of such parenchymeus organs as liver and pancreas, where the cells are uniformly distributed and are mainly of the same kind. In order to get sufficiently large signals from such elements, it is convenient to stain the nuclei so that a sufficient light absorption difference is obtained in relation to the cytoplasm (cf. § 11).

81. Impulse shape experiments. In order to decide if it is at all possible to count the cell nuclei of a histological tissue section, some experiments were performed on liver sections. The rotating stage described in this paper could not be used for this type of counting, as it was necessary to pass light through the object from below. Consequently, it has so far not been possible to make any counting experiment similar to those described in chapter VIII. However, by use of a conventional microscope stage moved by hand, it was possible to determine whether or not detectable signals could be obtained from liver cell nuclei. After a few trials, detectable signals were obtained with the following experimental arrangement. Microtome sections from liver were stained by the Harris hematoxylin method and differentiated so that the nuclei were seen stained blue-black and the cytoplasm a faint gray. A microscope objective of 22 x, N. A. = 0.45 was used together with the original condenser supplied with the 'Ortholux' microscope (condenser according to Berek with both aperture and

field diaphragms) and a yellow light filter. The image was adjusted with the aid of the condenser so that the cytoplasm appeared optically as homogeneous as possible. It was found that if the cytoplasm appeared granular, spurious counts were obtained from these structures. With this system, light signals from the cell nuclei were represented by a decrease in light intensity and by a positive output impulse from the photo-

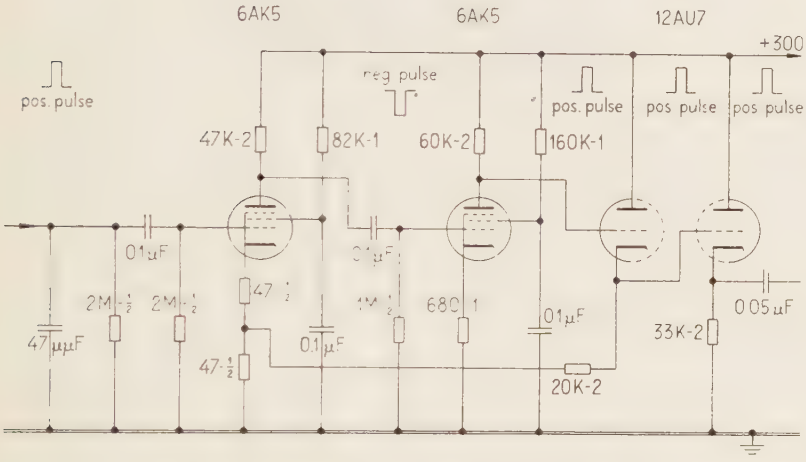

Fig. 58. Amplifier for positive input signals.

tube. An experimental amplifier was set up that gave positive output impulses for positive input signals. It consisted of a three stage feedback loop and a cathode follower output stage, and it was of a type similar to those described by ELMORE and SANDS (1949). It had a gain of about 180. A schematic diagram of this amplifier is given in Fig. 58.

By use of the arrangement described in § 53 for visualizing the impulse produced by a single cell or group of cells, the oscillograph pattern of the impulse produced by a liver cell nucleus given in Fig. 59 was obtained. From this pattern, it is seen that the field of vision scanned by the rotating aperture gives rise to a broad negative impulse. From the bottom of this negative impulse, the positive impulse corresponding to the liver nucleus is seen. This impulse is very well defined and

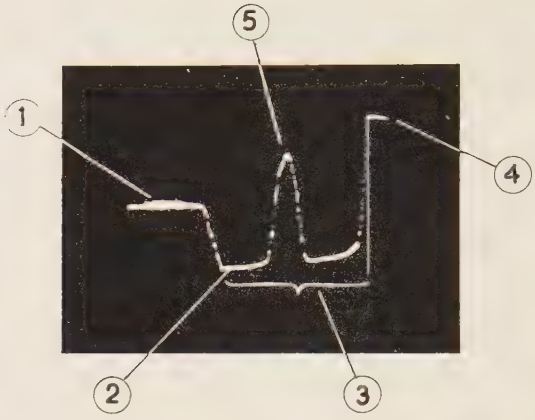

Fig. 59. Oscillograph pattern of the impulse produced by a liver cell nucleus. 1. Zero level. 2. Noise absent, amplifier overdriven. 3. Negative impulse referring to the field of vision. 4. Overshoot region. 5. Positive impulse referring to the liver cell nucleus.

is similar to those obtained from erythrocytes by use of dark field illumination. The pattern of Fig. 59 shows impulse distortion, which is due to overshoot produced by improper time constants in the experimental amplifier.

Summary.

A theoretical basis for the photoelectric method of counting individual microscopic cells by scanning described by the author (1947) has been advanced and an improved apparatus has been constructed. The counting procedure is effected by moving the area containing the cells relative to a microscope where the field of vision is limited to a size about that of a single cell, by means of a rectangular aperture placed in the eyepiece plane. A phototube is placed behind the aperture and is connected to an electronic recording system. When the cell distribution is scanned or swept by the aperture, cells or parts thereof pass through the aperture area in succession and give rise to impulses which are recorded. If no cells were missed during the scanning run, the following relation would be valid:

(i) $$N = u\,(a + 2\,\bar{z})\,L.$$

Here N is the number of cells recorded; u is the number of cells per unit area; a is the width of the aperture; $\bar{z}$ is a quantity depending on the sensitivity of the recording system and the light intensity change produced by individual cells; L is the length of the scanning track. Equation (i) contains two unknown quantities: u and $\bar{z}$. We perform two scanning runs with aperture widths a_1 and a_2, and obtain two equations of the form (i). Subtracting one of these from the other, we eliminate $\bar{z}$ and solve for u. Thus, we estimate u without knowing the size of the cells and without standardizing the sensitivity of the recording system, provided only that $\bar{z}$ has the same constant value during both scanning runs.

In a random distribution of cells, however, there are a certain number of cells situated so close to each other that they cannot be resolved and separately counted. Consequently, a certain number of cells are missed and equation (i) is not valid. It is found that the scanning counter does not count individual cells but rather a sequence of intervals between consecutive cells, and indeed only those intervals longer than a certain

minimum value l depending, among other things, on the aperture length; in fact, l is not the same for all pairs of cells. The fraction of missed elements can be estimated by the theory of probability and the result corrected for missed cells. It is shown that the number of recorded intervals N' is approximately equal to

$$N' \approx N \cdot e^{-u(a+2\bar{z})\bar{l}_{u,\nu}}. \tag{ii}$$

Here N is the true number of intervals between consecutive cells on the scanning track, and $\bar{l}_{u,\nu}$ is the arithmetic mean of all critical minimum intervals which actually occur. N is evaluated from equation (ii) by means of successive approximations and N is then used for evaluating u by use of equation (i).

A statistical treatment shows that we must consider the following mutually independent random variables: (1) the random distribution of the cells (distribution of Poisson type); (2) the random distribution of N' for given number N; (3) the apparatus error. It is found that the variation due to the random distribution of the cells is the most important one in most of the counting experiments performed.

The experimental apparatus is described. Dark field illumination is used, and the scanning motion is effected by means of a rotating stage constructed so that the scanning track has helical form. The electronic system is similar to that of a scintillation counter. An experimental arrangement for visualizing the impulse shape of a single cell or group of cells on an oscillograph screen has been devised. The impulse shape of human erythrocytes are given when different aperture sizes are used and certain time constants of the electronic system are varied. The impulse shapes experimentally obtained are compared with those derived theoretically, and the agreement is found to be good.

In order to determine whether or not the apparatus functions according to the theory, a number of counting experiments were performed on human erythrocytes settled at random from a diluted fluid suspension. It was found that the results obtained by the scanning method agree with the visual count after correction for missed cells, provided that the background

light and the sensitivity of the recording system are not too high. When these quantities are high, the quantity z in equation (i) is not equal in the two scanning runs and a systematic error is introduced.

Improvements of the method and apparatus are discussed. A two-channel system is proposed, in which scanning runs corresponding to two different apertures are performed simultaneously. Furthermore, a four-aperture system and counting by means of intermittent scanning are briefly discussed.

Finally, impulse shape experiments on differentially stained liver nuclei of a histological tissue section are recounted.

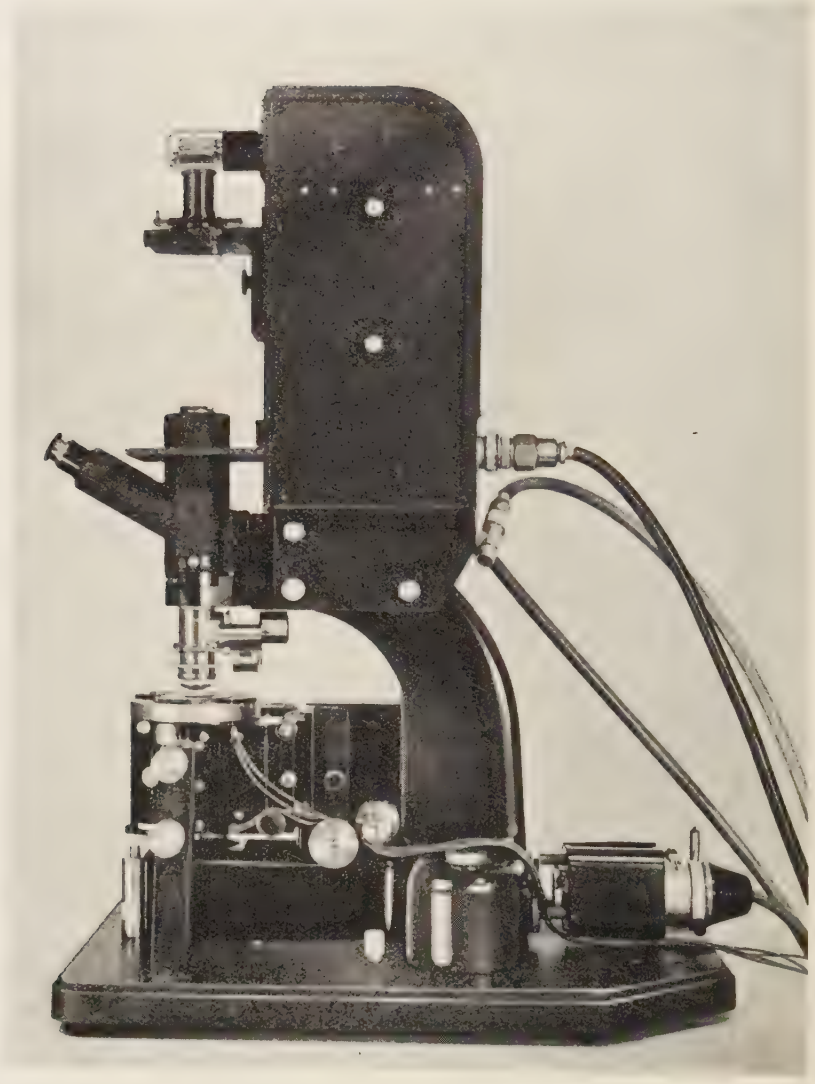

Fig. 60. View of the scanning and counting microscope mounted with the rotating stage. Light shield removed.

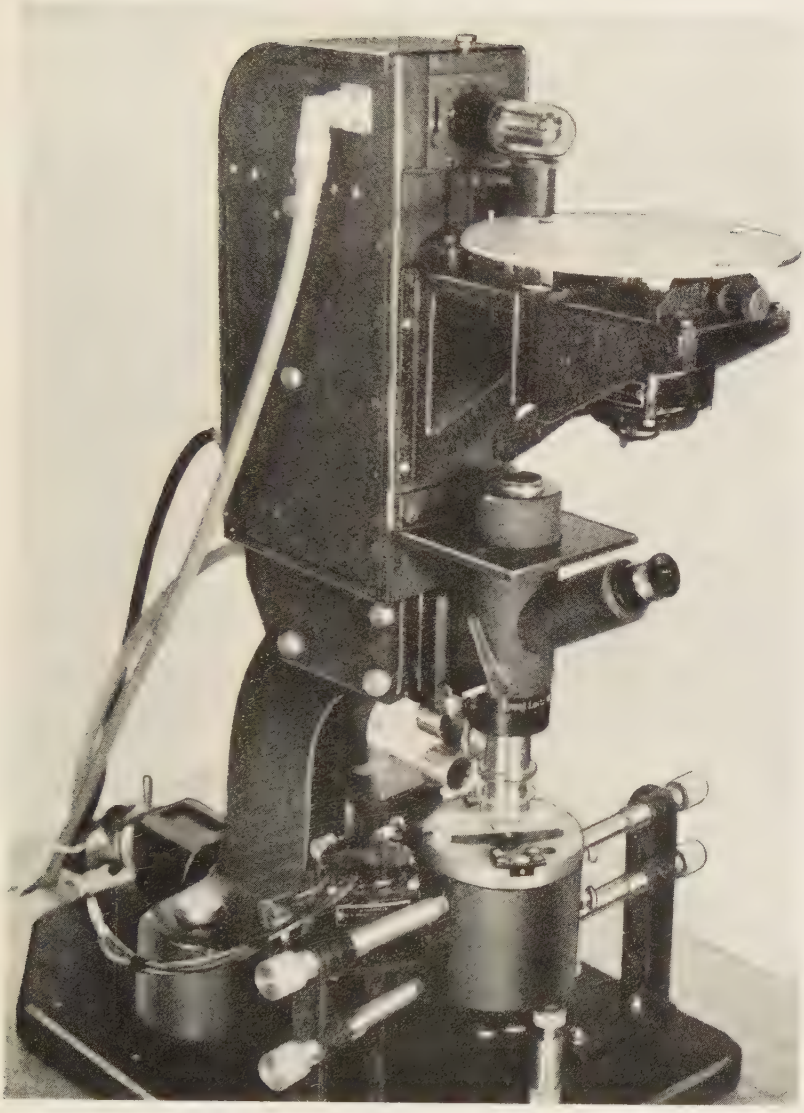

Fig. 61. View of the scanning and counting microscope equipped with the arrangement for visualizing the impulse of a single element or group of elements. The five holders (mentioned in § 42) for supporting the rotating stage can be seen clearly.

Acknowledgements.

The present work was begun in the Institute of Medical Chemistry and later continued in the Central Laboratory of the University Hospital. The author is indebted to professor Gunnar Blix and to laborator Anders Grönwall for their interest and support.

The author is indebted to docent Bo Kjellberg for much valuable help and advice in developing the mathematical part of the work.

Furthermore, the author would like to thank professor Ernst Bárány, diplomingenjör Jonas Björkman, docent Gösta Brogren, laborator Torbjörn Edlund, fil. lic. Knut Medin and docent Einar Stenhagen for helpful discussions.

The author is obliged to ingenjör Georg Eriksson and instrumentmakare Folke Högberg for excellent assistance in the design and construction of the mechanical parts of the apparatus.

To Mr. Lars Finn, Mr. Endel Sepp, and ingenjör Eric Köiv the author is indebted for the preparation of figures and diagrams.

Finally, the author wishes to express his best thanks to professor and Mrs Edwin Hewitt for linguistic revision.

Part of the expenses involved in this work have been defrayed by grants from the Medical Faculty of the University of Uppsala.

References.

ARLEY, N., and K. R. BUCH, *Sandsynlighedsregning,* København 1943.

BLAU, M., R. RUDIN, and S. LINDENBAUM, Rev. Sci. Inst. 1950, *21,* 978.

BOSSELAAR, C. A., and N. SPRONK, Nature 1952, *169,* 18.

BRYAN, W. R., and W. E. GARREY, J. Amer. Med. Assoc. 1934, *103,* 1059.

CRAMÉR, H., *Sannolikhetskalkylen,* Uppsala 1949.

ELMORE, W. C., and M. SANDS, *Electronics, Experimental Techniques,* New York 1949.

ENGHOFF, H., Uppsala Universitets Årsskrift, 1937, *9.*

GUCKER, F. T., Science, 1949, *110,* 372.

HEIGL, J. J., B. F. DUDENBOSTEL, J. F. BLACK, and J. A. WILSON, Analyt. Chem. 1950, *22,* 154.

HIGINBOTHAM, W. A., J. GALLAGHER, and M. SANDS, Rev. Sci. Inst. 1947, *18,* 706.

LAGERCRANTZ, C., Upsala Läkareförenings Förhandlingar 1947, *52,* 287.

——, Nature 1948, *161,* 25.

LAWRENCE, J. H., and J. G. HAMILTON, *Advances in Biological and Medical Physics* Vol. I p. 210, New York 1948.

LOESCHCKE, H. H., and R. WEVER, Brochure published by Hellige & Co., Freiburg 1951.

MARGENAU, H., and G. M. MURPHY, *The Mathematics of Physics and Chemistry,* New York 1943.

MARSDEN, E., and T. BARRATT, Proc. Phys. Soc. London 1911, *23,* 367.

MARSHALL, F.-H., J. W. COLTMAN, and A. I. BENNETT, Rev. Sci. Inst. 1948, *19,* 744.

MATTHES, M., and H. SCHARPF, Klinische Wochenschrift 1951, *29,* 266.

MCCUSKEY, S. W., and R. M. SCOTT, Rev. Sci. Inst. 1934, *5,* 196.

MELLORS, R. C., and R. SILVER, Science 1951, *114,* 356.

MICHEL, K., Die Grundlagen der Theorie des Mikroskops, Stuttgart 1950.

MOLDAVAN, A., Science 1934, *80,* 188.

POST, R. F., and N. S. SHIREN, Phys. Rev. 1950, *78,* 81.

VALLEY, G. E., and H. WALLMAN, *Vacuum Tube Amplifiers,* Radiation Laboratory Series Vol. 18, New York 1948.

WOLFF, H. S., Nature 1950, *165,* 967.

YOUNG, J. Z., and F. ROBERTS, Nature 1951, *167,* 231.

UPPSALA 1952
APPELBERGS BOKTRYCKERI AB